Design of Software Defined Radio Based Testbed for Smart Healthcare

Aboajeila Ashleibta

Submitted in fulfilment of the requirements for the
Degree of Doctor of Philosophy

School of Engineering
College of Science and Engineering
University of Glasgow

February 2022

Abstract

Human Activity Recognition (HAR) help to sense the environment of a human being with an objective to serve a diverse range of human-centric applications in health care, smart-homes and the military. The prevailing detection techniques use ambient sensors, cameras and wearable devices that primarily require strenuous deployment overheads and raise privacy concern as well. Monitoring human activities of daily living is a possible way of describing the functional and health status of a human. Therefore, human activity recognition (HAR) is one of genuine components in personalized life-care and healthcare systems, especially for the elderly and disabled. Recent advances in wireless technologies have demonstrated that a person's activity can modulate the wireless signal, and enable the transfer of information from a human to an RF transceiver, even when the person does not carry a transmitter. The aim of this PhD project is to design a novel, non-invasive, easily deployable, flexible and scalable test-bed for detecting human daily activities that can help to assess the general physical health of a person based on Software Defined Radios (SDRs). The proposed system also allows us to modify the power level of transceiver model, change the operating frequency, use self-design antennas and change the number of subcarriers in real-time. The results obtained using USRP based wireless sensing for activities of daily living are highly accurate as compared to off-the-shelf wireless devices each time when activities and experiments are performed. This system leverage on the channel state information (CSI) to record the minute movement caused by breathing over orthogonal frequency division multiplexing (OFDM) in multiple sub-carriers. The proposed system combines subject count and activities performed in different classes together, resulting in simultaneous identification of occupancy count and activities performed. Different machine learning algorithms namely K-Nearest Neighbour, Decision Tree, Discriminant Analysis, and Naıve Bayes are used to evaluate the overall performance of the test-bed and achieved a high accuracy. The K-nearest neighbour outperformed all classifiers, providing an accuracy of 89.73% for activity detection and 91.01% for breathing monitoring. A deep learning convolutional neural network is engineered and trained on the CSI data to differentiate multi-subject activities. The proposed system can potentially fulfill the needs of future in-home health activity monitoring and is a viable alternative for monitoring public health and well being.

Contents

List of Tables

List of Figures

List of Abbreviations

CSI - Channel State Information
WCSI - Wireless Channel State Information
CFR - Channel frequency response
ADC - Analog to Digital Converter
AI - Artificial Intelligence
CP - Cyclic Prefix
DAC - Digital to Analog Converter
DDC - Digital down Converter
DUC - Digital up Conversion
FFT - Fast Fourier Transform
IFFT - Inverse Fast Fourier Transform
ISI - Inter Symbol Interference
LOS - Line of Sight
LPF - Low Pass Filter
OFDM - Orthogonal Frequency Division Multiplexing
PCA - Principal Component Analysis
QPSK - Quadrature Phase Shift Keying
RF - Radio Frequency
RSS - Received Signal Strength
USRP - Universal Software-Defined Radio Peripheral
NCO - Numerically Controlled Oscillator
BER - Bit Error Rate
QAM - Quadrature Amplitude Modulation
ML - Machine Learning
NIC- Network Interface Card
MIMO - Multiple Input Multiple Output
DL- Deep learning
DTW - Dynamic time warping
FPGA - Field Programmable Gate Array
HAR - Human Activity Recognition

HMM - Hidden Markov Model
IOT - Internet of Things
KNN - K-nearest neighbors
DT - Decision Tree
DA - Discriminant Analysis
NB - Naive Bayes
UWB - Ultra-wide band
Wi-AR Wireless Activity Recognition
Wi-Fi Wireless fidelity
Wi-GeR - Wi-Fi-based gesture recognition
Wi-hear - Wireless Hear
Wi-motion - Wireless Motion
Wi-See - Wireless See
Wi-Vit - Wireless Vitality
AWGN - Additive white Gaussian noise channel
CV - Cross Validation
CM - Conjugate Multiplication
FMCW - Frequency Modulated continuous wave
FOG - Freezing of Gate

Acknowledgements

First and foremost, I would like to express my heartfelt gratitude to my supervisor, Prof. Mohammad Ali Imran, for their unwavering support and invaluable edification throughout my Ph.D. studies, as well as for providing me with the opportunity to work in this exciting field. I would also like to thank my co-supervisor, Prof. Qammer H. Abbasi, for his technical guidance and support throughout my PhD period. A special thanks to the Abbasi lab group for amazing memories, dinners, parties, and trips. None of the work in this study would have been possible without the help of the CSI group members. I would also like to thank friends for their help and support during my studies. Last but not least, I wish to express my deepest gratitude to my family. Without their unconditional love and understanding, I could not insist on my dream and work for it. This thesis is dedicated to you all!

List of Publications

The work presented in this thesis has culminated in the following journal publications and conference proceedings:

[Journals]

1. Ashleibta, A.M.; Zahid, A.; Shah, S.A.; Abbasi, Q.H.; Imran, M.A. Flexible and Scalable Software Defined Radio Based Testbed for Large Scale Body Movement. Electronics 2020, 9, 1354. https://doi.org/10.3390/electronics9091354.

2. A. M. Ashleibta, Q. H. Abbasi, S. A. Shah, M. A. Khalid, N. A. AbuAli and M. A. Imran, "Non-Invasive RF Sensing for Detecting Breathing Abnormalities Using Software Defined Radios," in IEEE Sensors Journal, vol. 21, no. 4, pp. 5111-5118, 15 Feb.15, 2021, doi: 10.1109/JSEN.2020.3035960.

3. Ashleibta, A. M., Taha, A., Khan, M. A., Taylor, W., Tahir, A., Zoha, A., Imran, M. A. (2021). 5g-enabled contactless multi-user presence and activity detection for independent assisted living. Scientific Reports, 11(1), 1-15.

4. Shah, S.A.; Tahir, A.; Ahmad, J.; Zahid, A.; Pervaiz, H.; Shah, S.Y.; Ashleibta, A.M.A.; Hasanali, A.; Khattak, S.; Abbasi, Q.H. Sensor fusion for identification of freezing of gait episodes using Wi-Fi and radar imaging. IEEE Sens. J. 2020, 20, 14410–14422.

[Conferences]

1. Ashleibta, A., Shah, S. , Zahid, A., Abbasi, Q. and Imran, M. (2020) Software Defined Radio Based Testbed for Large Scale Body Movements. In: 2020 IEEE International Symposium on Antennas and Propagation and North American Radio Science Meeting, Montreal, QC, Canada, 05-10 Jul 2020.

2. Taylor, W., Ashleibta, A. M. A., Shah, S. A. , Imran, M. and Abbasi, Q. (2020) Software Defined Radio Based Activity Recognition for Remote Healthcare Driven by Machine Learning. In: 9th IEEE Asia-Pacific Conference on Antennas and Propagation (APCAP 2020 on-line), Xiamen, China, 4-7 August 2020,

Chapter 1

Introduction

Human activity detection has received considerable attention in recent years due to their applications in many emerging indoor environments such as healthcare systems, intrusion detection, and search & rescue. Notable applications include monitoring patients, fall detection for elderly and physically challenged individuals [1]. Technology advancement in the healthcare system improves the quality of life by providing a robust wireless communication system that reduces costs, facilitates quick access, and ensures high-quality patient care. Additionally, the detection of human activity in buildings can be used by environmental control systems to create a comfortable indoor atmosphere while maintaining a high level of energy efficiency [2]. Numerous innovative technologies for activity monitoring have been presented in industry and academic sectors, these technologies are categorised primarily into two types: contact and contactless. Contact with body-based technology is defined as monitoring via wearable sensors [3–9], which may include the usage of wearable devices such as smartphones or smartwatches equipped with accelerometers. Contactless technologies are either camera-based or RF-based. Camera-based monitoring employs images or videos to monitor humans [10–13]. Whereas radio frequency-based technology employs changes in channel state information (CSI) induced by human body motions. Furthermore, Wi-Fi [14–17], radar [18–21], and SDR [22–25] are all examples of RF sensing-based technology.

Each of these technologies involves a trade-off between benefits and drawbacks. For example, wearable sensors can be viewed as an effective tool for gathering detailed information about human activities and health issues. However, wearable devices, require direct contact with the body or keep it within proximity for detection, this may cause discomfort and the user needs to remember to keep these devices close. Additionally, patients may forget to wear their wearable sensors. Certain patients may come into contact with individuals suffering from skin disorders, and infants are also discouraged from wearing such sensors [26]. Similarly, camera-based systems need to be in Line of Sight to cover the full detection area [27].

Wireless sensing devices have become increasingly popular because of their ease of use and accessibility. Consumers do not need to wear any form of hardware support equipment when

using this type of technology.

Numerous wireless sensing-based devices for monitoring and recognising human activity have been presented [28–31]. The fundamental premise for detecting human body motions through the use of wireless sensing technologies is that the human body is primarily composed of water. As a result, wireless signals can easily be reflected, altering the course of propagation. Consequently, human body movements result in multipath fading.

Radar technology is also capture body movement's variations, making it ideal for detecting human activity in a non-line-of-sight (NLOS) environment. Radar technology is widely employed in military applications. It provides advantages such as precise localisation, coverage, and vital sign monitoring. However, it has several limitations, deployment of infrastructure, spectrum licencing, and equipment costs. In addition, very expensive and difficult to handle and needs professionals to operate.

Wi-Fi-based RF sensing systems are also used for activity recognition, relying on RSSI variations or the more detailed channel state information (CSI). However, RSSI based systems capture the propagation attenuation of the wireless signal to recognize activities [32]. They are inaccurate and are faced with performance degradation in complex indoor environments because of interference and multipath fading, which in turn cause the signals to be changed at receivers [33]. Furthermore, it has limited accuracy due to the effect of environmental changes on the received signal.

Researchers recently used the much finer-grained channel state information (CSI) reflecting channel frequency response to recognizing human activities. Commercial Wi-Fi devices have been extensively used for detecting activities of daily living as it uses small wireless devices such as Wi-Fi routers, network interface card (NIC) and off-the-shelf antennas operating at 2.4 GHz [15, 16]. The combination of Wi-Fi technology and machine learning algorithms helps in detecting intricate body motions as presented in [34].

Although prior studies offer an adequate solution for the detection of human activities in an indoor setting using CSI signals. However, the main limitation of the extracted CSI data from off-the-shelf small wireless devices is the limitation of only 30 subcarriers that are revealed. Furthermore, the data obtained is inconsistent. Therefore, affecting the overall performance of the system. The loss of OFDM sub-carriers sometimes cause loses valuable information. [35]

Hence to receive all sub-carrier transmitted, we have used Universal Software Radio Peripheral (USRP) where the hardware can be controlled over the software. The USRP platform allows for modifying the number of frequency carriers, changing the transmitted and received power and the operating frequency swing can be altered as well [35]. Furthermore, the ease in implementation of signal processing algorithms and the ability to reuse hardware encourages researchers to choose Universal Software Radio Peripheral (USRP) for their applications [23, 24].

1.1 Problem Statement

Non-contact sensing based activity recognition in a remote and unobtrusive manner provides considerable significant value to healthcare applications. The ratio of the number of health care problems and patients is increasing exponentially, such as in COVID-19 infection prediction. Furthermore, falls for elder people during physical activities are a significant cause of fatal and non-fatal injuries.

Wearable sensors can detect and recognize human physical activities, but it is not a realistic approach. Similarly, camera-based human monitoring technologies have privacy concerns. These technologies also fail in the monitoring in dark places. Therefore, It is important to develop innovative solutions to provide non-contact and remote assistance to reduce the risk and assisting patients suffering from serious health issues. The proposed system provides a flexible and scalable software defined radio peripheral for human activity recognition. Our system helps the researcher to reduce such devices and targeting a promising device-free sensing system.

1.2 Motivation

Human activity (HA) sensing is becoming one of the key components in future healthcare system. With the increasing number of health problems worldwide because of a lack of physical activity during the quarantine period, it is necessary to do indoor physical activities to prevent non-communicable diseases. They cannot spread from one person to another, but can last a long time. Cardiovascular diseases, cancer, diabetes, and other chronic respiratory diseases are categorized as non-communicable diseases. Sometimes, sudden falls due to physical activities may damage the human body, especially when a person is alone.

The prevailing detection techniques for human activity uses ambient sensors, cameras and wearable devices that primarily require strenuous deployment overheads and raise privacy concerns as well.

The technologies are growing and we are looking for new ways to sense the surrounding world. This motivates our work to develop a non-contact system for monitoring human movements and health work in a contactless way. furthermore, enhancing the system by using portable, flexible, and multi-functional SDR platform.

1.3 Aims and Objectives

Monitoring human activities of daily living is an essential way of describing the functional and health status of a human. Therefore, it is one of the genuine components in personalized life-care and healthcare systems.

• This work aims to investigate and develop wireless system based on Universal Software Radio

Peripheral (USRP) for connected health application. The proposed SDR technology monitors health while protecting individual privacy and offering patients comfort. In addition, it is affordable and accessible from any location at any time. It is intelligent, dependable, portable, flexible, and multipurpose in addressing the difficulties identified in the healthcare sector.
• The developed platform faithfully captures critical events such as falls and small-scale movements that include chest movement and heartbeat. This system more generalize, acquiring data in elderly care centre or hospitals in different geometrical settings.

1.4 Main Contributions

This thesis proposes human activity detection based on wireless sensing system to provide non-contact monitoring and remote assistance for patients. The contributions of this thesis can be summarized as follows:

• The development of a flexible and scalable software defined radio that can transmit and received N number of multiple sub-carriers to extract wireless channel state information that carry information for activities of daily living. The channel frequency response (CFR) is used to extract the fine-grained channel state information (CSI) by using the multi-carrier orthogonal frequency division multiplexing (OFDM) technique. Machine Learning algorithms are used for classification purposes, and their performance is evaluated on the basis of accuracy, prediction speed, and training time. The results demonstrate that this platform can recognize and classify activities with high classification accuracy. The developed platform is intelligent, flexible, portable, and has multi-functional capabilities.

• The developed platform faithfully captures different human abnormal breathing patterns and intelligently classifies normal, shallow, and elevated breaths using different machine learning algorithms. This platform allows medical professionals and caretakers to remotely monitor individuals in a non-contact manner. The developed platform is also suitable for both COVID-19 and non-COVID-19 scenarios.

• Finally, a novel 5G-enabled presence and activity detection system of multiple subjects is presented. The proposed RF-sensing system was designed to operate in the 5G frequency band, particularly at 3.75 GHz. The ultimate goal is to enable the incorporation of 5G-based non-invasive in-home activity monitoring systems in our community to maximise the utilisation of the opportunities offered by 5G and its enabling technologies.

1.5 Thesis Outline

The thesis consists of six chapters:

Chapter 1 Introduction include.

- Problem Statement.
- Research Motivation.
- Aims and Objectives.
- Main Contributions.
- Thesis Outline.

Chapter 2 This chapter presented human activity recognition methods in a wide range of applications. Moreover, discuss the existing studies of wire and wireless techniques and their evaluation in most recent researches in healthcare application. This chapter divided into two sections: Contact with body based system which include wearable sensors. Contactless body based systems are camera based and RF based systems.

Chapter 3 This chapter provided contactless activity monitoring of single subject based on SDR technology. It started by presenting background of the USRP platform and signal propagation, then discuss the principle of generating OFDM signal of the designed system, followed by the experimental setup and discussion of the results.

Chapter 4 In this chapter, vital signs monitoring of single subject was presented. it started by presenting the basic principle of the proposed system involved transmitting and receiving operation over multiple sub-carriers, then discuss the data collection, data extraction, feature extraction, and experimental scenario. In addition, the results and discussion of the this chapter.

Chapter 5 Multiple subject activity monitoring was introduced. It starts by presenting methodology and framework adopted to conduct the experiments, followed by a detailed outline of the experimental design stage including experimental variables, data collection, data processing, system training, and testing. In addition, experimental results included discussion was provided.

Chapter 6 This chapter conclude the work presented in this thesis and discusses future work that will be completed throughout the project's duration. Future work is explored, as well as ideas for how to enhance the human activity recognition given in this thesis.

Chapter 2

Literature Review

Human activity recognition has accelerated in recent years, owing to contactless inexpensive cost, widespread deployment, and privacy protection [36]. The core idea is that when a person lives in an environment with wireless signals, his or her body movement will have an impact on the wireless signals as they pass through the environment, generating a variety of distinct signal patterns. By examining the underlying patterns of several signal metrics, the original activities can be recognized. Machine learning's recent advancement opens up new avenues for more intelligent and accurate recognition performance.

This chapter provides an in-depth background overview of activity recognition using wireless sensing and learning. It started by introducing traditional approaches recognition methods based on camera and sensors, then present wireless-based activity sensing which include RSSI based systems, CSI based systems, Radar based system, Multiple subjects activity recognition and vital signs monitoring.

2.1 Vision and Sensor based Activity Recognition Systems

Computer vision-based systems use multiple high-resolution cameras to record the target with a series of video frames [36]. Camera-based systems are used to detect a wide range of human activities [37, 38]. For example, Motion History Images (MHIs) technique was presented to detect human movement and recover the full three dimensional of human [39]. The problem of recognising human activities with video cameras has been addressed using computer vision techniques with contentious outcomes, particularly in unconstrained real-world applications [40]. However, computer-vision-based approaches raises privacy concerns, mobility and energy consumption constraints. Furthermore, advanced infrared LED and depth camera technologies are sensitive to light illumination and can not recognise activities in dim or dark environments [41]. Sensor-based systems recognise activities by combining inputs from multiple sensors, such as geomagnetic, accelerometer, temperature, and gyroscope [42]. Wearable sensors are also popular for human activity recognition due to their high recognition accuracy [43]. Furthermore, it

has the advantages of portability, mobility, low energy consumption, and scalability. They are widely used in a variety of fields (e.g.,healthcare [44], living assistant, fitness). For example, [3] BodyScope, which records sounds using acoustic sensors to classify activities such as eating and coughing. Chen et al. [45] also used a smartphone with an accelerometer sensor to recognise human activity.

Another commonly used sensor for detection is ambient sensors which include motion detectors and pressure mats. These sensors are widely used in residential settings to support daily life monitoring such as tracking and resignations. Chiang et al. [46], proposed an approach that uses these types of sensors to detect individual and cooperative activities among different residents. However, the method based on wearable sensors requires users to carry sensing devices, which are considered invasive and raise the issue of personal privacy disclosure as seen in Figure 2.1 . Furthermore, because ambient sensors cannot capture specific user actions, their use should be limited to applications requiring coarse-grained activity recognition [46]. Children and the elderly dislike wearing wearable devices because they are uncomfortable. Under these conditions, non-contact based sensing technologies such as WiFi, SDR, and radar-based human activity sensing systems are gaining popularity because they monitor human activities without requiring human contact.

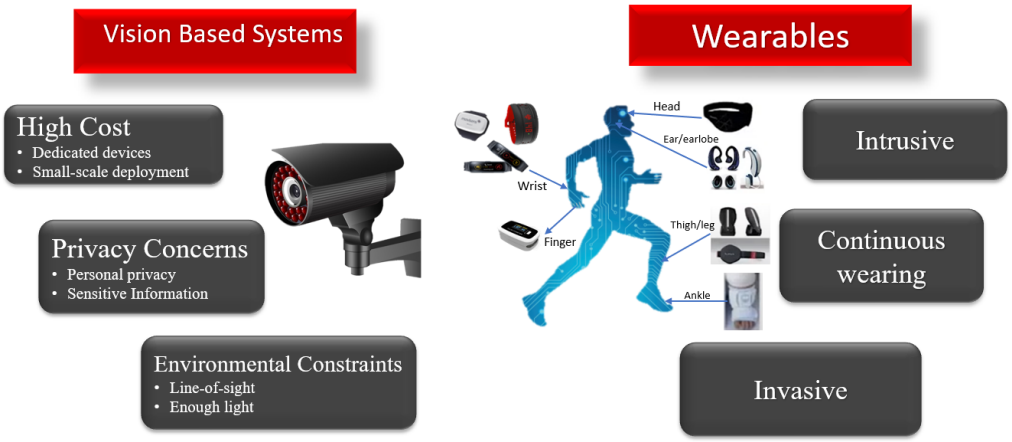

Figure 2.1: Invasive and Intrusive sensing

2.2 RF Signal based Activity Recognition Systems

Researchers have recently made significant progress in activity recognition using wireless signals. Existing systems are typically classified into three types: RSSI-based systems, Radar based systems, and CSI-based systems. Figure 2.2 shows general human activity sensing based on wireless signal.

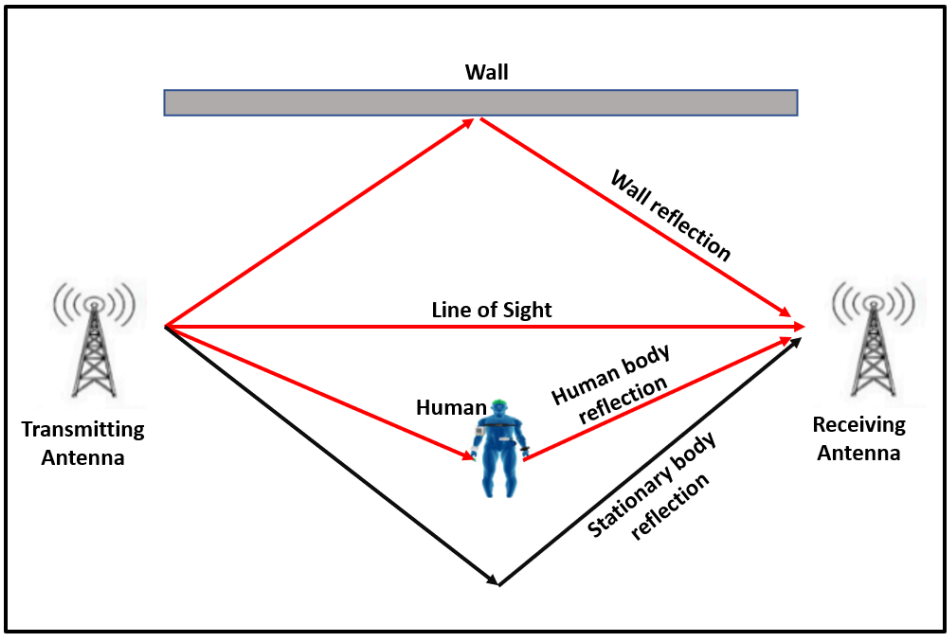

Figure 2.2: General wireless sensing system

2.2.1 RSSI based Systems

Various applications that use RSSI to detect ambient characteristics have emerged in recent years. RSSI is commonly employed in mobile computing applications such as indoor wireless localisation and passive human identification due to its universality. RSSI is a measure of total received power across all subcarriers, which limits its stability and reliability. Moreover, it has been used by researchers to perform activity recognition through identifying the closest fingerprint [47]. The work of [48] presented gesture recognition system known as WiGest using RSSI measurements. This system uses RSSI signal to recognise human hand gestures around a user device without any wearable device or any modification to the wireless equipment. The data processing component of the system is shown in Figure 2.3.

The authors of [15] use RSSI signal to recognise human activities. Their system extracted some representative features manually from the raw RSSI measurements, then they used unique fusion algorithm that combines the k-NN and a decision tree algorithms to classify human activities, such as sitting, standing, and walking.

Several researchers have successfully used RSSI signals to detect human activity in indoor environments, the received signal strength indicator (RSSI) of a wireless signal fluctuates due to object movement in indoor setting. As a result, such fluctuations can be used to track human motions without the need for cumbersome equipment [49] [50]. Moore et al. [51] presented a system-positioned human motion that takes into account changes in the standard deviation of received signal strength between stationary wireless transmitters and receivers at fixed locations. Kosba et al. [52] used an anonymous parametric technique and analysed RSSI features to improve the accuracy of human detection in various environments. In [53] passive and active

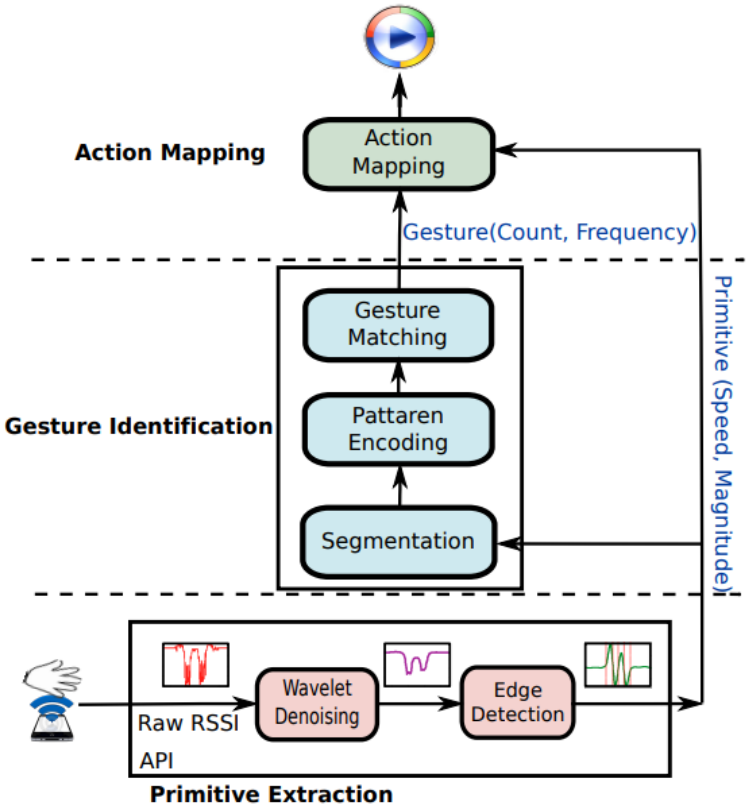

Figure 2.3: Data processing component [48]

system used USRPs as specialized hardware devices to collect RSSI signal for detecting different simple activities. In [54] device free recognition system was proposed to detect static and dynamic activities of single individuals using RSSI signal. In [55] the authors demonstrated a method for detecting and tracking human motion using RSSI. This method defined two functions: one to improve the collection and measurement of RSSI signals affected by human motion, and the other to detect human motion in indoor environments using a predefined threshold and zone selection method. The work of [56] used an RF-channel to design a passive and active system for detecting human activity based on variations in the RSSI signal caused by human motion.

Previously, a hand gesture recognition scheme based on easily deployable ubiquitous WLAN devices was proposed in [57], employing a sophisticated WARP board outfitted with two RE14P directional patch antennas, their system was implemented and tested in two scenarios: gesture-based electronic activation from a wheelchair (up to 25 gestures tested with 92% accuracy) and gesture-based control of a car infotainment system (84% accuracy on average). However, because of the multi-path and fading effects, RSSI measurements are highly unstable and noisy, limiting the performance of RSSI-based activity recognition systems, even for some simple activities. Furthermore, these systems are incapable of recognising fine-grained activities with comparable accuracy [57]. RSSI has the problem of having coarse grain resolution, being highly

vulnerable to noise, and exhibiting variations, making it an impractical solution for occupancy detection.

2.2.2 CSI based Systems

Due to recent advancements in 802.11n and the availability of advanced technologies, it is now possible to extract fine-grained channel state information (CSI) from cheap WiFi devices. Channel state information (CSI) can captures signal amplitude information which reflects channel frequency response of OFDM subcarriers [58], and it can be extracted from commodity wireless Network Interface Card (NIC) and Universal Software Radio Peripheral (USRP). It attracts more attention in activity recognition recently since it discriminates multipath characteristics. Several researchers have focused on different approaches and technologies for human activity detection based on CSI signal. This subsection reviews the existing literature available on CSI-based systems to recognize human activity in an indoor environment.

In today's world, Wi-Fi access points are readily available almost anywhere, and human presence between the access points contributes to the creation of a distinct CSI. In order to classify human movements, CSI data is extracted and processed using machine learning [59]. In [60], the CSI based on Wi-Fi signals recognises human behaviour in two different locations and address the effect of the environment on the received signal to introduce the change in CSI of human motion detection. The work of [61] made use spatial diversity based on Wi-Fi to extract the CSI of human present in the dead zone. The work of [62] presented a Fresnel zone model for human activity recognition using CSI signals, the proposed model achieved very high accuracy detection. RF signal was proposed to detect human behaviour like walk, sit, stand and run, this system is used to extract fine-grained CSI for human activity analysis [63]. In [64] the author exploits the CSI that extracted from commercial WiFi device to recognise human activity which consists two key model, a CSI-speed model and a CSI-activity model.

Lv et al [65]. also presented an indoor intrusion system based on CSI, this system uses a Hidden Markov model to classify human intrusion actions. In [6] human activity recognition was presented through analyzing the CSI at the receiver side to classify four human activities (standing, sitting, walking, laying), their system showed good result without radio frequency interference environment (RFI). Figure 2.4 indicates that RFI has a significant impact on CSI. The diagram depicts a CSI without RFI and a CSI with RFI on a certain radio channel. De Sanctis et al [66]. presented WIBECAM to recognise human activity through WiFi Beacon-Enabled Camera.

Wang et al [67] proposed E-eyes indoor recognition system to collects CSI information using commercial WiFi device to detect 11 human activities such as cooking, washing dishes, and walking. It is a method that can enable accurate tracking and recognition with low infrastructure requirements and without the need for a specialised device as shown in Figure 2.5. However, This system identify activities only in fixed position and E-eyes can be enhanced by increasing the signal bandwidth, transmission rate, and number of Wi-Fi devices.

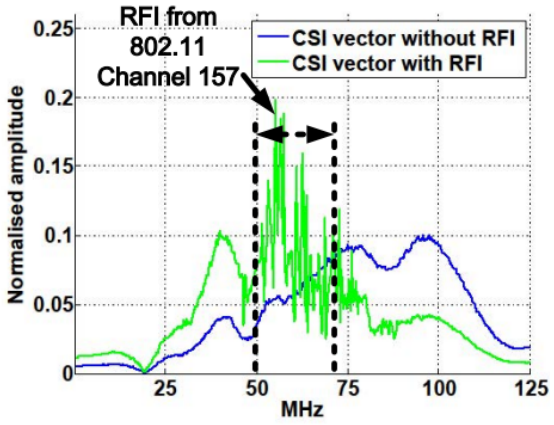

Figure 2.4: CSI with and without RFI [6]

Many approaches exploit CSI signal to detect human walking. In [68], device free passive detection system was presented to detect human moving with dynamic speed using both amplitude and phase information of CSI signal. The research published in [69] have presented human detection using non-linear techniques to extract CSI by examining the amount of nonlinear correlations between subcarriers. A non-contact sensing-based Wi-Run system estimated human steps using commercial Wi-Fi devices [70]. In addition, the authors of [71] presented the estimation of human's walking direction based on Wi-Fi channel state information in an indoor environment.

Channel state information has the capability to detect human behaviour through the wall as well. In [72], through the wall (TTW) human presence sensing systems was proposed to detect both moving and stationary persons from a single Wi-Fi access point (AP), allowing for greater efficiency and researchers conducted trials in an empty room, in which a person moved or remained fixed, and the channel frequency response (CFR) was evaluated to determine whether or not there was any human activity.

In [73]. Wi-Fi CSI-based occupant activity recognition system was proposed to recognize activities in smart office. In [74] Wi-Chase wireless system to track human presence using CSI, their system collects data from all subcarriers in order to identify and classify human behavior. A Wi-AR human activity recognition system collected data from ten persons performing sixteen different indoor activities using Wi-Fi signals. This approach reduces costs and enhances performance in a variety of areas [75].

Wi-Motion based human activity detection system, it is capable of sensitively to identify five human activities. This system exploits both amplitude and phase of CSI sequence to improve the recognition accuracy [76]. Device-free imaging-based occupancy recognition system used WiFi router and omni directional antenna for future smart buildings, and detecting different human activities, their system achieved high accuracy recognition [77]. Increasingly, Wi-Fi technology is being used in mobile devices to track human actions on a regular basis [78].

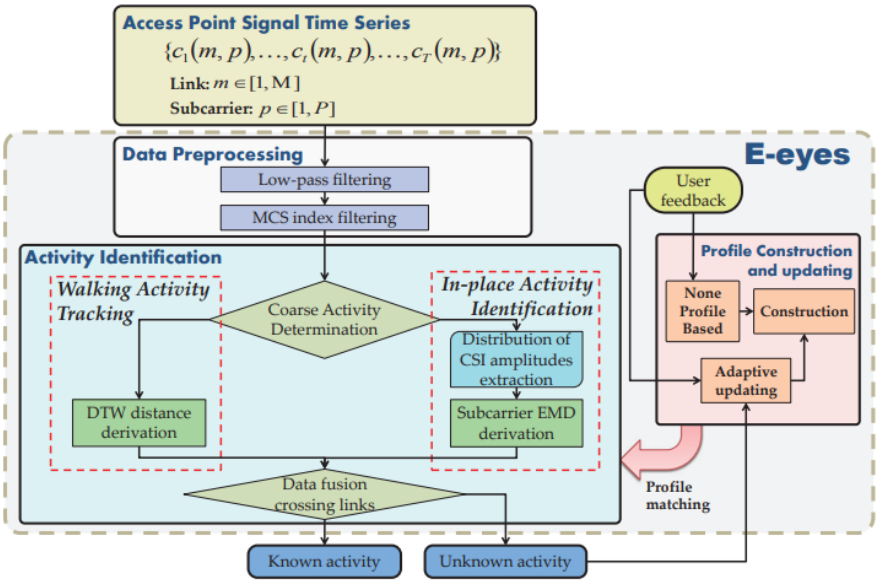

Figure 2.5: Framework of E-eyes [66]

Building upon these successes, researchers have applied CSI-based system to recognise fall activities. Khan, [79], developed a non-contact sensing platform is to monitor fall sports activities using software-defined radio (SDR) technology. This system exploits the amplitude response of the CSI signal to recognize different activities such as, walking, running, standing and bending, then he applied different machine learning algorithms for classifying the activities and achieved accuracy of around 93%. In [80], the authors proposed deep fall detection using spectrograms that present the propagation of CSI signal based on the variations of human through different places of the environment.

The work of [81] provided multi-stages fall detection using channel state information, this work can be distinguished the different between falling action and sitting action. The authors of [82] presented human fall detection in indoor environments using channel state information (CSI). Wang et al. [83] proposed RT-Fall algorithms to detect falls and achieved high accuracy.

In [84] Robust and unobtrusive device free fall detection based on Wi-Fi was propsed that can be applied into dynamic indoor environment. Wi-Fall [85], a system used for monitoring the fall of independent living people, especially old age. This system detects the fall of the human in a non-contact manner using commodity 802.11n network interface card (NIC) and achieves high fall detection accuracy for a single person. Borhani and Pätzold [86] proposed Wi-Fi-based fall detection system using a stochastic 3D trajectory model. In the simulation, human body, such as the head, arms, and legs, are molded as moving scatters, and fixed scatters represents static objects (e.g., the walls, appliances, or furniture). The simulation model detects when a fall occurs during random walking by analyzing the time-variant Doppler effect caused by an occupant's activity.

The wireless detection system makes use of 5G band technology to precisely capture people's

Table 2.1: Summary of non-contact human activity WiFi based sensing literature

NO	Technology	Activities Monitoring	Classification Method	Performance
1	Wi-Fi [15]	Walking, sitting and standing	k-NN classifier	92.58%
2	Wi-Fi [65]	Fall	SVM and RF	94%
3	Wi-Fi [63]	Walking, running, sitting and falling	CSI-speed mode	96%
4	Wi-Fi [62]	Walk, Sit, Stand, Run	SVM and LSTM	95%
5	Wi-Fi [72]	Human motion	HMM	94.2%
6	Wi-Fi [74]	Whole-body and partial-body movements	Machine Learning	94.82%
7	Wi-Fi [75]	Upper, Lower and whole body	CNN	90%
8	Wi-Fi [76]	Bend, walk, sit down and squat	SVM	98.4%
9	Wi-Fi [77]	Walking, jogging and sitting	Deep auto-encoder	91.1%
10	Wi-Fi [69]	Standing and sitting	Soft-max regression	97.5%
11	Wi-Fi [58]	Walk, stand, empty and sit down	RNN	90%
12	Wi-Fi [78]	Moving area, path walking	Path matching	90.83%
13	Wi-Fi [69]	Quantifying running	SSF	93.18%
14	Wi-Fi [87]	Post-surgical fall	SVM	90%
15	Wi-Fi [88]	Breathing rate and falls	Machine Learning	98%
16	Wi-Fi [89]	Danger Pose	SVM	96.23%
17	Wi-Fi [130]	Breathing and heart rate Patterns	DTW	94%
18	Wi-Fi [73]	Walking, running and moving hands	kNN and SVM	97%
19	Wi-Fi [81]	Distinguished between falling action and sitting action	Deep learning	89%
20	Wi-Fi [84]	Fall	SVM and k-NN	91%

falls and body movements [87]. Passive Wi-Fi sensing is used to monitor a person's health status, which includes breathing rate and falls [88]. The detection of a passive Wi-Fi system gathers two-dimensional phase information for the purpose of tracking human falls [89]. Summary of non-contact human activity WiFi based sensing literature is shown in Table 2.1.

2.2.3 Radar Based Systems

Human activity recognition based on radar system provides adequate information regarding human movement recognition. It can also provide a complete and stable development environment that enables researchers to create radio signals [31]. For instance, the work of [90], proposed SDR based through-wall radar system for detecting human presence and extract the micro doppler signature of humans walking through the wall. In [91], the system was able to extract four human motions using micro doppler signature based on universal software radio peripheral USRP N210. The work in [92] has proposed universal software radio peripheral platform to calculate and analyze the doppler shift of the propagation signals reflected from human movement. In [93] Micro-Doppler Radar signal for human gait detection has been proposed. This system designed a feature mechanism to extract six features from the human behavior signature using Short Time Fast Fourier Transform (STFFT). Furthermore, other studies [94] have provided human detection based on doppler radar signal to identify human subjects using a physical characteristic of target. Wi-Vi leverages the ubiquity of Wi-Fi chipsets to track target behind walls using USRP N210 radios [95]. Gao et al [96] proposed activity recognition system based on radio image features and deep learning. WiTrack based on FMCW signal can track the 3D motion of single subject involving 3D localization [97].

Yang, X. [98], proposed wandering scenarios with patients suffering from dementia using an S-band sensing technique to monitor and characterize different scenarios including random, lapping, and pacing movements in an indoor environment, their system shows high classification accuracy up to 90%. Fioranelli, [99] proposed radar for healthcare system to detect human activities and monitoring vital signs.

RADAR technology is also used in the human gesture recognition system to monitor and identify complex movements made by individuals to interact with objects without pressing buttons or touching screens [23, 100, 101]. WiSee leverages the USRP to measure small doppler shift to recognize nine whole-body gestures [102].

The researches in [103, 104] employed the FMCW radar scheme to acquire data on fall and recognize human activities such as running, walking, jumping, stepping, and squatting, the data were processed by a cross-validation technique over the K-NN algorithm and the achieved accuracy of around 95.5%. Unique micro-doppler signature for walking and running is the periodic motion of arms and legs, producing sidebands for the main doppler frequency used for the detection and classification of the respective activity [105]. Similarly, other studies used radar-based systems to track occupancy through the use of frequency modulated continuous-wave (FMCW) and orthogonal frequency division multiplexing (OFDM) techniques [106].

System based on ambient radar has been proposed to detect human activity in indoor environment. The operating frequency of 7.8 GHz detected human activity by sending 16 pulses per second and their system can distinguish between human movements in order to recognise various activities [18]. Radar-based devices are capable of capturing micro-doppler signatures for

Table 2.2: Summary of non-contact human activity radar based sensing literature

NO	Technology	Activities Monitoring	Classification Method	Performance
1	Radar SDR [91]	Human motion classification	Decision tree	97.3%
2	Radar [93]	Human walk detection	Artificial Neural Network (A-NN)	96%
3	Radar [94]	Human Detection	SVM	96%
4	Radar [96]	Human Walk	CNN	91%
5	Radar [98]	Patients Monitoring	SVM	90%
6	Radar [100]	Gesture Recognition	KNN	95 %
7	Radar [103]	Fall Detection	KNN	95.5 %
8	Radar [104]	Human Activity Recognition	KNN, SVM	81%
9	Radar [105]	Human Detection Outdoors	KNN, SVM, CNN	97%
10	Radar [107]	Walk, Running and Crawling	KNN, SVM, CNN	88%

human movements that can be used for recognition [107]. A passive-Doppler radar was employed in a wireless sensing strategy to detect changes in human body movement, irregular breathing rate, and various human physical activities in order to assess health status [108].
However, radar technology is not commonly used due to the high cost of the hardware configuration. Besides, the need for specialised hardware prevents them from being widely deployed at this time. Summary of non-contact human activity radar based sensing can be seen in Table 2.2.

2.3 Multiple subjects activity recognition

Recently, several approaches for recognising and counting multiple human activity have been developed using radio frequency methods and analysis of the reflected signal from the human body, without the use of any wearable device, using existing radio types such as Bluetooth, ZigBee, Wi-Fi, and RF. Jonsson et al. [109] used the Bluetooth function on the phone to detect multi-purpose activities via RSSI. Guerra et al. [110] employed ZigBee technology to develop CARDEA, a system that recognises human behaviours and facilitates daily life for multiple subject environments. The two approaches outlined above both make use of RSSI in order to identify human activity. However, they had difficulties with fine-grained localization.
WiFi based system has been developed to enable indoor localization to recognise multiple subject motion detection. Jose et al. [111] demonstrated a group detection method based on time-series Wi-Fi signal intensity measurements. In [75] WiFi-based activity recognition was utilised to recognise sixteen distinct activities performed simultaneously by ten persons. This technology is cost effective and performs well in a variety of applications. Tan et al, and Feng et al. [112] suggested a commercial Wi-Fi multi-system that utilises CSI to detect several individ-

uals' activities. In [113] the authors proposed multi-user gesture recognition system (WiMU) for recognising multiple persons executing movements simultaneously. In [76], the authors exploits the CSI collected from commercial WiFi device to detect and improve the accuracy of recognition for different participants, this system leverage both amplitude and phase information of CSI sequence to improve the accuracy.

FMCW are utilised to monitor people daily activities. The authors of [114] presented frequency-modulated carrier (FMCW) with a doppler range to detect human gestures in the presence of multiple moving targets and demonstrate the benefits of an FMCW radar in recognising human gestures when numerous human subjects are in the sensor's field of view. In [115] Multiple-target detection using a doppler radar system has been proposed. The system use of two elements receiving array for detecting multiple moving targets.

People counting can be useful in a variety of applications. One example is smart building management, in which heating can be optimised based on the number of people present, resulting in significant energy savings. Mostofi et al. [116], proposed a Wi-Fi-based system that counts the number of people walking in an area using only RSS measurements between a pair of transmitter and receiver antennas, the proposed framework is based on two important ways in which people affect the propagation of the RSS signal: blocking the line of sight signal and scattering effects. In [117] Multiple Wi-Fi nodes and RSS measurements were used to count up to four people, they reported an accuracy of around 84% within error of one person. A similar approach was used in [118], but with fewer nodes, they could count up to three people using RSS measurements. In [47] a transmitter-receiver pair was used to estimate the number of people, the underlying model was developed using extensive training data, and errors of up to 6 people were reported in experiments limited to 9 people.

Xi et al. [119] proposed a system for crowd counting based on the changes of CSI caused by human movement and their results show that CSI is very sensitive to the influence of the environment. The authors of [120] proposed algorithm to classify and estimate the number of people. The work of [121] presented a system capable of recognising the gestures of multiple users. Arai et al. [122] proposed a method for correlating crowd movement patterns with radar chart features, this method necessitates a survey of the used areas in order to create a fingerprint database, the main limitations of this approach are the effort, cost, inflexibility, and the dynamics of the environment, the training cost is a major limiting factor in crowd counting, especially for large-scale scenarios; additionally, it is extremely difficult to obtain the ground truth when the number of people is large.

2.4 Vital Signs Monitoring

With the advances in wireless communication devices and signal processing, researchers have qualified their findings to be taken into consideration while tracking human vital signs and respi-

ration. The majority of them were relevant to our work. Systems based on radio frequency (RF) technology have received considerable attention because they provide non-invasive breathing rate monitoring by extracting and analysing the RF signal that is reflected off the human body, such as those mechanisms based on universal software radio peripheral (USRP), FMCW, and doppler radar [123, 124]

Authors in [125], flexible and portable SDR technology is used to monitor vital signs such as respiration and other related health indicators, with the use of the multi-carrier orthogonal frequency division multiplexing (OFDM). They were able to extract the channel state information CSI from the channel frequency response (CFR) using OFDM technique and their method captures minute movements in human breathing and automatically classifies them into four categories: normal, slow, quick, and deep breaths, using three machine learning algorithms, they were able to obtain classification accuracy of approximately 99%.

Ashleibta [126] demonstrated a non-contact breathing detection system based on SDR technology. The system makes use of channel state information (CSI) to record minute movements caused by breathing over orthogonal frequency division multiplexing (OFDM) in multiple subcarriers and detect normal, shallow, and elevated breathing, which is then compared with a wearable sensor to determine which is the most appropriate (ground truth), then, a variety of machine learning techniques were used to attain high accuracy of around 91%. The authors of [127] proposed a contactless sensing system to detect COVID-19 symptoms such as irregular breathing and coughing in order to prevent the virus from spreading. This system can be further investigated and classified using cutting-edge machine and deep learning algorithms. The study of [128] also offered breathing detection of humans using SDR technology. This work created an SDR platform to monitor human breathing and overcome the challenges associated with null detection locations.

In [129] smart homes that monitor breathing and heart rate has been proposed, the authors introduce Vital-Radio, a wireless sensing technology that monitors breathing and heart rate without body contact and even when the user is up to 8 metres away from the device or behind a wall, their experiments show that the technology has accuracy of 99.3% for breathing and 98.5% for heartbeats. Vital-Radio can detect periodic chest movements generated by inhaling and exhaling and skin vibrations induced by heartbeats as shown in Figure 2.6.

In addition, a new way takes advantage of the CSI based on Wi-Fi devices to measure the breathing and heart rate of a human. For example, the work published in [130] demonstrated breathing identification based on the CSI signal, this approach made use of the Dynamic Time Warping algorithm to discern between the variance of the signal caused by breathing and that caused by the heartbeat of the human. The accuracy of this approach has been demonstrated to be 94%. In [131], the authors developed a method for detecting multi-person breathing using a common WiFi device, they used channel state information (CSI) phase difference data to make intelligent estimations of numerous breathing rates, their experimental study demonstrates that

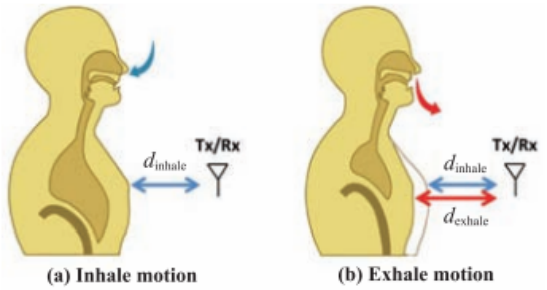

Figure 2.6: Chest movement affects signal reflection time [129]

their method is capable of accurately estimating multi person breathing. The work presented in [132] proposed track vital signs such as breathing rate and heart rate during sleep using off-the-shelf WiFi without the use of any wearable or dedicated devices, this system takes advantage of the fine-grained channel information to capture the minute movements caused by breathing and heartbeats during sleep. Additionally, their system is capable of monitoring vital signs for up to two people. The framework of the system's data processing is shown in Figure 2.7

Recent work presented in [133] uses RSS measurements on the link between two commercial wireless devices to determine a single person's respiration and position. Additionally, the authors of [134] proposed the use of a single commercially off-the-shelf WiFi-enabled devices to monitor respiratory rate. Nasser et al. [135] demonstrated the design and architecture of a non-intrusive system for predicting breathing rates and detecting apnea, as well as extracting the concealed breathing signal from a noisy WiFi RSS. Their system overcomes a variety of obstacles, including noise reduction, interference from humans, unexpected user movements, and the detection of anomalous breathing circumstances, the technology is more than 96% accurate in detecting sleep apnea.

In [136], mmVital employed a 60 GHz millimetre wave (mmWave) signal for breathing and heart rate monitoring with high bandwidth of nearly 7GHz, but it does not operate well over a longer distance and requires high gain directional antennas for the transmitter and receiver. In [137], a monitoring and detection system for human breathing was proposed. The authors use RSS measurements to track and estimate human breathing rates.

In [138] demonstrated how to develop and execute a real-time breathing detection system using cheap WiFi devices, they overcome the blind spot issue by employing conjugate multiplication (CM) of CSI between two antennas to achieve complete coverage of respiration detection. In [139], the authors proposed human respiration sensing via WiFi devices and used the Fresnel Model to examine the effect of human respiration on receiving radio frequency signals and to construct a theory relating human's breathing depth, position, and orientation. WiSleep [140] was the first work to use CSI in cheap WiFi devices to identify human breathing rate for sleep monitoring, this work was expanded in [141], which takes into account sleeping postures and abnormal breathing patterns.

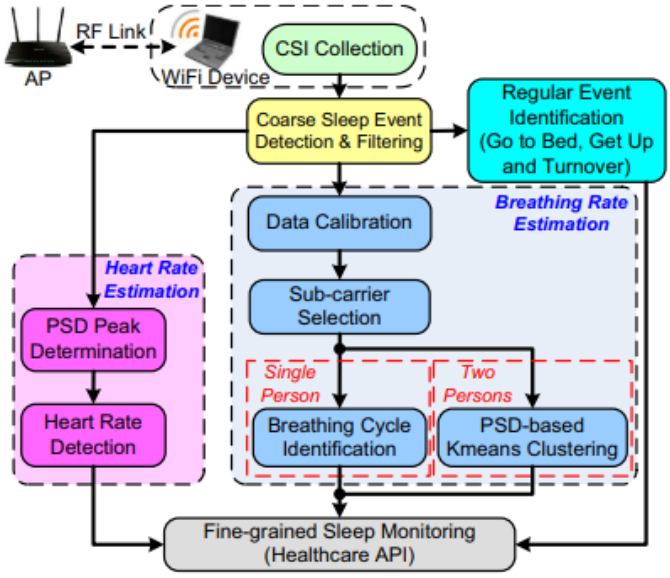

Figure 2.7: System Architecture[129]

Table 2.3: Summary of non-contact human breathing literature

NO	Technology	Activities Monitoring	Classification Method	Performance
1	SDR [125]	Normal, slow, fast and deep breathing	KNN, SVM, DT	99.3%
2	SDR [126]	Normal, shallow, and elevated breathing	KNN, DT, DA, NB	91%
3	WiFi [130]	Breathing detection	DTW algorithm	94%
4	Radar [136]	Breathing estimation	Deep learning	98.4%

However, the prior technique, such as received signal strength RSS, requires additional wireless network equipment. channel state information CSI in comparison to RSS, comprises both amplitude and phase data at the subcarrier level for orthogonal frequency-division multiplexing (OFDM) channels, providing a more reliable and accurate depiction of channel parameters. The aforementioned radar-based approach is constrained by infrastructure deployment, spectrum licensing, and the requirement for specific hardware. Summary of non-contact human breathing literature is shown in Table 2.3.

2.5 Summary

In this chapter, we presented a comprehensive review on existing vision and sensor based activity recognition systems and wireless-based activity sensing approaches with different types of signals or devices, we also have summarized and reviewed the deployment of wearable sensors

and vision based system in the healthcare system, and provided some traditional approaches that use camera based system and wearable sensor for recognise human activities. In addition. the advantages and disadvantages of both camera and sensor based have been introduced. We reviewed various human activity detection using wireless based system include received signal strength indicator RSSI, channel state information CSI, radar based system, multiple subjects detection and vital signs monitoring. The above approaches make use of different devices, signal and different activities performed in indoor environment.

Chapter 3

Contactless Activity Monitoring of a Single Subject

3.1 Introduction

Human activity monitoring domain has received significant research attention over the last two decades because it represents an effective solution to a variety of human-centric problems, HAR can provide numerous benefits to elder care, healthcare, and surveillance applications. Additionally, the availability of smart devices, artificial intelligence (AI), the Internet of Things (IoT), and computer vision has enabled enormous advancement in the HAR sector, allowing for effective and efficient life quality improvement. Numerous research attempts have been done to analyse human activities at various scales utilising a variety of sensing technologies. In [142], examples of systems that use cameras to detect human activity. Camera-based systems have the advantage of being able to detect even the tiniest motions of the human body. However, there are certain drawbacks to these systems, such as the impact of lighting and worries about privacy. Wearable sensors are also useful for human activity recognition due to their excellent recognition accuracy [143]. However, wearable sensor-based systems require users to bring additional devices for activity identification, which is difficult and obstructive for users.

Recent advancements in wireless technologies provide fresh and innovative solutions to the concerns listed above. Numerous monitoring systems such as WiFi, radar are helpful for detecting activities. For instance, WiFi based on RSSI signal is considered to address those concerns. and the systems that use the Received Signal Strength Indicator (RSSI) to capture the propagation attenuation of wireless signals can detect and identify activities [144]. However, they are imprecise and suffer from performance loss in complicated indoor situations due to interfering signals and multipath fading.

Researchers have recently adopted much finer-grained Channel State Information (CSI) reflecting channel frequency response for recognise activities. CSI provides more fine-grained features including both the amplitude and phase of multiple subcarriers. In [145] the authors propose hu-

man activity recognition based on Wi-Fi channel state information and machine learning. However, the CSI data were collected using off-the-shelf wireless devices and a low-cost Intel 5300 network interface card (NIC) that reports just a group of 30 data subcarriers natively. However, the total number of data packets transmitted by a Wi-Fi router is 56. Additionally, one or several subcarriers contain specific data, such as diverse bodily movements (i.e. sitting down, standing up, walking and so on). The unidentified subcarriers from 31 to 56 occasionally carry unique body movements. Additionally, NIC establishes the frequency range, power level, and operational frequency [146].
In this work, we have used software-defined-radio model named (USRP) by transmitting and receiving N number of multiple OFDM subcarriers as compared to its counterpart where limited numbers are available. The proposed system also allows us to modify the power level of transceiver model, change the operating frequency, use self-design antennas and change the number of subcarriers in real-time. The results obtained using USRP based wireless sensing for activities of daily living are highly accurate as compared to off-the-shelf wireless devices each time when activities and experiments are performed.

3.2 Background and System Overview

3.2.1 Universal Software Radio Peripheral

The Universal Software Radio Peripheral (USRP) enables engineers to rapidly design and implement powerful, flexible software radio systems. In addition to providing best-in-class hardware performance, the open source software architecture of the USRP X300 and X310 provides cross-platform UHD driver support making it compatible with many USRPs supported development frameworks, reference architectures, and open source projects. In our system, two USRPs X310 and X300 are used to implement the wireless channel state information of human behaviour, the software offered by national instrument, USRPs X300/x310 is a high performance hardware device that combines two extended bandwidths with a range covering DC – 6 GHz with up to 120 MHz . It is connected to the PC computer through 1Gb Ethernet cable to interface the USRP with PC. The maximum output power provided by USRP is 17 dB with a frequency range of 1GHz to 10 GHz, the FPGA of USRP X300/X310 sends and receive at a sampling rate from 200 MS/s to the DACs and ADCs respectively. Figure 3.1 shows the block diagram of the USRP. Some important features of USRP X300/X310:
• Xilinx Kintex-7 XC7K325T FPGA
• 14 bit 200 MS/s ADC
• 16 bit 800 MS/s DAC
• Frequency range: DC - 6 GHz with suitable daughterboard
• Up 160MHz bandwidth per channel

• Two wide-bandwidth RF daughterboard slots
• Multiple high-speed interfaces (Dual 10G, PCIe Express, Express Card, Dual 1G) •

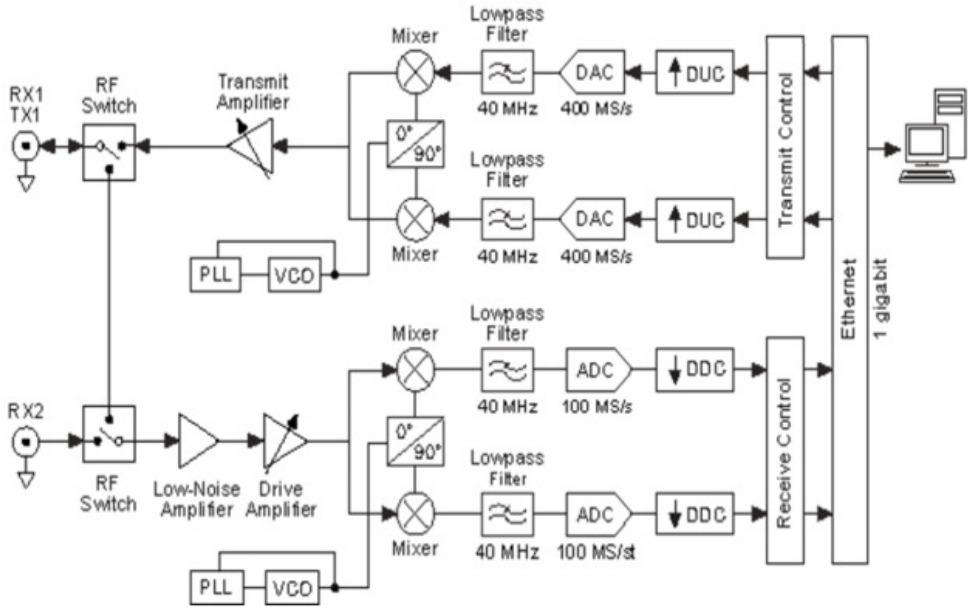

Figure 3.1: Block diagram of USRP X300/310 [147]

The existing wireless communication system communicates primarily through the use of high frequency transmissions. The SDR implementation down converts the majority of the data to sample and transport those high-frequency signals. The universal software defined radio peripheral is a family of hardware that is hosted by a computer and is part of this category. Matt Ettus has designed an SDR system that is both versatile and cheap cost at the same time. used to establish a connection between the RF-world (radio frequency) and a personal computer USRP is made up of a USRP motherboard [147], as well as a variety of daughterboards and the associated antenna, among other things. When it comes to conventional USRP products, each individual block is made up of two parts: a motherboard with high-speed signal processing FPGA and one or more daughterboards with different frequency ranges that can be swapped. They must be combined to produce the bit stream data that is sent from the antenna to the host computer, which serves as the receiver. Alternatively, data can be transmitted from the host computer to the antenna as a transmitter. on a number of daughterboard configurations The USRP series covers the complete frequency range from DC to 5.9GHz, which includes all frequencies ranging from AM radio to the IEEE802.11 standard. The USRP is made up of a number of different components, each of which is described in greater detail below.

• USB 2.0 Controller
• ADC (Analog to Digital Converter)
• DAC (digital to Analog Converter)
• PGA (Programmable Gain Amplifier)

• Daughterboards
• FPGA (Field programmable Gate Array)

Figure 3.2 illustrates the particular configuration of the modules above and their workflow. [148]

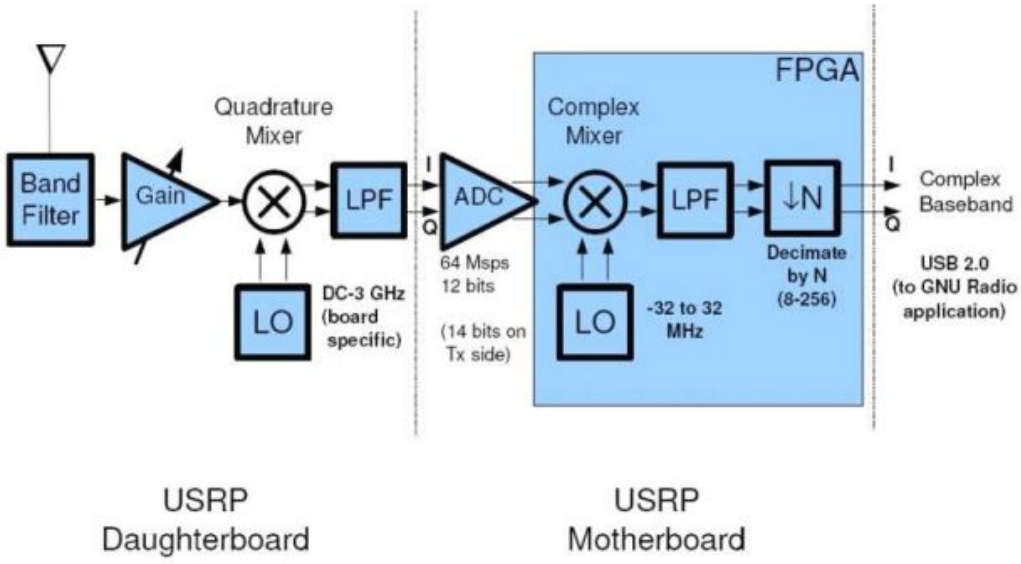

Figure 3.2: Universal Software Radio Peripheral Block configuration [148]

3.2.2 The Motherboard

The motherboard's primary functions are intermediate frequency sampling (IF sampling) and conversion between IF and baseband signals. As illustrated in Figure 3.2. The motherboard contains four slots for connecting the daughters boards to the mothers boards.

The motherboard features a 12-bit analogue to digital converter (ADC) with a sampling rate of up to 64Msps (samples per second), as well as four 14-bit digital to analogue converters (DACs) with a maximum sampling rate of 128Msps. Two Digital up Converters (DUCs) to up convert the baseband signal to 128Msps before translating it to the selected output frequencies, a programmable USB2.0 controller for communication between the USRP and GNU radio, or software supporting the USRP and FPGA for implementing four Digital Down Converters (DDCs) as defined in the figure 3.3.

The digitised samples from the ADC are mixed down to the desired IF by multiplying them by sine and cosine functions, resulting in the I and Q paths. The frequency is generated by a numerically controlled oscillator (NCO) within the FPGA, which synthesised a discrete-time, discrete-amplitude wave form through the employed NCO frequency hopping at high speeds is possible. Following that, the sampling rate is decimated using an arbitrary decimation factor N. The sampling rate (fs) divided by N yields the output sample rate, which is sent to the host. In

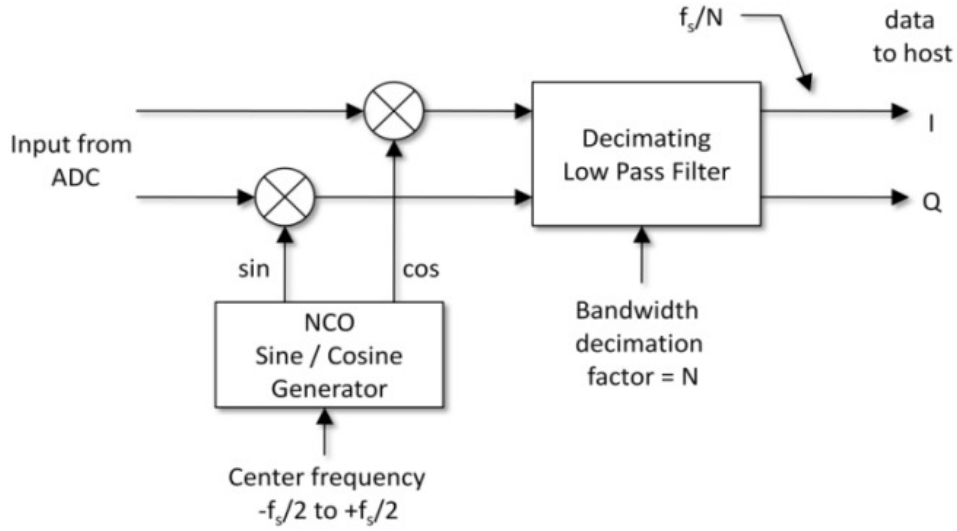

Figure 3.3: Digital to analogue converter Block diagram [148]

the transmit path, the same procedure is carried out by employing a Digital Up Converter (DUC) and a Digital Analog Converter (DAC).

3.2.3 The daughterboard

The daughterboard serves as the SDR's RF front end. Most daughterboards already filter, amplify, and tune the signal to a baseband frequency based on the board's IF bandwidth and local oscillator frequency. There are also basic RX/TX boards that lack frequency conversion and filtering. They only offer a direct RF link to the mother board. Table 3.1 shows the details for the majority of the available daughter boards.

3.2.4 Basic Principle of the Wireless Sensing System

Wireless sensing systems integrate radio-frequency, digital signal processing, and machine learning technologies to create a novel kind of ambient perception via wireless signals. This technique collects environmental data from modulated wireless signals dictated by the environmental state and employs digital signal processing to acquire current environmental states of interest in order to accomplish the goal of experiencing the environment.

The most common method of transmitting wireless signals is by the use of radio waves, which can be classified as direct wave, reflected wave, scattered wave, refracted wave, and diffraction wave. Wireless signals propagate to the receiver over a variety of paths in a typical indoor setting with human bodies and obstructions in the way. These paths include reflection, diffraction, and scattering. Each propagation path affects the received signals, which exhibit different physical characteristics at the receiver terminal, such as received signal strength and phase [149].

Wireless signals in free space suffer from propagation loss in a wireless communication system.

Table 3.1: USRP daughterboard list [148]

Identifier	Frequency range	Area of application
	Transceiver	
WBX	50-2200 MHz	Broadcast TV; GSM; WSN
SBX	400-4400 MHz	WiFi, WiMAX
RF X900	750-1050 MHz	GSM (Low Band)
RF X1200	1150-1450 MHz	GPS
RF X1800	1.5-2.1 GHz	DECT, GSM (High Band)
RF X2400	2.3-2.9 GHz	WLAN, Bluetooth
XCVR 2420	2.4 GHz -5 GHz	WLAN
	Transmitter/Receiver	
Basic TX, Basic RX	1-250 MHz	Misc. baseband operations
TCRX Receiver	50-860 MHz	VHF, DAB
DBRX2 Receiver	800-2300 MHz	Cellular and PCS.DECT

The distance between the transmitting and receiving antennas is represented by d in the free space propagation model, and the received signal power obtained by the transmission formula is as follows 3.1. [149].

$$P_{r1}(d) = \frac{P_t G_t G_r \lambda^2}{(4\pi d)^2} \tag{3.1}$$

where P_t denotes transmission power and $P_r(d)$ denotes received signal power as a function of distance. d, G_r denotes the gain of the reception antenna,G_t denotes the gain of the transmitter antenna, λ represents the wavelength in metres, and d denotes the distance between the transmitter and receiver in metres. Taking into account the reflection routes created by the ceiling and floor, the power received is denoted by 3.2.

$$P_{r2}(d) = \frac{P_t G_t G_r \lambda^2}{(4\pi)^2 (d^2 + 4h^2)} \tag{3.2}$$

where h is the distance from the reflection point on the ceiling or floor to the LOS path. When a person is present in an indoor environment, the human body generates a number of dispersed paths. Those scattered powers should be included in the final received power, which is denoted as follows 3.3. [149]:

$$P_{r3}(d) = \frac{P_t G_t G_r \lambda^2}{(4\pi)^2 (d^2 + 4h^2 + \Delta^2)} \tag{3.3}$$

where Δ is a brief representation of the path length caused by the human body. As a result, human body actions in radio-frequency coverage change the signal propagation path, causing the received signal power $P_r(d)$ to fluctuate significantly. In the absence of motion interfer-

ence, $P_r(d)$ remains essentially stable [150], and the total received power by the receiver is the sum of received power from multiple propagation paths. If the magnitudes of the LOS path, the roof reflection path, the ground reflection path, and the human scattering path are $E_{\text{los}}, E_{\text{ref1 1}}, E_{\text{ref 2}}, E_{sca}$, respectively, then the total received power $P_r(d)$ can be expressed as 3.4. [149].

$$P \propto \left| E_{los} + E_{ref1} + E_{ref2} + E_{sca} \right|^2 \tag{3.4}$$

While in a static environment the values of $E_{los}, E_{ref1}, E_{ref2}$, and E_{sca}, and E_{sca} are almost constant. While signal transmission is disrupted by the movements of the human body, E_{sca} changes for a short time. According to the principle of signal propagation, the phase of a signal is a linear function of the distance between two points on a propagation path. Information changes in the propagation channel induced by human actions, such as moving objects, will therefore be reflected in the phase of the received signal. Human actions, in addition, can alter the size and phase of the received signal [150]. The wireless sensing system is suitable because wireless signals carry sufficient physical information to accurately describe the condition of the environment in which they are received.

3.2.5 Channel State Information (CSI)

The key to the wireless sensing system is to figure out how to get information about the environment from wireless signals:
When a person move within range of wireless networks, the signal is effected and change. This is due to wireless signal scattering caused by changes in human posture. As a result, the wireless channel is made up of signals reflected and scattered by static objects in the environment, such as furniture, walls, as well as moving objects, such as humans. The Channel State Information (CSI) represents the effects of signal propagation in a channel, these additional reflections caused by various human activities can also be observed [149].
In the frequency domain, the transmitted and received signal vectors represented as **x** and **y** respectively 3.5.

$$\mathbf{y} = H\mathbf{x} + \mathbf{n} \tag{3.5}$$

where **y** represents the received signal vector, H is a complex channel matrix consisting of CSI values, **x** represents the transmitted signal vector and **n** is the channel noise vector. The CSI represents the estimation plural matrix of the wireless channel, that is, the estimation of the channel state matrix H and the CSI essentially describes the channel frequency response of each subcarrier [151]. In the MIMO system, the CSI matrix is the $N_T \times N_R \times N_c$ dimension matrix, and each element provides the amplitude and phase information of the corresponding subcarrier channel, as follows: 3.6.

$$H = \begin{bmatrix} H_{11} & H_{12} & \dots & H_{1N_R} \\ H_{21} & H_{22} & \dots & H_{2N_R} \\ \vdots & \vdots & \ddots & \vdots \\ H_{N_T1} & H_{N_T2} & \dots & H_{N_TN_R} \end{bmatrix} \tag{3.6}$$

where $H_{ij} = (h_1, h_2, \dots, h_{N_C})$ describe the communication channel state matrix between the transmitting antenna i and receiving antenna j. Where, h_k represent the channel state of the subcarrier, N_R denotes the number of receiving antennas, N_T represents the number of transmitting antennas and N_C is the number of OFDM subcarriers. In wireless OFDM systems each subcarrier has amplitude and phase and the received OFDM signal can be represented as follows: 3.7. [152]

$$h_k = |h_k| \, \mathrm{e}^{j \sin \theta} \tag{3.7}$$

where $|h_k|$ represents the amplitude, and θ represents the phase.

It is possible to create wireless sensing systems because the CSI signals can convey enough information about human actions in a specific area to enable wireless sensing systems to be implemented. In actuality, equal motion creates varying degrees of signal disturbance on different subcarriers as a result of frequency-selective fading, which is a property of the signal. In particular, due of constructive and destructive phase superposition, the same motion does not consistently raise or decrease the received signal power [152].
Therefore, in comparison to the Received Signal Strength Information (RSSI), the CSI is more refined. Current research findings indicate that the wireless signal is sufficiently sensitive to actions in the environment to allow for the detection of macro-scale body movements, such as walking, as well as the extraction and recognition of large-scale motions, such as gestures, breathing, and heartbeats.

3.2.6 Principle of Generating OFDM Signal and CSI Propagation

In this section, Figure 3.4 shows the block diagram of the MATLAB Simulink model, also we discussed the working principle of generating the channel sensing model using Universal Software Radio Peripheral Platform USRP.

3.2.7 Transmission of Multiple Frequency Carrier

Initially, the transmitter model based on OFDM transmitting multiple subcarriers was designed using MATLAB/Simulink to generate the transmitted data through the USRP, and transmitting it using an omni directional antenna. Random bits are sampled and obtained by the signal from the

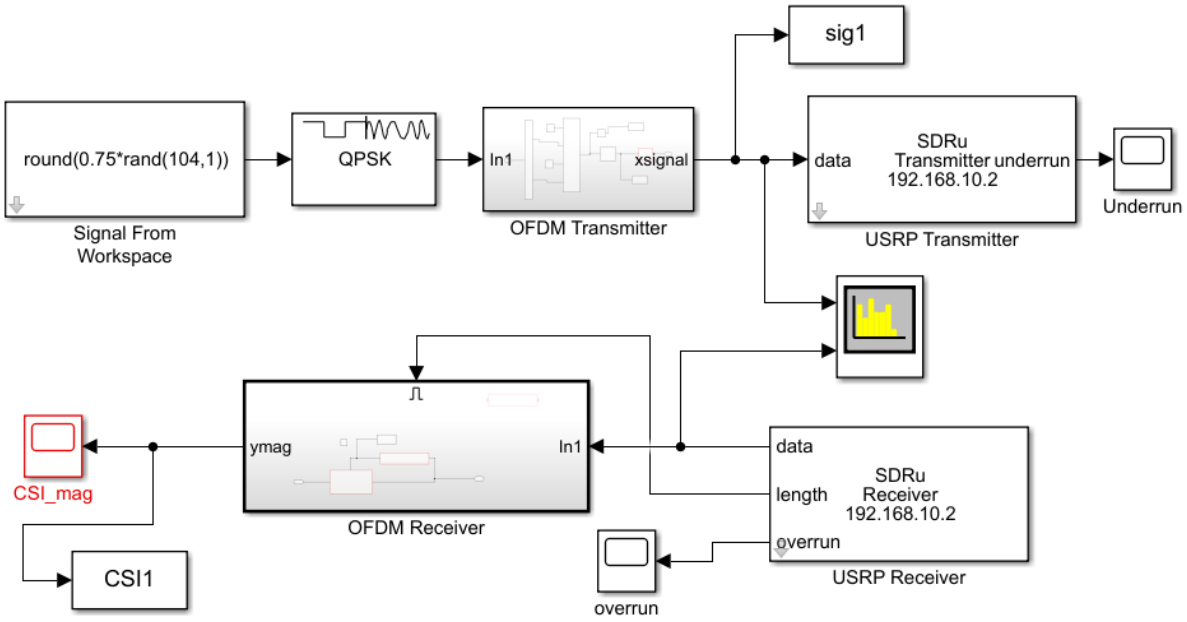

Figure 3.4: Simplified OFDM Simulink Model using QPSK.

workspace at successive sample time, the random bits have 0.75 probability. Next, the quadrature phase shift keying QPSK modulation scheme was used to convert the bits into symbols, every two bits is one symbol and mapped into phase shift format, two bits can also be used to define 4 possible values. Therefore, one QPSK symbol carries the equivalent of two bits of information. This block accepts either a column or a scalar vector as input. Depending on the input signal, bits or integers can be used. When you adjust the parameters of input signal and set it as 'Bit' the width of input signal must be an integer. Once the modulation is done, these symbols will link to a single subcarrier system. A de-mux block divides vector signals into scalars. Then, they are transferred from serial to parallel converter. After that, a DC subcarrier and a null subcarrier are added to generate output signal. Phase and magnitude of the signal are calculated in the frequency domain. Inverse Fast Fourier Transform IFFT is carried out because QPSK symbols are viewed as if they are in the frequency domain and hence IFF blocks convert them to the time domain and perform orthogonality between the subcarriers. Inter symbol interference ISI always occurs in the OFDM system. This can be removed by appending a cyclic prefix in the guard interval of an OFDM symbol, where a guard period is added at the start of each symbol to avoid multipath propagation of the reflected transmitted signal caused by physical objects, then the signal is upconverted through Digital-to-Analog Converter (DAC) which is used in USRP devices, and transmitted wirelessly through the USRP antenna. The designed system was deemed Additive White Gaussian Noise channel in a laboratory environment. Transmitting process can be seen in figure 3.5.

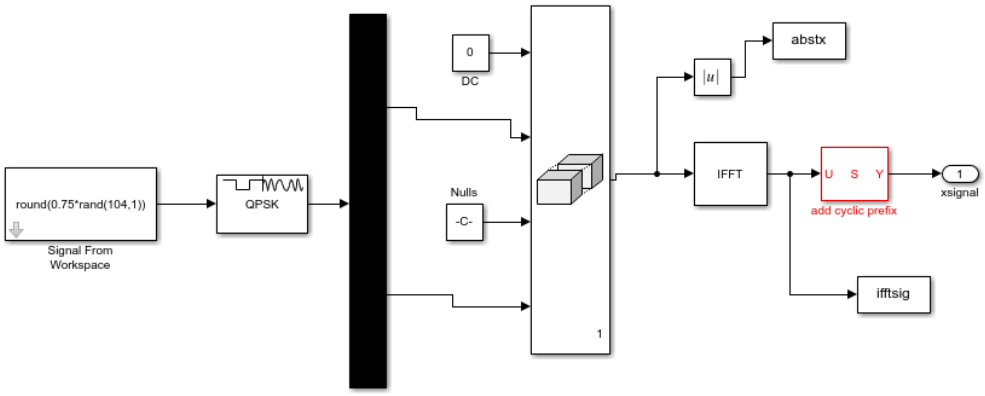

Figure 3.5: OFDM transmitting multiple subcarriers .

3.2.8 Reception of Multiple Frequency Carrier

On the receiver side, USRP X310 was fitted with an omni-directional antenna to receive the signal and then analyzed analogue to digital conversion (ADC) of the received signal. This was then converted down to the base band and passed through a low pass filter to remove the effect of high-frequency terms. Additionally, the carrier tone is removed at the mixer of the USRP. This operation is applied at the receiver of the USRP. Besides, OFDM bits are normally sorted into frames so that the received signal needs to be synchronized in time and frequency to obtain the start of the OFDM symbol. Also, the cyclic prefix is eliminated from each symbol and then Fast Fourier Transform FFT is performed to recover the signal from the time domain to the frequency domain. De-mux block is applied to split the vector output signals into scalars or smaller vectors then data is converted to parallel through serial to parallel converter to obtain the original signal. The DC and null subcarriers are disconnected. Then, the input signal is demodulated using QPSK modulation scheme. Finally, a vector of inputs with integer values is converted to a vector of bits. The receiver operation can be seen in figure 3.6.

3.2.9 Data Collection and Standardization

In this experiment, USRP was utilized to collect the CSI signal. Whereas, the CSI represents the properties of the channel in a wireless communication system. It is explaining how the signal transmits in free space comprises the amplitude and phase of each subcarrier in the OFDM channel. The CSI signal can be represented using the following equation 3.8 [153].

$$H(f_i) = H(f_i)\, e^{j\angle H(fi)} \tag{3.8}$$

Where, H(f_i) refers to the amplitude information of CSI, and $\angle$H(f_i) describes the phase of CSI. The system collects N of CSI packets and the measured OFDM subcarrier can be represented as

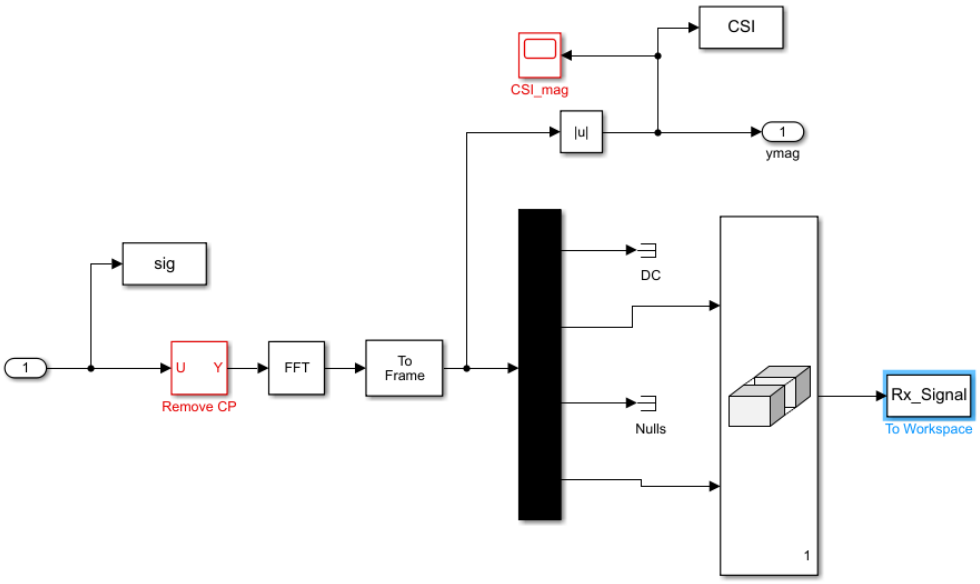

Figure 3.6: OFDM receiving multiple subcarriers .

follows in 3.9.

$$\mathrm{H} = (h_1, h_2, h_3, \ldots\ldots, h_N) \tag{3.9}$$

In our design, the amplitude and phase of channel frequency response (CFR) are measured by IFFT at the transmitter process and FFT at the receiver operation. Channel response measurement of our system is illustrated in equation 3.10. [24].

$$H(f) = \frac{Y(f)}{X(f)} \tag{3.10}$$

Where H(f) represent the channel response of the system, X(f) is the transmitted signal frequency response Y(f) refers to the received signal frequency response.

Figures 3.7 and 3.8 represent the system architecture and workflow of the proposed design. Therefore, our novel system consists of the following modules: CSI data collection. Processing the data on MATLAB and applying machine learning algorithm for data classification.

3.2.10 Additive White Gaussian Noise

Additive White Gaussian Noise Channel (AWGN) was considered for the simulated results. This wireless medium model has been widely exploited in identifying the most feasible modulation scheme. The main advantage of this wireless channel model is its least complexity in terms of test and deployment and represents the real man-made noise regarding multi-user interference [154].

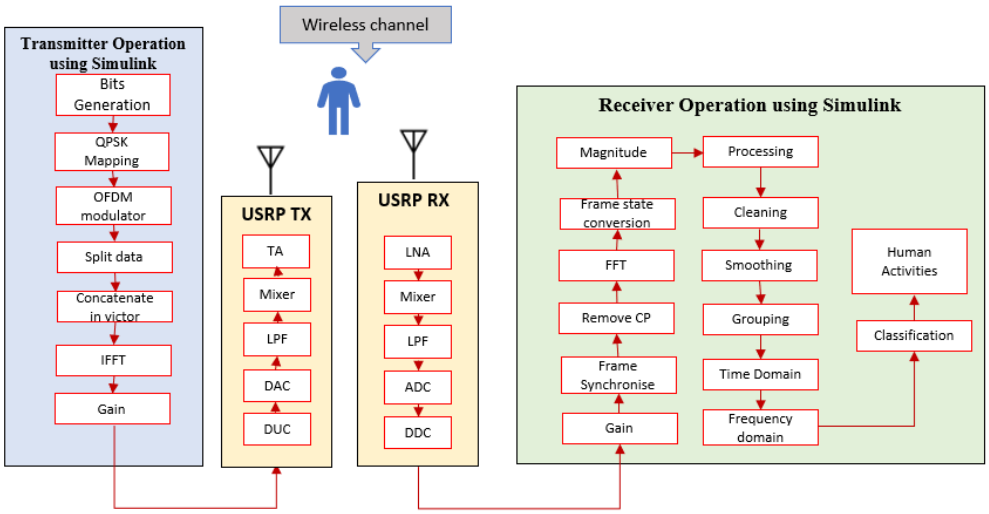

Figure 3.7: Simplified OFDM Simulink Model for Transceiver Operation.

3.2.11 Bit Error Rate of the USRP Model

Bit error rate (BER) gives the number of bits in error per unit time and the most important parameters to analyse the performance of any robust, efficient, and accurate wireless communication system. Figure 3.9 shows BER versus SNR (Eb/No in dB) performance analysis of various modulation techniques. The additive white Gaussian noise wireless channel was used to obtain simulated results. It is clear from the figure that BPSK has lower BER than QPSK and QAM. For instance, at SNR 10 BER for BPSK is 0 but for QPSK and 16 QAM is greater than 10^{-4}. In addition, at SNR 14 BER for QPSK is 0 whereas for 16 QAM is approximate 10^{-3}. Therefore, Quadrature Amplitude Modulation (16-QAM) has greater Bit Error Rate (BER) as compared with lower order Binary Phase Shfit Keying (BPSK). This is also proven for our proposed model as well.

3.2.12 Data extraction

At the receiver side, the OFDM signal utilized for fine grained wireless channel state information extraction then the amplitude frequency response for each activity will be observed constantly for 10 seconds. And each collected signal consists of several OFDM samples and subcarriers. Time and samples can be represented as the received number of samples in a unit time.
The obtained data from CSI is in the row form and needs processing to provide meaningful information using the three following steps.
I- Data cleaning is a process to remove and replace missing or bad data. It detects abrupt changes and local extrema, which is useful to find significant data trends.
II- The smoothing process remove noise using filtering and other signal processing techniques.
III- The grouping technique is performed to detect the correlation between the CSI values.

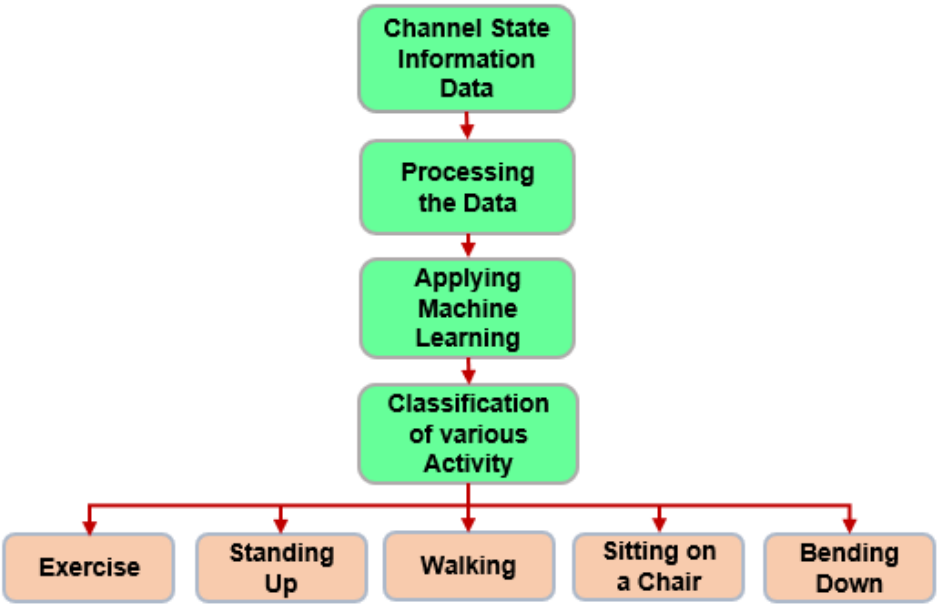

Figure 3.8: Flowchart of the System.

3.2.13 Feature extraction

CSI information represent fine-grained data and feature extraction is used for transferring the CSI data into meaningful information. The extraction of features from data is a critical step in the reduction of data size and the provision of useful information in the development of a classification model [155] [156]. The majority of researchers extracted features using statistical characteristics methodologies. Several features in the time domain are implemented. (1) The mean value provides information about the signal's steady component.(2) the normalized Standard deviation indicates the dispersion degree among the sampling points of the CSI signal.(3) the root mean square (RMS) is used to calculate the magnitude of CSI information.(4) peak to peak value is used to calculate the difference between the maximum and minimum amplitude values of the collected CSI signal. (5) the peak factor indicates if there is influence on the CSI information. (6) waveform factor is used to represent the ratio of the root mean square value to the average value. (7) FFT is used to excerpt the frequency component with peak to peak values of the signal. (8) spectrum probability and signal energy are used for the extraction of frequency domain analysis. (9) The variance gives information about the fluctuations from the mean. (10) The kurtosis is used to measure of the tailedness in the WCSI data. (11) The skewness is used to represent symmetry of the WCSI data. (12) the mean value gives information about the stable component of the signal. (13) Interquartile range is used to obtain statistical dispersion. Table 3.2 illustrate feature extraction equations.

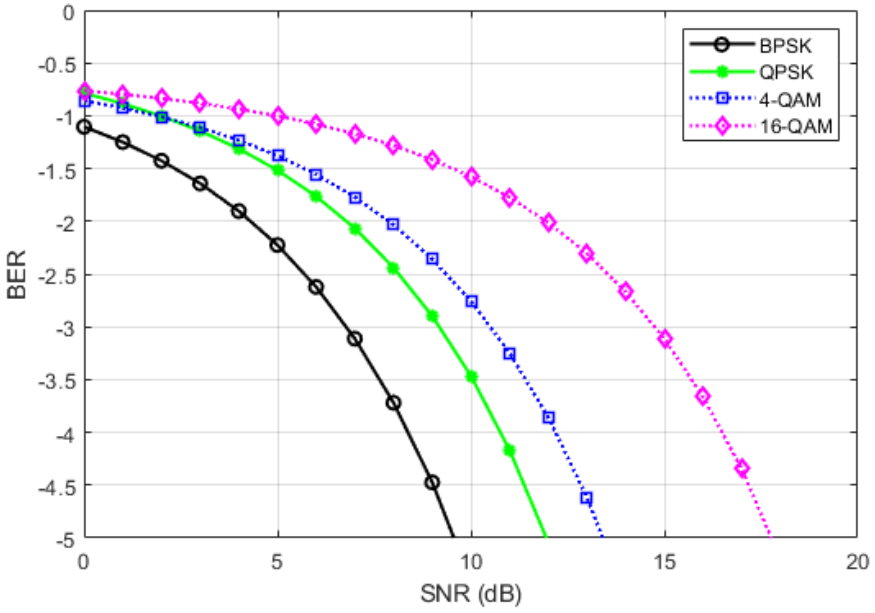

Figure 3.9: Simulated Bit error rate analysis of OFDM system.

3.3 Machine Learning for Activity Recognition

The dataset's performance was evaluated using different of machine learning algorithms implemented via the SciKit library. Scikit is a machine learning package that is widely used in the field of data science [157]. The SciKit library is used to process the samples after they have been converted to CSV format. Because the data is of varying length across the samples, the labels are added as the first column on the data frames. The data frame of each sample is then combined to form the full dataset; the varying lengths result in NAN values being included in the dataset [158]. To solve this problem, SciKit includes a function known as simple imputer. This function is used to replace all NAN values with a 0. As a result, the shorter samples of the dataset will have 0 values at the end of the row on the CSV file. This is not regarded as a problem because the differences in length are minor and the pattern of the RF signals remains visible. This is part of the variation between samples. The data set is then split into two variables, one for labels and one for the data itself. The four algorithms used to test this dataset are K nearest Neighbours (Knn), Discriminant Analysis (DA), Naive Bayes (NB) and Decision Tree (DT).

We have used MATLAB tool to process the USRP data and apply different machine learning algorithms. The parameters and configurations for each algorithms are as:

1-The K nearest Neighbours algorithm is known for its simplicity. The algorithm operates by comparing the testing and training data [159]. The training data features are assigned to a K sample, and the testing data is assigned to the K sample that most closely matches the new data [160]. SciKit uses the Euclidean KNN equation, which is shown in equation (3.11).

Table 3.2: Feature extraction equations for data classification

NO	Feature	Expression
1	Mean	$Y_m = \frac{1}{N}\sum_{i=1}^{N} x_k$
2	Normalized standard deviation	$Y_{SD} = \sqrt[2]{\frac{1}{N-1}\sum_{i=1}^{N}(x_k - Y_m)^2}$
3	The root mean square (RMS)	$Y_{RMS} = \sqrt[2]{\frac{1}{N}\sum_{i=1}^{N} x_k^2}$
4	Peak to peak value	$Y_{PPV} = Y_{\max} - Y_{\min}$
5	Peak factor	$Y_P = \frac{\max(x_k)}{Y_{RMS}} (i = 1,2,\ldots,N)$
6	Waveform factor	$Y_W = \frac{N * Y_{RMS}}{\sum_{k=1}^{N} \lvert x_i \rvert} (i = 1,2,\ldots,N)$
7	FFT	$Y_{FFT} = \sum_{n=-N}^{N} x(n) e^{-j2\pi \frac{k}{N} n}$
8	Signal energy	$Y_E = \sum_{n=-N}^{N} \lvert p(k) \rvert^2$
9	Spectrum probability	$Y_{SE} = \sum_{i=-N}^{N} p(k)\ln(p(k))$
10	Variance	$Y_V = \sum_{i=1}^{n} (x_k - Y_m)^2$
11	Kurtosis	$Y_K = \frac{\frac{1}{N}\sum_{k=1}^{N}(\lvert x_k \rvert - Y_{MV})^4}{Y_{RMS^4}}$
12	Skewness	$Y_S = \frac{\frac{1}{N}\sum_{i=1}^{N}(\lvert x_k \rvert - Y_{MV})^3}{Y_{RMS^3}}$
13	Interquartile range	$Y_{IQ} = Q_3 - Q_1$
14	Minimum frequency value	$Y_{f\,\min} = \mathrm{Min}(\Upsilon_{FFT})$
15	Maximum Frequency value	$Y_{f\max} = \mathrm{Max}(\Upsilon_{FFT})$
16	Spectral Probability	$\mathscr{Y}_{SP} = \frac{FFT(k)^2}{\sum_{i=-N}^{N} FFT(k)^2}$

$$\sqrt{\sum_{i=1}^{k} (x_i - y_i)^2} \tag{3.11}$$

$k =$ is the number of samples

$x =$ the data

$y =$ the label

2-The decision tree is a tree-like structure in which each internal node represents an attribute judgement, each branch reflects the output of that judgement, and each leaf node represents a classification result. The procedure of obtaining the classification result using the decision tree approach is a step-by-step process that begins at the top root node and progresses down to the leaf node. The decision tree's root node holds all of the data, whereas each non-leaf node indicates a segmentation of the samples [161]. Decision Tree (DT) is ML algorithm that progressively divide data sets into smaller data groups based on a descriptive feature, until they reach sets that are small enough to be described by some label. They require that you have data that is labelled (tagged with one or more labels, like the plant name in pictures of plants), so they try to label new data based on that knowledge. DTs are being used in the healthcare industry to improve the screening of positive cases in the early detection of cognitive impairment, and also

to identify the main risk factors of developing some type of dementia in the future. The decision tree algorithm performs classification based using two predictors, $x1$ and $x2$ to classify and do prediction, start at the top node, represented by a triangle $\wedge$. The first decision is whether $x1$ less than the value of 0.5. If it is smaller than the specific value, it follows the branch on left side, and identifies the particular tree that classifies the data as type 0. When the value of $x1$ increase from 0.5, it then follows the right branch of the tree to the lower-right triangle node.

3-Discriminant analysis (DA) is a multivariate technique used to separate two or more groups of observations (individuals) based on variables measured on k each experimental unit (sample) and find the contribution of each variable in separating the groups. DA works by finding one or more linear combinations of the k selected variables [162]. The discriminant analysis algorithm used mean for unweighted data as:

$$k = \frac{\sum_{n=1}^{N} M_{nk} x_n}{\sum_{n=1}^{N} M_{nk} w_n} \tag{3.12}$$

the value for k was selected as 1 in this case.

4-The Naive Bayes classifier is based on the Bayes theorem, which is illustrated by the following equation:

$$P(A \mid B) = \frac{P(B \mid A) \cdot P(A)}{P(B)} \tag{3.13}$$

where P is the probability and $P(A \mid B)$ is the conditional probability. In the case of a Naive Bayes classifier, the probability of each occurrence is calculated based on equation 3.13. The candidate is the event with the highest probability. The Naive Bayes classifier is based on two fundamental assumptions: (1) The features are distinct from one another. (2) Each feature is given equal weight. In general, a Naive Bayes classifier goes through two stages: offline training and online testing [162]. A Naive Bayes classifier estimated each class for all activity by assuming equiprobable classes by computing an approximation for the class probability from the training set.

For each algorithm, two separate experiments are conducted. The first experiment used a 10 fold cross-validation procedure. Machine learning models can be tested using the 10 fold cross-validation, where the data is split into training and testing sets.The number 10 denotes the number of groups. Each group serves as test data for a turn, while the remaining groups serve as training data. This ensures that there is variance in the test data. The final results are obtained by averaging the results of the 10 runs. The second experiment employs the train test split method, with the dataset divided 70/30. 70% of the dataset was used to train the dataset, and 30% of the dataset was used for testing.

3.4 Experimental Setup and System Parameters

In this section, we evaluate the performance of the proposed system as follows: (I) Data collection using two USRP models. (II) Data analysis using state-of-the-art machine learning techniques. The transmitter and receiver involved two Universal Software Radio Peripheral equipment USRPs X310/X300 from a national instrument (NI), each equipped with extended-bandwidth daughter board slots covering DC– 6 GHz with up to 120 MHz of baseband bandwidth. The USRP X300 worked as a transmitter and USRP X310 performed as a receiver. The system had two PCs to run the initial trial. Both USRPs were connected to the PCs through a 1G Ethernet cable. Furthermore, the experimental hardware comprised of two omni directional antennas, VERT2450 that were driven by the USRPs. The simulated transceiver model was designed using MATLAB/Simulink program linked to the software-defined radio.
The experimental campaign was undertaken in a lab environment, the distance between the USRPs was kept as 4m in line of sight (LOS), to achieve optimum performance. Ethical approvals have been acquired through University of Glasgow Ethics Review committee. Volunteer was asked to perform five different human activities in the area of interest. The subjects going under various activities were: (a) Walking (b) Sitting on a chair (c) Standing from a chair, (d) Doing exercise, and (e) bending down to pick up an object from the ground. Each volunteer was asked to repeat the aforementioned activities 10 times. The test was performed in a 7 by 8 meter room having furniture such as tables, chairs, etc. Machine learning algorithms such as K-Nearest Neighbour (KNN), Discriminant Analysis (DA), Naive Bayes (NB) and Decision Tree (DT) were applied to process and classify the collected data. The experimental setup is shown in figure 3.10.

Figure 3.10: Schematic depiction of experimental setup along with pictorial representation of five different activities classified and actual snapshot of lab environment

We have performed the experiment in laboratory settings using healthy volunteers and asked them to perform different activities under test. We have repeated the experimental campaign multiple times and each time almost identical results were obtained. Due to ethical approval issues outside university environment i.e. on actual patients and elderly people, we have only undertaken the experimental campaign in a controlled setting.

3.5 System Parameters Selection

We performed our experiments with varying parameters to evaluate the performance of the system. Tables 3.4-3.5, lists the parameters which were used in the designed software. The USRPs used in the study have a frequency range from 1 GHz to 10 GHz. Center frequency for both USRPs was set to 5.32 GHz and the operational frequency of omni directional antenna was the same as well, with 3 dBi gain. The gain of USRP chosen to be 70 for transmitter and 50 for the receiver. The parameters values were used to test the software are summarized in Table 3.3. For selecting hardware parameters, firstly we test QPSK Simulink examples in MATLAB to

Table 3.3: Software Configuration Parameters Selection

Parameters	Values
Input data (Signal)	round(0.75*rand(104,1))
Sample time	132/104*(1/132e4)
Modulation type	QPSK, BPSK, 4QAM, 16QAM, 64QAM
Bit per symbol M	2 bits
OFDM Subcarrier	64 subcarriers
Pilot subcarrier	4
Null subcarrier	12
Cycle prefix	NFFT-data subcarrier
Samples per frame	Used subcarrier log2 (M)

calibrate and choose the correct parameters of our USRP platform. Then applied the designed system using Simulink. The parameters of the hardware configuration for both transmitter and receiver USRPs shown in the following table 3.4.

Table 3.4: Hardware Configuration Parameters Selection

Platform	USRP X300/X310
TX IP address	192.168.11.1
RX IP address	192.168.10.1
Channel mapping	1 TX, 2 RX
Centre frequency	5.32 GHz
Local oscillator offset	Dialog
PPS source	Internal
Clock source	Internal
Master clock rate	120 Mhz
Transport data type	Int16
Gain (dB)	TX 70, RX 50
Sample time	1/80e4
Interpolation factor	500
Decimation factor	500

3.6 Results and Discussion

3.6.1 Large Scale body Movement for one subject

This section addresses the findings of a comprehensive experimental campaign conducted using the proposed SDR-based human activity recognition system. Five different activities were considered in this experiment, including walking, sitting on the chair, standing up from a chair, bending down and exercising. When the data was recorded, multiple factors were taken into account. Factors of the environment such as physical objects: chairs, tables, computers and people could affect the wireless received signal or leads to attenuation of the collected signal during testing the activity of the human. To address this issue, firstly, we tested our hardware devices with a simple MATLAB simulink QPSK example on the MATLAB simulink software such as QPSK transmitter and receiver with USRP to standardize and configure hardware parameters of the system. After ensuring that the system can receive an RF signal successfully, we then applied the actual simulink design of our system.

The results are divided into two cases: with and without human activity. In the first case: Figure 3.11 shows the result when no activity performed between the transmitter and receiver, as can be seen from the figure that the amplitude of the received signal remains constant ensuring no changes occurred between the transmitter and receiver antenna. The procedure of this case was repeated several times with no amplitude variations observed. The time duration of this case was 10 seconds and the number of transmitted packets in this trial was 10000. We received only 8063 packets out of 10000. Ten repetitions were performed and the same number of packets were obtained. Also, the packet index and colours represents the number of subcarriers of the OFDM signal. whereas, each color is one subcarrier. The amplitude and time duration of this

signal can be seen clearly in Figure 3.11.

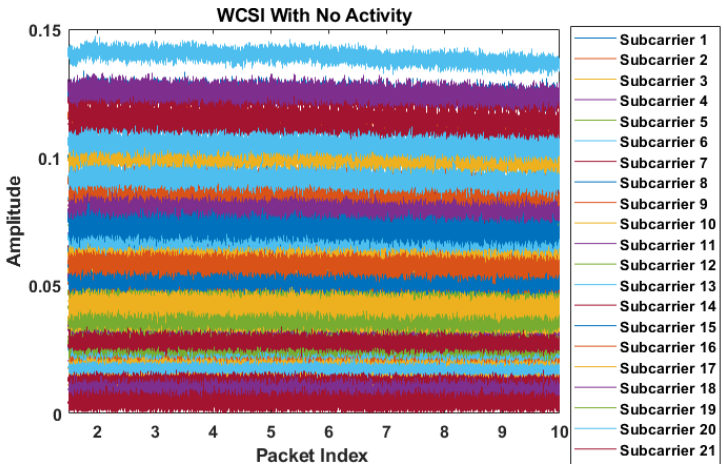

Figure 3.11: Wireless channel state information without any activity.

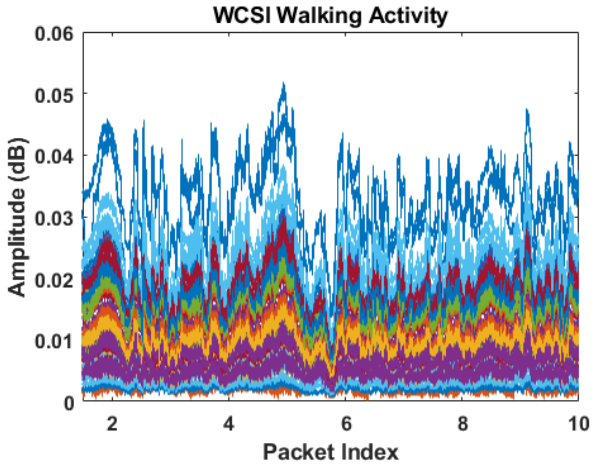

Figure 3.12: Wireless channel state information during walking.

In case 2, one volunteer performed the five activities. Figure 3.12 illustrates the changes in amplitude when a person is walking. The motion of hands and legs affect the amplitude of the received signal. The variation in amplitude of the collected signal was prominent compared to the original signal as depicted in Figure 3.11. The time duration, in this case, was 10 seconds. we received 8063 packets out of 10000 transmitted packets for each performed activity. Figure 3.13 demonstrates the results for the case of sitting on the chair. The chair was located between the USRP transmitter and receiver.

In addition, the distance among the USRPs and chair was kept as 2 meters. After transmitting the signal, the person commenced sitting on the chair. Therefore, we can observe only small changes in the amplitude of the received signal and drop down according to the sitting actions based on the type of human motion. We noticed the amplitude only changes during the action after that, it remains constant.The time duration in this activity is 10 seconds and contained the similar number of transmitted and received packets. Figure 3.14 presents results for the standing

up from chair activity. This action was opposite to the previous activity, when the person starts to stand up from the chair, the amplitude of the received signal changes based on the movement and starts going up according to human action.The time duration of this activity was 10 seconds as well.

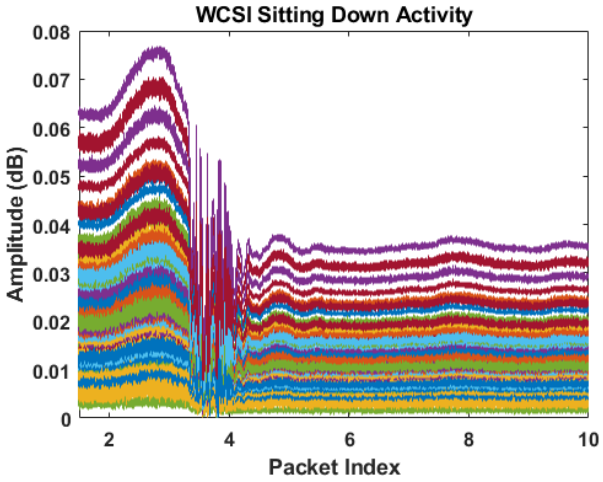

Figure 3.13: Wireless channel state information while sitting on a chair.

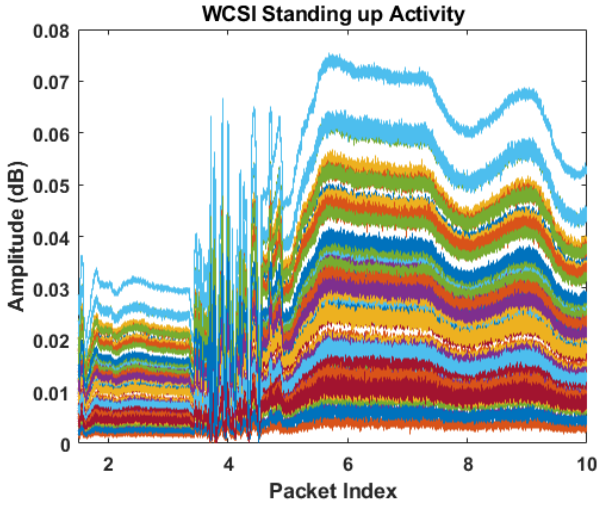

Figure 3.14: Wireless channel state information during standing up from a chair.

Besides, the transmitted and received packets were equivalent to the number of packets in the previous activities which, was 10000 transmitted packets and 8063 received packets. Figure 3.15 helps in explaining walking and bending down activity. From this figure, we can observe amplitude variation in the beginning and then reduced variation based on walking and bending down movement. The time duration of this activity was the same as previous sitting and standing activities including the similar number of transmitted and received packets. Figure 3.16 illustrates the variation in amplitude depending on the exercise activity, where different exercises have implemented between USRPs. In addition, the time duration and number of packets sent

and received were the same as previously observed.

We can see in the Figures 3.12-3.16 that the amplitude changes according to human behaviour. Figures 3.12-3.16 shows the performed activity and amplitude changes for each action. All these activities have repeated 10 times and every time we noticed distinguished amplitude variation. This change of amplitude represents the human information behaviour and confirms that different human actions implemented between the transmitter and receiver system. Furthermore, machine learning algorithms were applied to process and classify the five activities and evaluate the overall performance of the system.

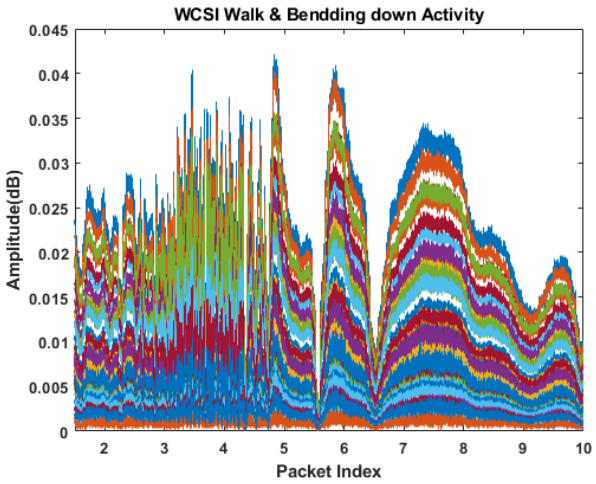

Figure 3.15: Wireless channel state information during bending down.

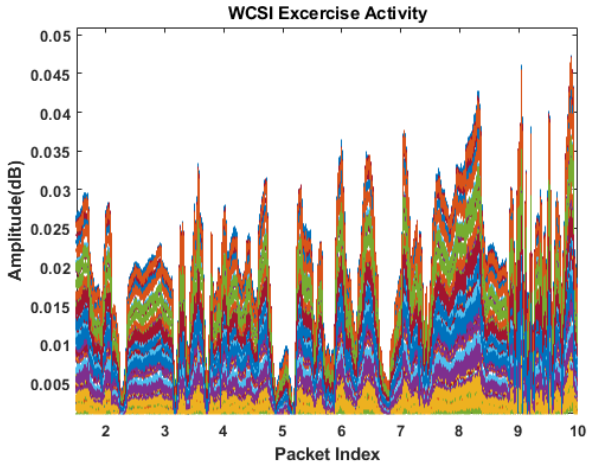

Figure 3.16: Wireless channel state information during exercise activity.

3.6.2 Machine Learning Classification for Large Scale body Movement

This section provided details on the discussion of machine learning algorithms used to classify various human activities and present the performance of proposed system based on percentage

accuracy. The four algorithms used are K-Nearest Neighbor (KNN), Discriminant Analysis (DA), Naive Bayes (NB) and Decision Tree (DT).

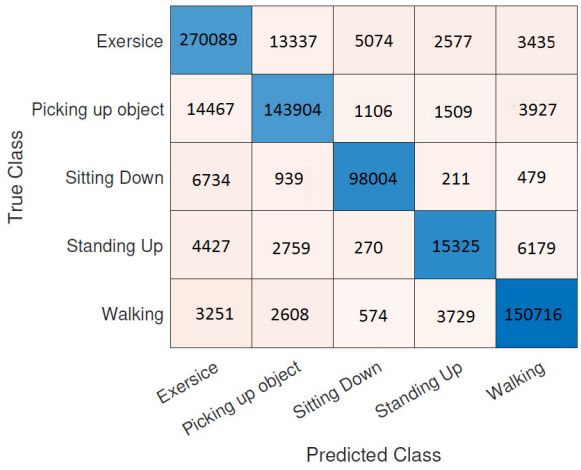

Figure 3.17: Confusion matrix for KNN classifier

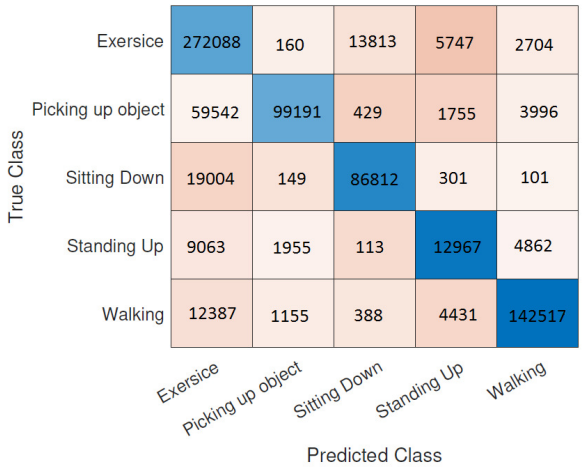

Figure 3.18: Confusion matrix for DT classifier

The KNN algorithm was used to classify 5 activities that provided the optimum results with ten-fold cross-validation leaving one subject out for validation. A total of 755630 samples were processed for all activities. For the activity exercise, 270089 samples were classified correctly, while a total of 24423 exercise samples were misclassified as other activities. The breakdown of the 24423 misclassified samples is 13337 samples classified as picking up an object, 5074 samples classified as sitting down, 2577 samples classified as standing up and 3435 samples classified as walking. These numbers can be seen in the above confusion matrix Figure 3.19. It also reveals how other activities have been considered for classification, with a blue representing the correct classification and the other boxes are identified as spurious observations and marked as incorrectly classified. It can be seen from Figure 3.19 that most of the samples have been correctly classified. The overall percentage accuracy using KNN classifier was obtained

as 89.73%. Compared to the KNN classifier, the efficiency of the DT algorithm classifier was found to be unsatisfactory, providing a total accuracy of 81.20%. For the first activity, there were 272088 classified correctly. A large chunk of the obtained data, 160 samples were identified as picking up object activity (false negative) and so on with most false negatives being classified as standing up 13813 as shown in the above confusion matrix in figure 3.20. Similarly, most of the sample was successfully classified in the KNN classifier, providing an accuracy of approximately 81.20%. The other algorithms tested were discriminant analysis and naïve bayes which produced poor results compared to KNN and decision tree algorithms with an accuracy of 49.21% for discriminant analysis and 23.28% for naïve bayes. the confusion matrix for DA and NB is shown in Figures 3.19-3.20. Table 3.5 shows the accuracy comparison for different classifiers.

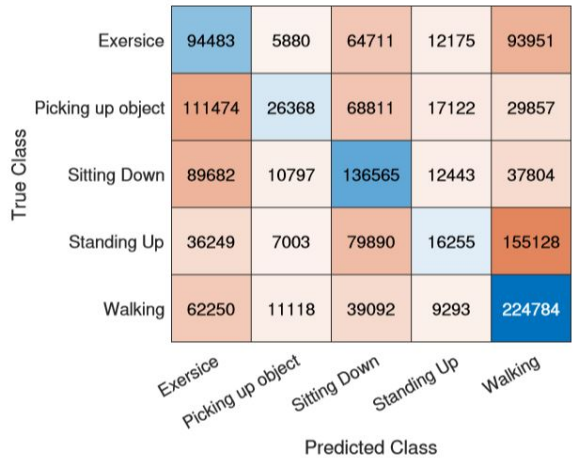

Figure 3.19: Confusion matrix for DA classifier

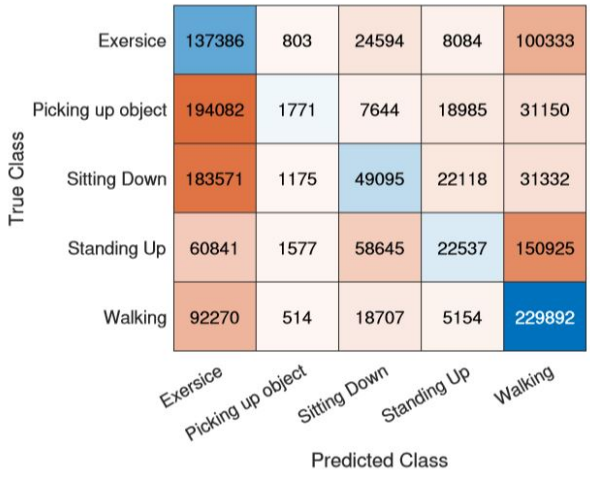

Figure 3.20: Confusion matrix for NB classifier

Table 3.5: Percentage accuracies of each classifier

Classifier models	Classification Accuracy %
Nearest Neighbor (KNN)	89.73
Decision Tree (DT)	81.20
Discriminant Analysis (DA)	49.21
Naive Bayes (NB)	23.28

3.7 Summary

In this chapter, we introduce the basic information and block diagrams of Universal Software Defined Radio Peripheral USRP. We then presented some fundamental properties of wireless channels that are critical in wireless sensing. Simplified OFDM Simulink Model using QPSK and generating the CSI have been explained as well, data collection and data extraction have presented includes result and discussion.

In our work, we proposed a flexible and scalable non-invasive wireless sensing system to detect activities of daily living using software defined radios. The core idea involved the analysis of channel state information using two USRPs platforms. The variances of amplitude information induced a unique imprint for each human activity including walking back and forth, sitting on a chair, standing up from a chair and doing exercise. All these activities were performed in a lab environment in the presence of furniture and involved volunteers. Compared with the CSI systems that extracted from off-the-shelf wireless devices, our system based on the USRP platform allows to modify the number of frequency carriers, change the transmitted and received power and the operating frequency swing can be altered as well. Different machine learning algorithms were applied on the CSI data collected where percentage accuracy was used as performance metric. The KNN classifier presented best classification accuracy of more than 89% among all four algorithms used.

Chapter 4

Vital Signs Monitoring of a Single Subject

4.1 Introduction

Non-contact continuous monitoring of biomarkers comprising breathing detection and heart rate are essential vital signs to evaluate the general physical health of a patient. Monitoring breathing rates assists in the diagnosis and possible prevention of a variety of health problems. It is a significant predictor of a variety of catastrophic complications, including cardiac arrests, strokes, and chronic obstructive pulmonary disease. [163] [164]. Traditional breathing detection method requires patients to carry devices such as pulse oximeter [165] and capnometer [166]. These specialised devices are frequently inconvenient for patients, restrict their movement, and, most significantly, are incompatible with remote patient monitoring.

The work of [167] proposes a camera-based monitoring method for extracting raw breathing signals from video streams. Moreover, camera based on a mobile phone has been utilised to determine a user's breathing rate by studying the user's chest motion [168]. However, this technique requires a specific amount of light to function properly, it cannot be used to monitor a sleeping infant's respiratory rate in a dark room. Additionally, in other instances, the use of the mobile phone camera would quickly drain the battery and raise privacy concerns.

Due to skin sensitivity and other issues that prevent sensors from being attached to the body, Radio frequency (RF) based systems were proposed and offer non-invasive breathing rate monitoring through analysis of RF signal reflected off the human body, including doppler radar [169] [170], and ultra-wide-band (UWB) radars [171] [172]. These systems can detect respiration rates with great accuracy due to the utilisation of a specific frequency band. However, their primary disadvantages are the limited range of high frequency devices available and their expensive cost.

Wireless sensing systems based on WiFi devices has been used to monitor human breathing. In [133] the authors extract received signal strength (RSS) values (for example, utilising 16 frequency channels in IEEE 802.15.4) from wireless sensor nodes and utilise these measurements to determine the breathing rate, their approaches necessitate the installation of additional wire-

less network infrastructure as well as the placement of sensor nodes in high-density areas. RSS is also unable to catch the heart rate.
Channel state information have also been used to determine a breathing rate. For instance, the authors of [173] demonstrated respiration detection using CSI derived from WiFi, their work achieves high accuracy of around 94%. However, The primary disadvantage of employing Wi-Fi routers is their limited scalability, adaptability, and lack of subcarrier reporting. The network interface card (NIC) used by CSI systems exploits only 30 subcarriers, not all 56 frequency channels sent by the Wi-Fi router, accounting for 42% of frequency carrier loss. Additionally, NIC-based systems lack the ability to increase or reduce the number of frequency subcarriers, the power level of the transmitter signal, remove noise, or adjust the operating frequency. [35].
In this chapter, we offer a flexible and scalable wireless sensing system for detecting human breathing that is powered by USRP and a machine learning algorithm. Our system, which was developed using a MATLAB Simulink model, utilises 64 OFDM subcarriers to receive all broadcast subcarriers and detect a single person's respiration rate.The software defined radio enables us to alter different factors in real time, such as the number of frequency carriers, the power level, and the radiation pattern. Additionally, systems based on SDR are adaptable, scalable, and capable of reliably and correctly delivering desired results. We presented a comparison of our breathing rate detection with wearable sensor (ground truth) results for single human subject.

Contributions and study motivation for this chapter Numerous studies have demonstrated CSI based on Wi-Fi signal to recognise human movement exploiting low cost small wireless devices such as Wi-Fi router, network interface card. The main limitation of using these devices is the scalability, flexibility, and under-reporting all group of subcarriers. The Wi-Fi sensing for human activity recognition only report limited number of subcarriers. The software defined radio allows us to change various parameters such as number of frequency carriers, power level and radiation pattern in real-time. In addition, systems based on SDR are also flexible, scalable and delivers desired result reliably and accurately.

4.2 Method

The material and methods used to develop a non-contact sensing platform for connected health using SDR technology and AI include the design of the SDR platform, data collection approach, data preprocessing techniques, feature extraction and selection, and classification algorithms.The schematic diagram of the transceiver operation can be shown in figures 4.1.

4.2.1 Transmitter Software Design

The transmitter operation was simulated with the help of a MATLAB Simulink programme, which generated the OFDM signal for the transmitter and reception processes over numerous

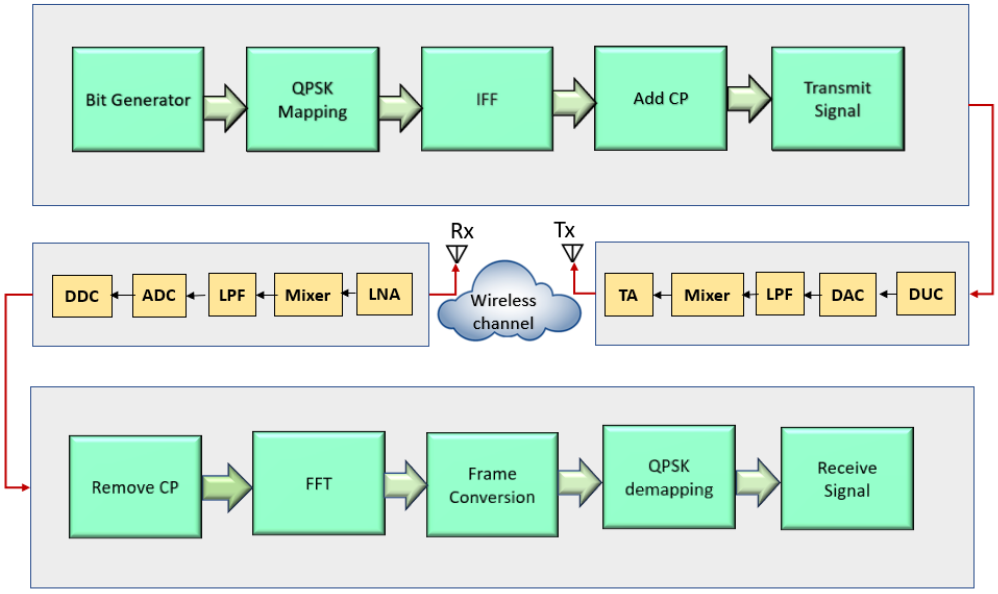

Figure 4.1: SDR-based human activity detection platform schematic diagram.

subcarriers using a universal software radio peripheral (USRP). Random data bits were generated from work space with probability of 0.75. The quaternary phase-shift keying (QPSK) technique is used to modulate this input signal, as shown in equation (4.1):

$$T(k) = x_I(n) + jx_Q(n) \tag{4.1}$$

where $x_1(n)$ and $jx_Q(n)$ are in-phase and quadrature components of the signal. Then, using a QPSK modulation technique, these bits were converted to symbols, with each pair of bits representing one symbol. The nulls and DC subcarriers are combined to generate a continuous output signal by concatenating signals of the same data type.The symbols were then attached to a single subcarrier and put into the converter, which converted them from serial to parallel using the Inverse Fast Fourier Transform (IFFT) operation and transferred them from the frequency domain to the time domain involves orthogonality between the subcarriers.The complex data signal is transformed into the time domain by using Equation (4.2):

$$t(n) = \frac{1}{N}\sum_{k=0}^{N-1} T(k)e^{-j2\pi\frac{k}{N}n} \tag{4.2}$$

Where, $T(k)$ contains the QPSK modulated complex data and $n = 0,1,2\ldots\ldots,N-1$, After that a cyclic prefix are then given into the system between each symbol to mitigate the effect of co-channel interference of the collected signal at the receiver side.The whole OFDM frame, including the CP, can be mathematically expressed as shown in Equation (4.3).

$$s(n) = t_{N+L}(n) \tag{4.3}$$

USRP hardware configuration is also a function of the transmitter PC. This function is used to control RF processing, such as carrier frequency operation, master clock operation, interpolation, and system gain.Then the received signal is up-converted through Digital-to-Analog converter (DAC) using USRP platform.

4.2.2 Wireless Channel

Modeling of the wireless channel is carried out for both the simulated and real-time wireless channels, respectively. It is necessary to evaluate the wireless channel characteristics and their effects on CFR by simulating ideal, AWGN, fading, and time-frequency dispersive channels.The wireless channel contains a significant information on the channel's noise, Doppler shift, multipath fading, reflection, and diffraction properties.The information obtained from human body reflections may be used to track human health.
In our experiment, additive white Gaussian noise channel (AWGN) was considered for simulated result. This wireless medium model has been widely exploited in identifying the most feasible modulation scheme. The main advantages of this wireless channel model is it's least complexity in terms of test and deployment and represents the real man-made noise with regards to other multi-user interference [154].

4.2.3 Receiver Software Design

At the receiver end, the OFDM signal was collected by the received antenna that equipped on the second USRPX310, then the USRP convert the OFDM signal from analogue to digital and next down converting it to the original base band signal, Afterwards a low-pass filter was used in the USRP to generate the I/Q base-band wave form and remove the effect of high frequencies. It then transforms the signal to a digital signal using an ADC and decimates it for software processing in the receiver's personal computer using a digital down converter (DDC). Additionally, because OFDM bits are typically grouped into frames, the received signal must be synchronised in time and frequency to acquire the start of the OFDM symbol and then converted to the frequency domain using the Fast Fourier Transform (FFT) technique. The transmitted OFDM frame, $s(n)$, is precisely received by the receiver without any channel impairment in the ideal channel. The received signal $r_I(n)$ is shown in equation (4.4):

$$r_I(n) = s(n) \tag{4.4}$$

The channel frequency response CFR $C_I(k)$ is calculated by taking the Fourier Transform of the received signal $r_I(n)$ as presented in equation (4.5) [174]:

$$C_I(k) = \sum_{n=0}^{N-1} r_I(n) e^{-j2\pi \frac{k_n n}{N}} \tag{4.5}$$

In the Additive white Gaussian noise channel (AWGN), additive noise $N(n)$ is added at the simulated channel to the transmitted OFDM frame $s(n)$. The received signal $r_A(n)$ can be shown as following in equation (4.6):

$$r_A(n) = s(n) + N(n) \tag{4.6}$$

The channel frequency response CFR for the Additive white Gaussian noise channel (AWGN) $C_A(k)$ is measured by taking Fourier Transform of the received signal $r_A(n)$ as illustrated in equation (4.7).

$$C_A(k) = \sum_{u=0}^{N-1} r_A(n) e^{-\vec{\pi}\,\underline{\delta^n n}} \tag{4.7}$$

the Doppler shift Δf In the fading channel is added at the simulated channel to the transmitted OFDM frame $s(n)$. The received signal $r_F(n)$ is illustrated in equation (4.8).

$$r_F(n) = s(n) e^{j2\pi(f+\Delta f)/N} \tag{4.8}$$

The CFR for the fading channel $C_F(k)$ in the presence of the Doppler shift is directly measured by taking the Fourier Transform of $r_F(n)$ as shown in Equation (4.9).

$$C_F(k) = \sum_{n=0}^{N-1} r_F(n) e^{-j2\pi k} n \tag{4.9}$$

The received signal, r(n), contains WCSI information which comprises channel noise, reflection from human body motion, carrier frequency and time offset, and so on.

After removing the CP, each OFDM frame will contain N points. After that, the FFT is employed to convert the OFDM samples from the time domain to the frequency domain. Equation (4.10) contains the expression for converting time domain data to frequency domain data in order to calculate CFR.

$$R(k) = \sum_{n=0}^{N-1} r_N(n) e^{-j2\pi \frac{k}{N} n} \tag{4.10}$$

Due to the fact that R(k) is the complex CFR value, it may be translated to the magnitude and phase responses specified in Equations (4.11) and (4.12).

$$|R(k)| = \sqrt{R_{Rc^2} + R^2_{Im^2}} \tag{4.11}$$

The R_{Re} is real part and the R_{Im} is imaginary part of the channel frequency response CFR.

$$\angle R(k) = -\tan^{-1}\left(\frac{R_{Im}}{R_{Re}}\right) \tag{4.12}$$

The magnitude and phase response of the multiple OFDM frames can be seen in equations

(4.13) (4.14) .

$$|R(k)|_{k,F} = \begin{bmatrix} \left|R\left(e^{j\omega}\right)\right|_{1,1} & \left|R\left(e^{j\omega}\right)\right|_{1,2} & \cdots & \left|R\left(e^{j\omega}\right)\right|_{1,F} \\ \left|R\left(e^{j\omega}\right)\right|_{2,1} & \left|R\left(e^{j\omega}\right)\right|_{2,2} & \cdots & \left|R\left(e^{j\omega}\right)\right|_{2,F} \\ \vdots & \vdots & \cdots & \vdots \\ \left|R\left(e^{j\omega}\right)\right|_{k,1} & \left|R\left(e^{j\omega}\right)\right|_{K,2} & \cdots & \left|R\left(e^{j\omega}\right)\right|_{k,F} \end{bmatrix} \tag{4.13}$$

k is used for the total number of subcarriers and F is used for the total number of OFDM frames received.

$$\angle R\left(e^{j\omega}\right)_{k.F} = \begin{bmatrix} \angle R\left(e^{j\omega}\right)_{11} & \angle R\left(e^{j\omega}\right)_{1,2} & \cdots & \angle R\left(e^{j\omega}\right)_{1,F} \\ \angle R\left(e^{j\omega}\right)_{21} & \angle R\left(e^{j\omega}\right)_{2,2} & \cdots & \angle R\left(e^{j\omega}\right)_{2,F} \\ \vdots & \vdots & \cdots & \vdots \\ \angle R\left(e^{j\omega}\right)_{k,1} & \angle R\left(e^{j\omega}\right)_{k,2} & \cdots & \angle R\left(e^{j\omega}\right)_{k,F} \end{bmatrix} \tag{4.14}$$

The magnitude and phase of the CFR are employed in Equations (4.13) and (4.14) for data preprocessing and identification.

4.2.4 Signal Model

The proposed system used CSI signal for the transmitter and receiver operation. The CSI represent the channel frequency response (CFR) for each OFDM subcarrier includes amplitude information and phase information. Figure 4.2 represent flow chart of data collection and processing using USRPs. This system has been developed and implemented only to extract the wireless channel state information amplitude response for human activities.
The CSI phase information is inapplicable due to presence of random noise. Therefore, it was not considered.. Equation (4.15) presented the received CSI signal.

$$H\left(f_i\right) = H\left(f_i\right) e^{j\angle H(f_i)} \tag{4.15}$$

In this expression, H(f_i) describes the information of amplitude and $\angle$ H(f_i) explains the phase information for CSI signal. The measured OFDM subcarriers contain the values of CSI packets and it can be shown in equation (4.16).

$$\mathrm{H} = (h_1, h_2, h_3, \ldots\ldots, h_N) \tag{4.16}$$

In this system, IFFT and FFT blocks measure the response of amplitude and phase. By performing IFFT at transmitter side and FFT at receiver side. The channel response can be expressed as following (4.17).

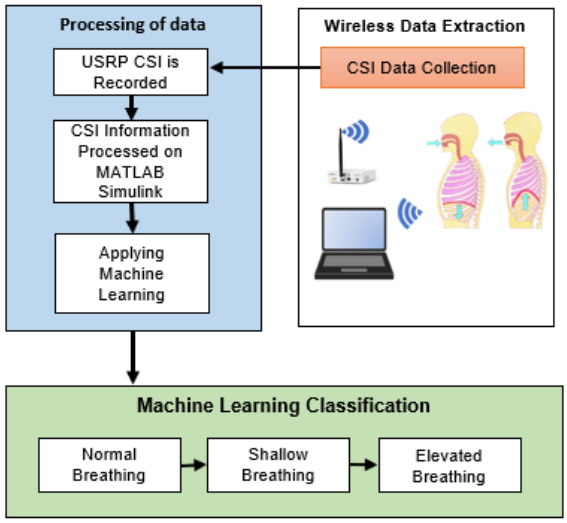

Figure 4.2: Flowchart of the proposed System for collecting channel state information using USRPs.

$$H(f) = \frac{Y(f)}{X(f)} \tag{4.17}$$

Where X(f) refers to the response of the OFDM transmitted signal, H(f) describe the system channel response and Y(f) represent the response of the OFDM received signal.

4.2.5 Data extraction

At the receiver side. The OFDM signal utilized for fine grained wireless channel state information extraction then the amplitude frequency response for each breathing activity will be observed constantly for 10 seconds. And each collected signal consists several OFDM samples and subcarriers. Time and samples can be represented as the received number of samples in a unit time.

The obtained data from CSI is in the row form and needs processing to provide meaningful information using three following steps.

I- Cleaning the data by eliminating the terrible CSI data.

II- Applying low pass filter for removing the noise.

III- The grouping technique is performed to detect the correlation between the CSI values.

4.2.6 Feature extraction

CSI information represent fine-grained data and feature extraction is used for transferring the CSI data into meaningful information. Several features in the time domain are implemented. (1) the normalized standard deviation indicate the dispersion degree among sampling points

of the CSI signal. (2) the root mean square (RMS) is used to calculate the magnitude of CSI information. (3) peak to peak value is used to calculate the differences between the maximum and minimum amplitudes values of the collected CSI signal. (4) the peak factor indicates if there is influence on the CSI information. (5) waveform factor is used to represent the ratio of the root mean squire value to the average value. (6) FFT is used to excerpt the frequency component with peak to peak values of the signal. (7) spectrum probability and signal energy are unique and essential for extraction of frequency domain analysis. Feature extraction equations can be seen in Table 4.1.

Table 4.1: USRP specification [8]

NO	Feature	Expression
1	Normalized standard deviation	$Y_{sd}= \sqrt{\frac{1}{N-1}\sum_{i=1}^{N}(x_i\text{-}y_m)^2}$
2	The root mean square (RMS)	$Y_{RMS}= \sqrt{\frac{1}{N}\sum_{i=1}^{N}x_i{}^2}$
3	Peak to peak value	$Y_{ppv} = Y_{max}$ - Y_{min} (i =1,2...,N)
4	Peak factor	$Y_P = \frac{max(x_i)}{Y_{RMS}}$ (i =1,2...,N)
5	Waveform factor	$Y_w = \frac{N*Y_{RMS}}{\sum_{i=1}^{N} X_i}$ (i =1,2...,N)
6	FFT	$Y_{FFT} = \sum_{n=-N}^{N} x(n)e^{-j\frac{2\pi}{N}nd}$
7	Spectrum probability	$Y_{SE} = \sum_{n=-N}^{N} p(d)^2$
8	Signal energy	$Y_M = \sum_{n=-N}^{N} p(d)\ln p(d)$

4.3 Machine Learning Processing

In this work, four machine learning algorithms are utilised to create classification models for predicting abnormalities based on breathing data.These adaptive algorithms distinguish between normal and abnormal patterns based on the trends seen in various breathing patterns.When a machine learning algorithm is trained on a larger amount of experimental data, processing on a large data set improves its recognition performance.The heterogeneous matrix is constructed using all of the features retrieved from the CFR data.The data from the Breathing CFR is read as a column vector with each row labelled with the corresponding breathing pattern.Cross-validation (CV) is a technique for evaluating a model's performance on new data by making predictions that have not been trained previously.The training of algorithms is accomplished using this technique by dividing the known dataset into subsets of known size for training and testing. CV divides the

original dataset randomly into training and testing groups for each iteration. After that, supervised learning techniques are utilised to train and test datasets for performance evaluation. This procedure is repeated several times, and the performance is measured as the average error. When training on model development, CV is critical to avoiding underfitting and overfitting. CV provides several approaches for partitioning the dataset in different ways in order to find the best algorithm to develop a model. In this experiment, the machine learning algorithm was used to classify three different breathing patterns that provided the optimum results with ten-fold cross-validation leaving one subject out for validation.Table 4.2 contains details about the experiments that were carried out.

Table 4.2: Information on the conducted breathing experiments

Experiments Information	Quantity
Number of subject	1
Number of activities	3
Time for each activity	10s
Number of experiments	30
Number of USRP devices	2
Number of PCs	2
Number of Antennas	2
Number of subcarriers	64
Number of classification algorithms	4
Response classes	3
Cross-validation	10

4.4 Evaluation

Our experiments were carried out to test human vital signs monitor the respiratory rates and identify anomalies. This section describes the hardware and software setup involves the parameters used in the designed system.

4.4.1 Experimental method

The experiment is performed in lab environment using two NI USRPX300/310 platforms that have been built for real time data acquisition. The USRPs is fitted with two omni directional antennas for the transmit and receive operation. The antenna has frequency range from 2.4 GHz to 5.9 GHz. The key advantage of using omni-directional antenna is that it can detect human activities in LOS and NLOS. Besides, directional antennas, yagi antennas have also been tested on our system and provided similar results. the experiment was conducted at 5.32 GHz,With the increase in frequency, the range resolution increases and vice versa. The respiratory rate will be best detected when the USRP transceiver model is tuned at higher frequencies. However, the

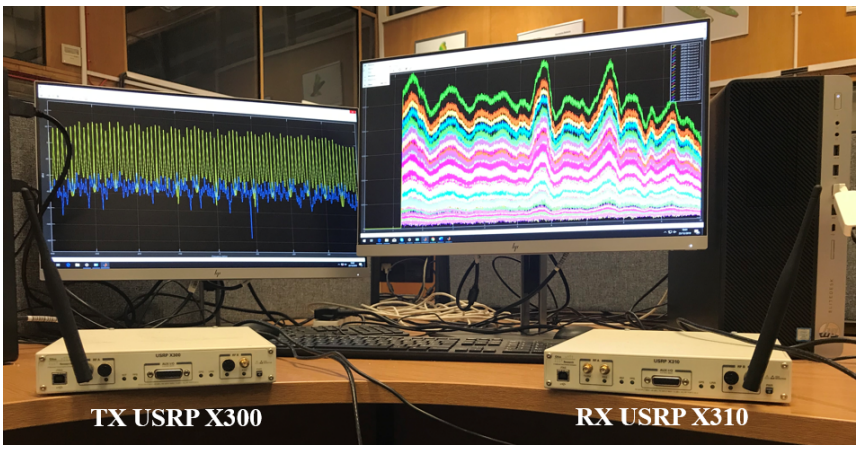

Figure 4.3: Hardware design of System Setup.

distance in terms of monitoring person will be decreases and signal will be highly susceptible to external noise. Furthermore, two PCs was used to implement the trial and a 1 GB Ethernet cable was used to transmit the data to the centralize personal computer to process the acquired USRP data and classify normal respiratory rate against abnormal breathing rate. The trial were processed using MATLAB SIMULINK software. For the demonstration, the experiment carried out in lab environment, which was a large room with office environment. Also, the volunteer was positioned 0.4 m away from the antenna, in order to achieve optimum performance. The experiment was undertaken to capture the changes occurred in CSI data due to chest movement cause by respiratory patterns. Moreover, we used wearable sensor (Ground truth) to ensure that the collected data from USRP is working properly. The breathing sensor used as a reference was SA9311M. The reference wearable sensor is a highly sensitive to chest movements and abdominal expansion/contraction and outputs the respiration waveform. Finally, four algorithms such as KNN, DA, NB and DT were applied to process and classify the collected data. In the same scenario, we have performed experimental campaign ask the volunteers to perform normal breathing, shallow breathing, and elevated breathing while they were under test. the experimental setup is shown in figure 4.3.

4.4.2 System Parameters Selection

In this part, we introduce the system parameters selected for software and hardware system setup. Firstly, Simulink model was implemented in MATLAB based on QPSK modulation scheme and OFDM signal. We tested the hardware parameters by running QPSK transmitter and receiver examples on MATLAB, then we applied our own hardware parameters of the USRPs X300/310 to capture the wireless CSI of different breathing pattern. The trial was conducted at 5.32 GHz for USRP platform and the sample rate chosen in this experiment was 80. Configuration for the hardware and software parameters are shown in Table 4.3.

Table 4.3: Software and Hardware Configuration and Parameters Selection

Parameters	Values
Input random bits	round(0.75*rand(104,1))
Sample time rate	132/104*(1/132e4)
Modulation type	QPSK
Bit per symbol M	2 bits
Used Subcarrier	64 subcarriers
Used Null subcarrier	12
Used Pilot subcarrier	4
Samples per frame	Used subcarrier log2 (M)
blackNFFTpoints	black64,128,256,512,1024 and 2048
Cycle prefix	NFFT-data subcarrier
Platform	USRP X300/310
TX serial number	192.168.10.1
RX serial number	192.168.11.1
Channel mapping	1, 2
Gain (dB)	70
Master clock rate	120 Mhz
Centre frequency of USRP	5.32Ghz
Sample time rate	1/80e4
Local oscillator offset	Dialog
Interpolation factor	500
PPS source	Internal
Decimation factor	500
Clock source	Internal
Transport data type	Int16

4.5 Results and Discussions

4.5.1 Experimental Results

In this section, we evaluated the overall performance of the breathing rate under three different pattern; normal breathing, shallow breathing, and elevated breathing. The three breathing regimes were measured by two devices USRPs and wearable sensor (ground-truth) after acquiring ethical approvals from University of Glasgow. Firstly, the volunteer was asked to breath normally followed by shallow breathing and the elevated breathing for 10 seconds each. We collected the data from sensor and the USRP simultaneously. The wearable sensor was attached to the participant body's chest. While testing our experiment and recording of the data, multiple factors were considered in real-time environment such as the physical objects that could affect the wireless received signal. First, we tested our system with QPSK transmitter and receiver examples with USRP to ensuring that there is no error acquired for the device configuration and whether working properly. Then we used our own Simulink model to captivate the wireless

signal for small scale body movement of the human. The number of packets characterise the number of subcarriers of the OFDM signal. Figure 4.4 shows wireless channel state information (WCSI) waveform of normal breathing for both USRP and wearable sensor. We have used The Breathing Rate Belt and Pressure Sensor 'product code 3190 as reference sensor. The human started sitting in front of the USRP and kept the distance as 0.4 meters. Also covered the sensor around his body and started breathing normally and recorded the data of both the USRP and sensor. We noticed that the amplitude changes were normally based on the usual breathing of the human. In this case, the practice was repeated several times with same amplitude differences detected.

During recording of the wireless data from human respiration, we set the time to 10 seconds. Transmitted packets were 10000 and received 8642 out of 10000 packets for 10 second time duration. We repeated the normal breathing activity 10 times and received same number of packets of each activity performed. We used the wearable sensor as reference. As the measured data of wearable sensor are reliable and presents the ground truth of the breathing detection. The wireless value is close to the wearable value. This ensures that the system can measure the human breathing without wearing any sensor and it can be alternative of wearable devices. Figure 4.5 shows the results when of shallow breathing. The figure illustrates the prominent changes in the amplitude. The time duration in this practice was also set for 10 seconds including the same number of send and received packets of the previous activity of normal breath. In this work, we have used software-defined-radio model University Software Radio Peripherals (USRP) by transmitting and receiving N number of multiple OFDM subcarriers as compared to its counterpart where limited numbers are available. In our experiment, The Orthogonal Frequency Division Multiplexing (OFDM) with 64-subcarriers is used to extract the Wireless Channel State Information of breathing activities.

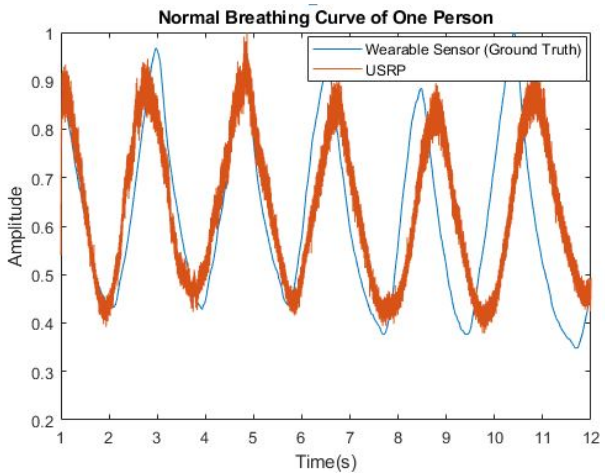

Figure 4.4: WCSI during Normal Breathing for USRP and Sensor.

Figure 4.6 represents the results of the elevated breathing. It can be seen that the signal increased in the cycle of the amplitude compared to the waveform of normal breathing. Also,

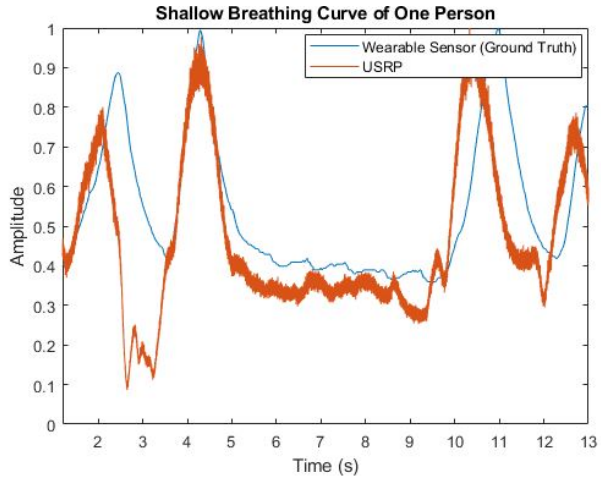

Figure 4.5: WCSI during shallow Breathing for USRP and Sensor.

comprised the similar number of the transmitted and received packets for 10 seconds time duration. Besides, the referenced signal is reliable and has less noise compared with the signal obtained from the SDR or is effected by any physical factors as a result of performing the breathing activities.

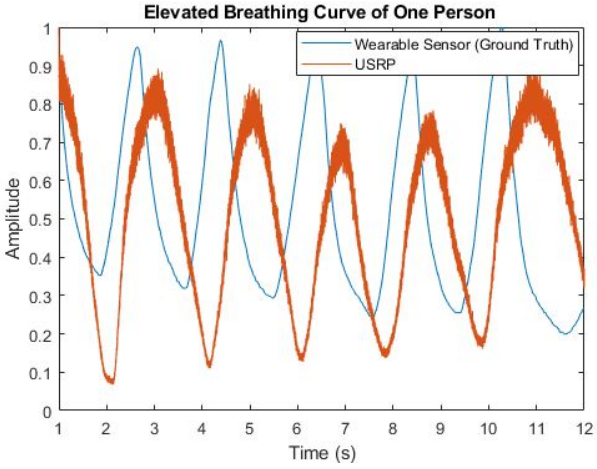

Figure 4.6: WCSI during elevated breathing for USRP and Sensor.

4.5.2 Machine Learning Classification

This section provided details on the discussion of four different machine learning algorithms used to classify three breathing events and evaluate the suggested system based on percentage accuracy. The dataset performance was obtained using different ML techniques as listed above. A 10-fold cross validation technique was used on the USRP data containing different respiratory patterns.

The accuracy is calculated as an average of the 10 sets of testing data used in each of the 10 cross fold validation process. The below Figures 4.7-4.8 shows the confusion matrix of KNN

and DT algorithms. It can be seen from Confusion matrix in figures 4.7-4.8 that the y axis represents the predicted classes and x axis symbolizes the true class of the algorithm.

The machine learning algorithms were run using the following parameters. KNN is configured using 3 K-samples using the Euclidean distance. Discriminant Analysis DA was configured as linear. Naive Bayes NB used the normal distribution method. DT algorithm is set up to use 50 splits in the decision tree. Table 4.4 shows the parameters were used for KNN and DT classifier.

The KNN classifier provide the best classification accuracy among other algorithms. The value for KNN algorithms was selected as 3. The confusion matrix in figure 4.7 represent a total of 1075851 samples were received over a period for all breathing events. For a combined activity of elevated breath, 15.4598% were correctly classified as elevated breath. While 1.3388% samples were incorrectly classified as breath normal and 0.3538% samples as shallow breath activity. Almost similar number of samples were correctly identified as breath normal and 1.4372% samples were determined as elevated breath besides 5.3134% CSI samples as shallow breath. 40.84745% samples were predicted as shallow breath while a combine of nearly 0.5765% were unclassified as other remaining activities. The overall percentage accuracy using KNN classifier was obtained as 91.0105%.

KNN Classifier		Predicted Class			
		Elevated Breath	Normal Breath	Shallow Breath	Total
True Class	Elevated Breath	**15.4598 %**	1.3388 %	0.3538 %	17.1524 %
	Normal Breath	1.4372 %	**34.6732%**	5.3134 %	41.4238 %
	Shallow Breath	0.2915 %	0.2850 %	**40.84745%**	41.42395 %
	Total	14.1885 %	36.237 %	46.51465%	**91.0105%**

Figure 4.7: Confusion matrix for KNN classifier.

Table 4.4: Following parameters were used for KNN and DT classifier

Classification Algorithm	Parameters	Setup
Decision Tree	Maximum number of dataset splits. Split Criterion	4 Gini's diversity index
K–Nearest Neighbour	Number of Neighbours. Distance Metric	2 Euclidean

DT algorithm performed worse, providing overall accuracy of only 71.131%. It can be seen in Figure 4.8 that for first activity, there were 5.7335% classified correctly. 4.5800% CSI samples were identified as breath normal activity (false negative) and 6.8390% samples as shallow breathing. The classification of normal breathing samples slightly more accurate. 1.4247% and 14.7483% samples were classified incorrectly as elevated breath and shallow breath, this leaves the remaining 25.2507% breath normal samples as being correctly classified. For the shallow breath activities, 40.1471% samples were classified correctly, then 0.3909% and 0.8858% samples were misclassified. The other algorithms tested were discriminant analysis (DA) and native bayes (NB) which produced poor results compared to KNN and DT algorithms with accuracy of only 59.72% for DA and 48.99% for NB. Table 4.5 shows the accuracy comparison for all used classifiers.

DT Classifier		Predicted Class			
		Elevated Breath	Normal Breath	Shallow Breath	Total
True Class	Elevated Breath	**5.7335 %**	4.5800 %	6.8390 %	13.1525 %
	Normal Breath	1.4247 %	**25.2507 %**	14.7483 %	41.4237 %
	Shallow Breath	0.3909 %	0.8858 %	**40.1471 %**	41.4238 %
	Total	7.5491 %	30.7165 %	61.7344 %	**71.1313%**

Figure 4.8: Confusion matrix for DT classifier.

Table 4.5: Percentage accuracies of each classifier

Classifier models	Classification Accuracy %
Nearest Neighbor (KNN)	91.0105
Decision Tree (DT)	71.131
Discriminant Analysis (DA)	59.72
Naive Bayes (NB)	48.99

4.6 Summary

In this chapter, breathing rate detection based on SDR techonolgy and CSI. In particular, we designed a MATLAB Simulink model based on universal software radio peripheral (USRP) to capture human breath monitoring. The simulated results improved understanding of wireless channel characteristics for CFR measurement. Our algorithms grounded on channel state

information (CSI) information in time domain can detect the breathing rate for individual non invasively. Three breathing scenarios was implemented; normal, shallow and elevated breathing. then compared our results with a data harvesting sensor as the ground truth. Our results show high correlation between the two methods. Machine learning algorithm were applied for processing and classifying the data to provide excellent performance and robustness on breathing rate. For future work, we will increase complexity of the data collection by monitoring multiple people simultaneously, increase other movements in the surrounding and so on. Our aim is to make this system more generalized, acquiring data in elderly care centre or hospitals in different geometrical settings. The CSI at heterogenous environment varies also, we will develop an algorithm for calibration in future work that is independent of geometrical structure.

Chapter 5

Multiple Subject Activity Monitoring

5.1 Introduction

In recent years 5G-based technologies, pointing at seamless integration of the world into a single system, have been making significant innovations in numerous real-world implementation and thus introducing significant commercial possibilities for several fields such as healthcare and energy conservation. In healthcare, 5G is already creating new opportunities for areas such as medical imaging, data analysis, elderly care, diagnostics, and prognostication due to its ultra low latency, Massive-Machine Type Communication (mMTC), intelligent management and handling of Big Data [175]. However, Human Activity Recognition (HAR) has received increasing attention due to numerous applications in fields such as security, health care and smart utilisation of resources, but has not been introduced with 5G-based technologies. HAR and classification not only brings numerous benefits to elderly care [176, 177] but also is a basic key in providing higher-level appropriate information such as positions, activities, occupancy, and identities in an indoor environment that can be useful for health care, source utilisation, security, and in energy saving.

The risks of high carbon emissions on the environment have increased the need for solutions, across all societal domains, to achieve carbon neutrality. One of the key points to be considered is reducing energy waste, that is, consuming energy only when and if needed [178]. Presence and activity detection systems can play a vital role in this and can complement Internet of Things (IoT) use cases for smart cities, such as the wireless electricity data logger introduced in [179], to control in-home energy consuming systems such as lights, appliances, and so on.

Several studies in the literature have discussed and evidenced the relationship between building occupancy and energy consumption. For instance, a study was reported in [180] showing that forecasted energy consumption can be skewed by up to 300% if occupancy was not accounted. Another study [181] confirmed this by showing that actual consumption could be up to three times greater than the simulation and one of the factors contributing to this big gap is occupants' behaviour and their numbers [182, 183]. Thereby, it is fair to say there is a strong correlation

between occupancy and levels of energy consumption [184], which makes a compelling case for occupancy monitoring systems and their positive impact on the environment.

In recent years, the attention towards contactless monitoring/detection of human activity has greatly increased and a lot of promising research work has been reported in this area. Contactless monitoring/detection of human activity employs techniques such as ultrasonic sensing [185], vibration Sensing [186–188], mobile device [189], Radar [190] and Radio Frequency (RF) sensing. The primary disadvantages of using ultra sound, vibration and radar sensing systems is the cost and set up of additional equipment. The use of mobile devices can be beneficial due to higher powered mobile devices becoming more available however the mobile device cannot be considered fully contactless as users must have their device on person. The use of RF-sensing addresses these disadvantages as RF signals are already present within the home with the use of Wi-Fi and is completely contactless. The methods based on Radio Frequency (RF)-sensing [191, 192] are gaining considerable popularity due to their privacy-friendly feature and for being contactless in comparison with conventional systems either based on cameras or wearable sensors [3, 36, 193, 194] and thus an introduction of 5G-based HAR and classification will certainly revolutionise this area of research.

Generally, the existing HAR systems based on RF-sensing differ from each other on basis of various factors such as hardware specifications, operating radio frequency, classification techniques, number of activities to monitor and number of subjects performing those activities. Available HAR systems either make use of Received Signal Strength Indicator (RSSI) [116, 117, 195]or Channel State Information (CSI) [112, 113, 196], for the purpose of activity recognition. However, studies, such as [197], suggest that CSI is more robust to the complex environments as CSI is fine-grained and measured per Orthogonal Frequency-Division Multiplexing (OFDM) from each packet while RSSI contains the coarse information that is a single value per packet. This makes CSI more stable to be used for localisation and activity recognition. Furthermore, due to recent advances CSI based systems do not require the user to carry wearable devices and do not depend on lighting. Also, it can detect human behaviour through the wall and complex situations. Making them a good alternative for RSSI based recognition systems.

Recently, many CSI and machine learning-based approaches have been proposed to accurately detect and count people in a given coverage area of a Wi-Fi network. For example, in [113] the authors proposed a Wi-Fi-based multi-user gesture recognition method to recognise 6 different gestures performed by 10 volunteers. A similar approach based on CSI has been proposed in [119] for crowd counting. Both of these studies make use of 1 transmitter (Tx) and 3 receiver antennas (Rx) and use the intel wireless network card. However, Network Interface Card (NIC) usually presents numerous limitations. For instance, the transmitter used in those system sends a group of 56 subcarriers, however, the NIC only reports 30 subcarriers, nearly 46% of the information lost in this case. The authors in [198] exploit the CSI of Wi-Fi to detect multiple subjects' activities. This system applied a three-phase system Wi-multi to recognise three

different activities performed in parallel, including in a noisy environment. They achieved an accuracy of around 96% using 2 Tx and 3 Rx antennas. In another study [199], the authors presented a method of crowd counting based on CSI extracted from a Wi-Fi device with 2 Tx and 3 Rx antennas. The proposed method exploits both amplitude and phase information of CSI signal to perform crowd counting only and does not deal with activity recognition. The work presented in [75] used CSI data of Wi-Fi device with 2 Tx and 3 Rx antennas to detect sixteen different exercises performed by ten different subjects. However, the authors did not deal with the activities performed in parallel. 5G has been used in [200], [201] to detect breathing rates of people suffering from diabetic keto acidosis (DKA). The proposed system makes use of C-band sensing operating at $4.8GHz$. C-band communication is an important component of 5G communication. $4.8GHz$ was also used in the work of [202] to detect the Freezing of Gait (FOG). FOG is an abnormal gait pattern that accompanies Parkinson's disease. This work used the 5G spectrum to detect and classify FOG by sensing the human movements. The work of [203] made use of the 5G frequency of 3.45 GHz to detect human presence and walking speed using Radio Frequency sensing.

The brief overview of the literature, presented above, suggests some important insights. For example i) most of the studies involve CSI data extracted from commercial Wi-Fi devices such as NICs that report a limited number of data subcarriers and causes a loss of information and thus adversely affect the classification performance. Moreover, NICs are primarily used for networking functions, hence it's reliability can be significantly impacted if it was simultaneously utilised for sensing. Hence, to ensure high accuracy and reliability, this paper presents a system that makes use of Universal Software Radio Peripheral (USRP) devices, where the hardware can be controlled over the software, and parameters such as the number of subcarriers can be controlled and fully utilised. The USRP platform also allows to modify the transmitted and received power and the operating frequency swing, through which the system could be easily configured to operate in the $5G$-band ($< 6GHz$). Furthermore, the ease in implementation of signal processing algorithms and the ability to reuse hardware encourages researchers to choose USRP devices for their applications. ii) All of the above-mentioned studies use more than one Tx and Rx antennas to capture the maximum information, whereas in this paper experimental results show that the proposed method achieved even better performance in recognising multiple activities performed in parallel with one Tx and Rx antenna.

Contributions and study motivation In this chapter a novel $5G$-enabled presence and activity detection system, of multiple subjects, is presented. The proposed RF-sensing system was designed to operate in the 5G frequency band, particularly at $3.75GHz$. The ultimate goal is to enable the incorporation of $5G$-based non-invasive in-home activity monitoring systems in our community to maximise the utilisation of the opportunities offered by $5G$ and its enabling tech-

nologies. The contributions in this work can be summarised to the following with the motivation behind each described after every point:

1. Presence and activity detection of multiple subjects performing different activities in parallel.

   Activity recognition for single subjects has been greatly explored by several studies in the literature [102,204–206]. The research team presenting this paper, have led several studies on activity recognition using software defined radios, [23,207,208], which motivated them to take it to the next level and conduct one to explore the capability of the technology to do so for multiple subjects. By utilising RF-sensing technology and Artificial Intelligence (AI), a single system is presented that can simultaneously monitor occupancy, that is count the number of people in a room, and detect the parallel activities of all subjects. The contribution here has two folds, the first is accounting for a combination of three different activities occurring in parallel, amongst four different subjects. Secondly, the variation introduced in the training data by introducing intra-class variation, that is, training the system to classify the same activity or combination of activities performed in different positions within the room and by different test subjects, as the same class. This was performed to strengthen the machine learning model and improve its detection accuracy.

2. $5G$-enabled sensing, that is, the proposed RF-sensing system was designed to operate in the $5G$-band, particularly at $3.75GHz$.

   To the best of the authors' knowledge, the use of $5G$ for sensing applications has not been considered elsewhere in the literature. The motive and ultimate goal for the use of this frequency is to utilise $5G$ technology with its high data rates and ultra-low latency capabilities in developing real-time non-invasive activity and presence detection systems for assisted living. Moreover, primary findings from the experiments conducted in this paper have shown that the CSI, reflecting activities performed by a test subject, captured using the $5G$ frequency $3.75GHz$ are much more evident in pattern compared to those captured at the Wi-Fi frequency. To confirm this, the experimental setup, presented later on in section 5.2, was used to collected CSI samples at both frequencies for the "Standing Activity" and for "Empty Room" at the Wi-Fi frequency $5.00GHz$. All three captures can be found in Fig. 5.1, where Fig. 5.1a and 5.1b, are of a "Standing Activity" captured at $5GHz$ and $3.75GHz$, respectively. Whilst Fig. 5.1c, represents a capture of an "Empty Room", at $5.00GHz$. The evident pattern in the captured CSI, such as that in Fig. 5.1b is more likely to increase the accuracy of classification, compared to that in Fig. 5.1a, especially in a real-time system when massive amounts of data are captured and processed.

3. The data sets collected during the course of the experiments, presented in this work, are made publicly available through this link [209]. As part of the contributions reported in

this chapter, the data collected at the University of Glasgow. The lack of a comprehensive data set for this type of activities has motivated the research team to make the data available and benefit the wider community with this rich data set that covers a wide range of activities. Researchers can use the data set to apply different processing techniques, replicate the experiment and collect more data for bench marking. The online data set contains a total of 1777 samples divided amongst 16 classes, as detailed later on in section 5.2.2.

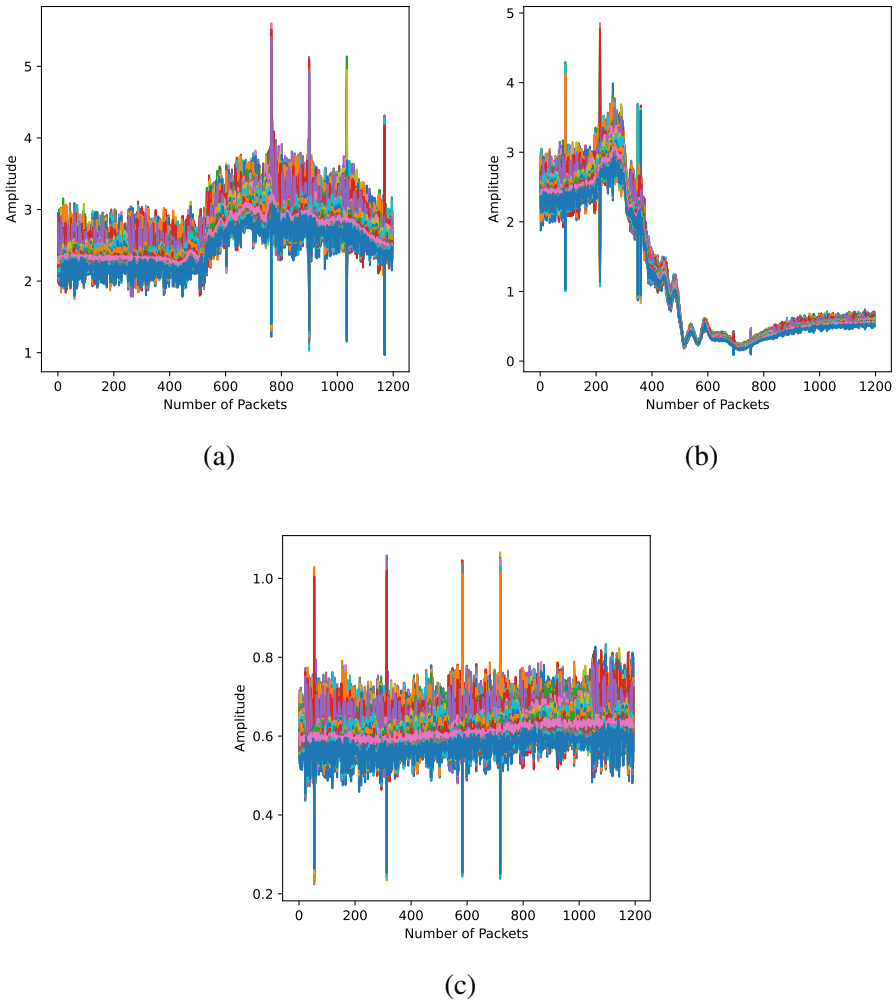

Figure 5.1: Channel state information patterns of activities performed at $5GHz$ (Wi-Fi frequency) and $3.75GHz$ ($5G$ Frequency); a) Standing Activity at $5GHz$, b) Standing Activity at $3.75GHz$, c) Empty Room at $5GHz$

5.2 Methodology and framework

This section details the methodology and framework adopted to conduct the experiments and achieve the reported results. It starts by presenting the specifications of the hardware design

stage, followed by a detailed outline of the experimental design stage including experimental variables, data collection, data processing, system training, and testing. The system conceptualisation and main building blocks are presented in Fig.5.2.

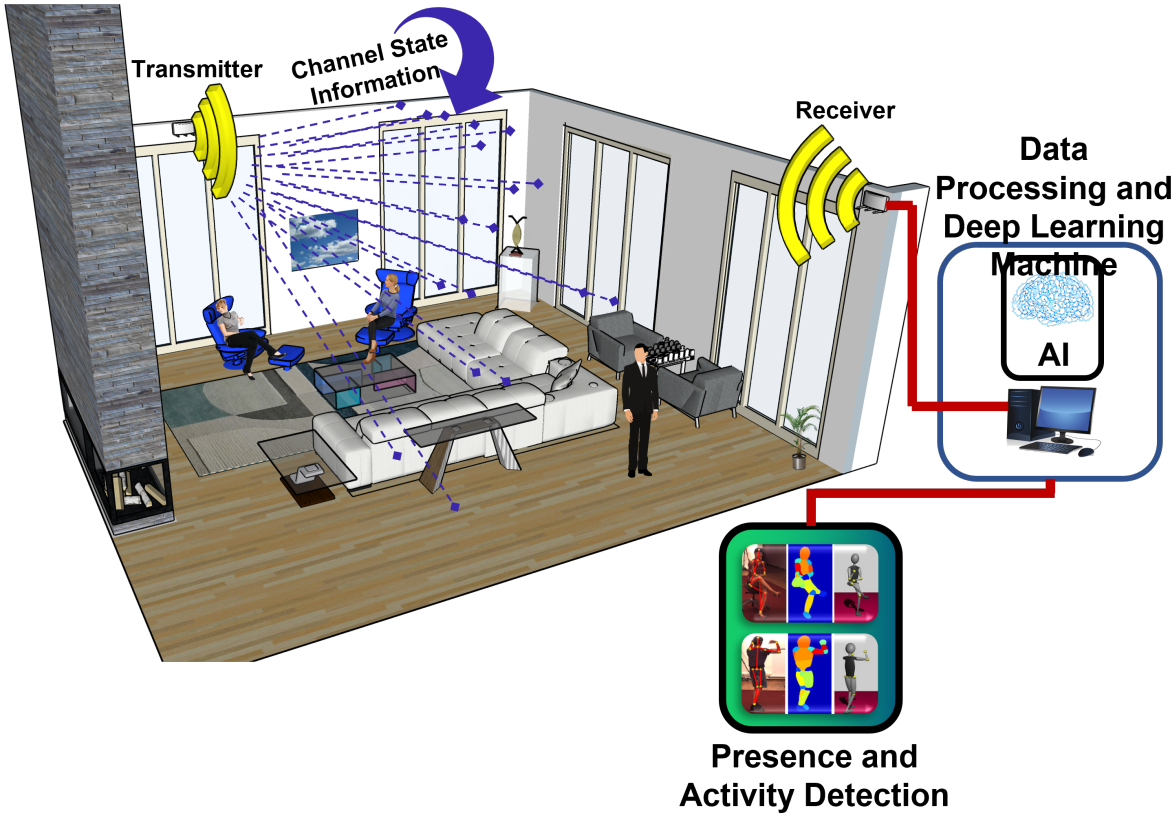

Figure 5.2: System concept diagram showing the contactless sensing system for multi-users using wireless signals

5.2.1 Hardware design specifications

The experiments conducted and reported in this work utilised two USRPs devices each equipped with the VERT2450 omnidirectional antenna. One USRP is used as the transmitter and the second USRP is used for the receiver. Each USRP is connected to a separate PC that uses the Intel(R) Core (TM) i7-7700 3.60GHz processors and has a 16 GB RAM. The system makes use of virtual machines to provide the Ubuntu 16.04 operating system. On the Ubuntu virtual machines, Gnu Radio is used to communicate with the USRPs. Gnu Radio allows for the creation of flow diagrams for the USRP function to be carried out. These flow diagrams can then be converted to python scripts. One python script is created to transmit data and another script is configured to receive the data from the transmitter. The transmitter transmits random numbers between 0 - 255 using OFDM. The receiver side is configured to receive the transmitting signal from the transmitter USRP. The script ran on the receiver side then outputs the CSI complex

number to the terminal. This output is then processed to extract the amplitude values from the CSI complex numbers. The system's main configuration parameters are shown in Table 5.1.

Table 5.1: Software Configuration and Parameters Selection

Parameter	Value
Platform	USRP X300/310
OFDM Subcarriers	52
Operating Frequency	$3.75GHz$
Transmitter Gain (dB)	70
Receiver Gain (dB)	50

5.2.2 Experimental design

To validate the effectiveness of the proposed framework, various experiments have been performed in a rectangular $2.8 \times 3m^2$ activity area as shown in Fig.5.3. The two X Series USRP devices for the transmission and the reception of CSI signals have been installed in the two corners facing each other. To capture maximum intra-class variation for all the activities that include sitting, standing and walking, the subjects have kept changing their positions randomly in the prescribed activity area while keeping a $1m$ distance among themselves during the course of multiple experiments. This is to simulate a small setting such as a care home with a limited number of people. Currently the focus of the experiment is to accommodate 4 people. Part of the future work will seek to increase this number.
Furthermore, the proposed deep learning-based classification methodology to recognise multi-user activities is comprised of two major modules: i) System Training and ii) System Testing, as depicted in a high-level signal flow diagram shown in Fig.5.4. The system training module is based on an offline process that involves already acquired and preprocessed CSI samples data set to train the 1-D Convolutional Neural Network (CNN). The system testing is performed in an online setting in which an input CSI data sample, after all necessary preprocessing is performed, is classified as one of the human activities. A detailed description of the two modules is provided in subsequent sub-sections.

System training

The system training module of the proposed classification architecture is mainly based on the three major components (see Fig.5.4): i) Data collection, ii) Data processing and iii) 1-D CNN. The CSI data acquisition was performed using the setup shown in Fig.5.3. To prepare the captured CSI data for subsequent classification, tasks are done in the data collection and data processing modules, respectively. Whereas the third component deals with the training and learning of the 1-D CNN model. A detailed discussion on each of these components is presented in the

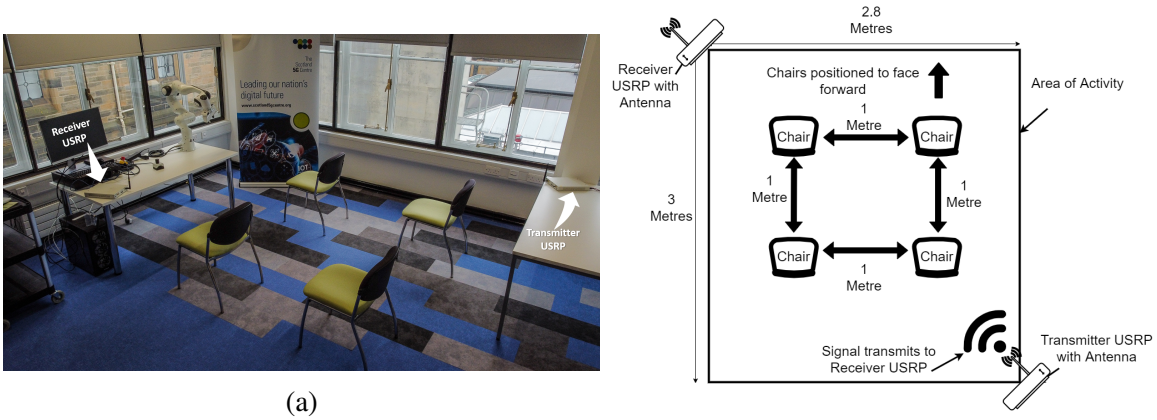

(a) (b)

Figure 5.3: Experimental setup for capturing activities using 5G

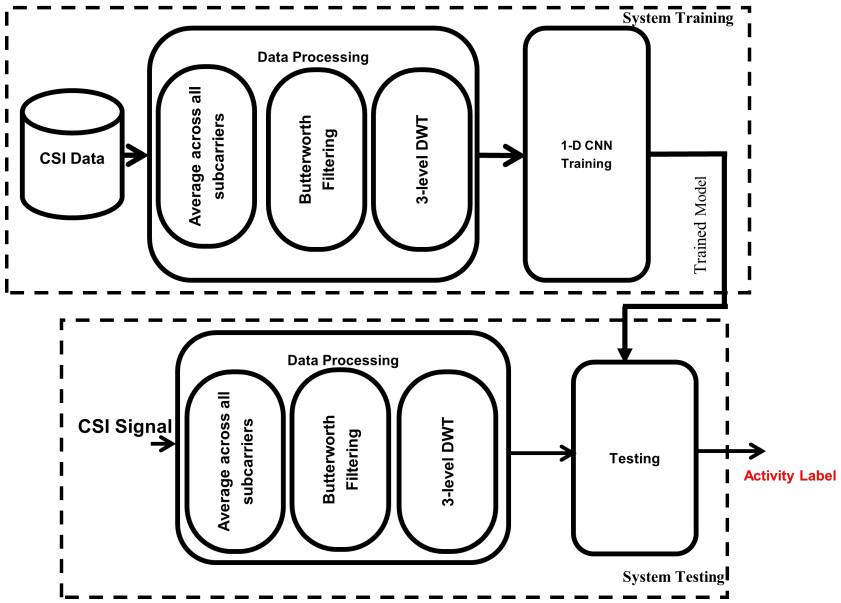

Figure 5.4: Signal flow diagram for multi-user activity classification.

following sections.

Data collection The data collection for the proposed system training involved five steps with four volunteers each performing three different activities, Sitting, Standing, and Walking in a lab environment, with the setup shown in Fig. 5.3b.The setup was replicated in two different lab environments as means of introducing different clutter levels which increases the variability of the data and further strengthens the model. Nevertheless, the data for a particular class collected in both environments were treated as the same data set, that is, clutter level due to environment was not a measured variable in the conducted experiments.

As with any experiment, there were some fixed attributes as well as variable ones. For

the experiments presented in this work, the fixed attributes included (1) The hardware and its configuration (2) The data processing and deep learning techniques and (3) The experimental setup, shown in Fig. 5.3. The experimental variables included (1) the number of subjects (2) The subject identity, in the data collection for one and two subjects and (3) The location of the performed activity, that is, for example, for one subject performing Sitting Activity it was performed in different chair locations, as per Fig. 5.3. The first variable was measured as will be highlighted in the remainder of this section and in the results, whilst the second and third variables were utilised to introduce maximum intra-class variation in the collected data. All the data was collected over a calendar week, with a random number of samples collected for all 16 classes in every day of the week to ensure the repeatability of the data over different days.

The ”Sitting” and the ”Standing” activities are representations of the action of performing these activities and not the posture or the position of the person in the sitting/standing state. Moreover, while capturing the activity data the volunteers were not stressed or forced to keep the upper body still and static so both "Sitting" and "Standing" activity data included the small variations of upper body.

In the first data collection step, the CSI data for a single subject were collected separately for all three activities, that is "Sitting", "Standing", and "Walking", where a total of 420 samples were collected. To introduce maximum variation into the data set, three different subjects participated in this data collection phase. Each subject contributed equally to the data collection, that is, each participant was involved in the collection of 140 samples, divided among the three activity classes. For each CSI data sample, 1200 packets in three seconds are transmitted.

The second step involved data collection for two subjects performing the above mentioned three activities, where a total of 400 samples were collected, as highlighted in Table 5.2. The same three participants were involved in this data collection stage, with equal contributions from each, that is, each participant was involved in the collection of at least 33 samples for each of the four classes identified for this stage of data collection.

In the third and fourth data collection steps, three and four participants were recruited to participate in collecting the data for three and four subjects performing activities, as outlined in Table 5.2. The participants recruited for these data collection stages were fixed throughout. In these two steps, 540 and 300 data samples were collected, respectively. In addition to the activity data, 117 data samples were collected for the class "Empty" which represents the status of the room when the subjects are absent from it. All the 16 classes are shown in Table 5.2. Some of the data samples representing different activities are shown in Fig.5.5. The inter-class variation in the data samples of different activity classes is obvious and can be exploited in subsequent classification process to get better results.

Table 5.2: Number of subjects and activity performed

No. of Subjects	Class Number	Class/Activity	Number of Data Samples
0	1	Empty	117
3*1	2	1 sitting	140
	3	1 standing	140
	4	1 walking	140
4*2	5	1 sit + 1 stand	100
	6	1 walk + 1 sit	100
	7	2 sitting	100
	8	2 standing	100
5*3	9	1 sit + 2 stand	120
	10	1 walk + 2 sit	120
	11	2 sit + 1 stand	100
	12	3 sitting	100
	13	3 standing	100
3*4	14	4 sitting	100
	15	4 standing	100
	16	2 sit + 2 stand	100

Data processing CSI for one transmitter and one receiver antenna forms a matrix that contains frequency responses of all $N = 52$ subcarriers as shown in Equation 5.1,

$$H = [H_1(f), H_2(f), \cdots, H_N(f)]^T, \tag{5.1}$$

here frequency of each subcarrier H_i can be represented as

$$H_i(f) = |H_i(f)|e^{j\angle H_i(f)}, \tag{5.2}$$

where $|H_i(f)|$ and $\angle H_i(f)$ are the amplitude and phase responses of the ith subcarrier. Each of these subcarrier response is related to system input and output as given in Equation 5.3,

$$H_i(f) = \frac{X_i(f)}{Y_i(f)}, \tag{5.3}$$

where $X_i(f)$ and $Y_i(f)$ are the Fourier transforms of input and the output of the system.
In general, the acquired CSI data is masked due to the high-frequency environmental noise and multipath propagation of CSI signal. Therefore, to denoise the data and to prepare it for the subsequent training of the 1-D CNN the data is passed through the following data processing steps:

- In the first step, each CSI data sample is averaged across all 52 subcarriers, see Equation 5.4, to get one averaged data sample to be used in subsequent processing,

$$x_i = \frac{1}{J}\sum_{j=1}^{J} y_{ij}, \tag{5.4}$$

where x_i is the ith data sample that represents the average across corresponding subcarriers y_{ij} for $(j = 1,2,\ldots 52)$.

- Afterwards, a Butterworth lowpass filter of order $n = 4$ is used to smooth out and to remove small variations from each averaged data sample x_i.

- Lastly, a discrete wavelet transform (dwt) at level 3 with a Haar basis function is applied to get the approximation coefficients A_i for each of the smooth data samples s_i. The approximation coefficients represent the output of the lowpass filter in dwt, therefore it further helps in reducing the noise. Mathematically, the convolution and downsampling process involved in the wavelet decomposition for all three levels is represented as follow:

$$A_i^0[m] = \sum_{k=0}^{M-1} s_i[k] \times g[2m-k], form = 1,2,\cdots,M. \tag{5.5}$$

$$A_i^1[t] = \sum_{k=0}^{T-1} A_i^0[k] \times g[2t-k], fort = 1,2,\cdots,T = \frac{M}{2}. \tag{5.6}$$

$$A_i^2[u] = \sum_{k=0}^{U-1} A_i^1[k] \times g[2u-k], foru = 1,2,\cdots,U = \frac{M}{4}. \tag{5.7}$$

where $g[k]$ for $k = 1,2,\cdots,K$ is the lowpass filter of length K for each decomposition level, $s_i[m]$ for $m = 1,2,\cdots,M$ is the smooth signal of length M after applying Butterworth lowpass filter, and A_i^l for levels $l = 0,1,2.$ is representing the approximation coefficient of three levels of dwt.

Figure 5.6 shows a raw data sample and the results obtained after each of the data processing steps. Once all the samples are processed, data set is ready to train the 1-D CNN.

1-D Convolutional Neural Network The CNN [210] is one of the most widely used Deep Neural Network (DNN) for the purpose of pattern classification from both 2-D images and 1-D data signals. 1-D CNNs that have been recently introduced and got a lot of popularity in dealing with the classification problems related to 1-D signals [211]. Motivated by its high accuracy rates in the classification applications [212], in this work, we have also adopted a 19 layers 1-D CNN to recognise multiple human activities performed by multiples subjects in parallel. The purposed 1-D CNN structure is comprised of 6 blocks of convolutional layers and one block of fully connected layers. Out of 6 blocks of convolutional layers, the first block contains one convolutional layer and one pooling layer whereas each of the remaining 5 blocks contains 3 convolutional layers and one pooling layer. Finally, the block of fully connected layers contains

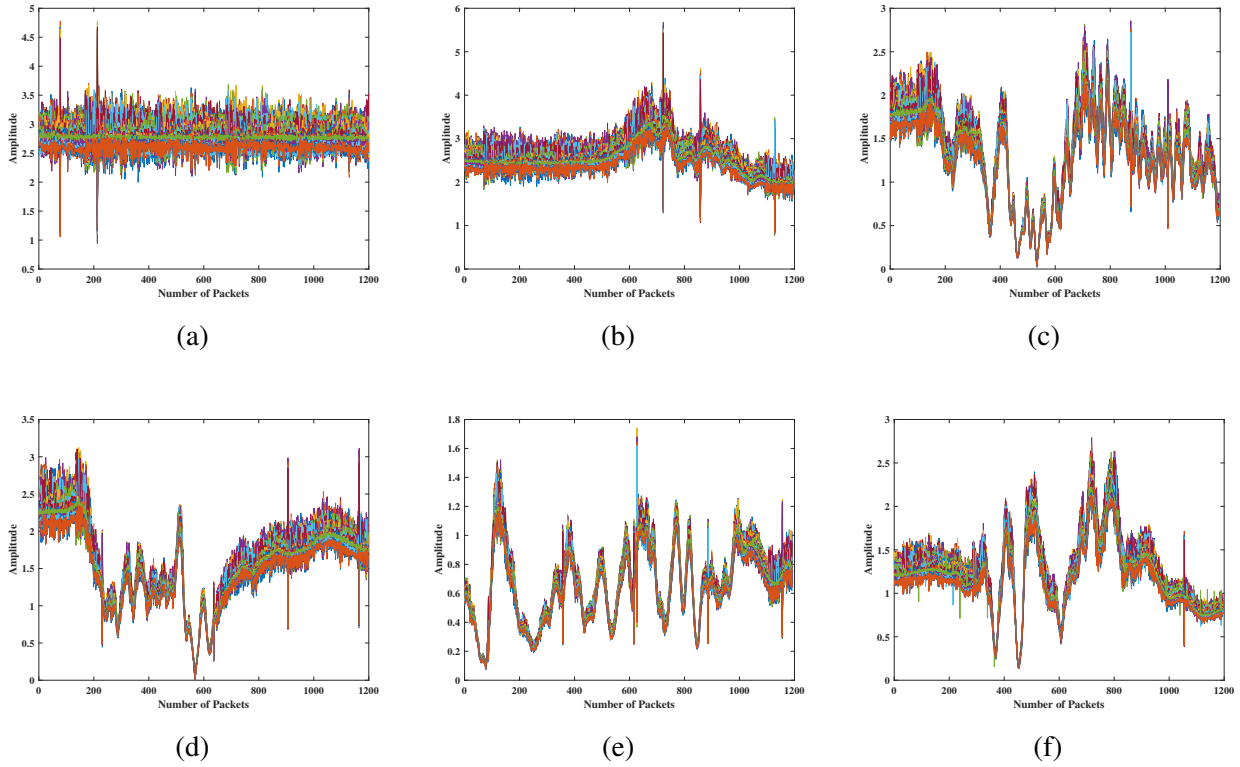

Figure 5.5: CSI data samples representing various activity classes: a) Empty, b) 1-Subject Sitting, c) 2-Subjects (1 Walking and 1 Sitting), d) 3-Subjects (1 Sitting and 2 Standing), e) 3-Subjects Standing and f) 4-Subjects Standing.

3 layers. The complete architecture of the network is shown in Fig.5.7 whereas the detail of various parameters used is given in Table 5.3. Once all the data is preprocessed and the 1-D CNN is trained the trained model is stored for the subsequent testing phase to classify incoming test CSI signal in one of the activity classes.

5.2.3 System testing

The second phase of the proposed methodology is the system testing that involves the following steps:

- In the first step, the CSI signal obtained from the USRPs is first processed by a Butterworth filter to make it smooth by removing small variations. Then the smooth signal is passed through Wavelet Transform, as described in the previous section, to get approximation coefficients at level three.
- In the second phase, the trained 1-D CNN model is used to classify the processed signal into one of the activity classes.

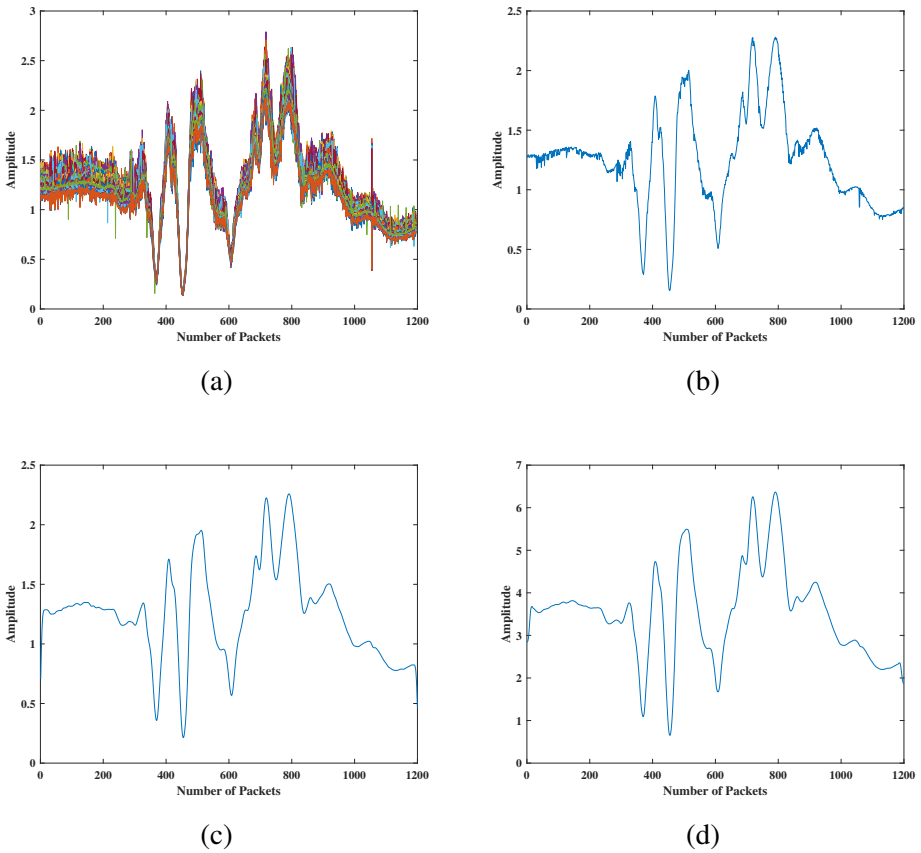

Figure 5.6: Data processing: a) Raw data sample, b) Averaged across all 52 sub-carriers, c) Butterworth low pass filtering and d) Approximation coefficients of a 3 level Discrete Wavelet Transform.

5.3 Results and discussion

The proposed human activity monitoring system was evaluated using two different types of experiments. The first set of experiments focused on determining the accuracy of the system to count the number of people performing particular activities in a room (see Phases 1 and 2 in Table 5.4). Whilst the second set was conducted to measure the system's accuracy in identifying different postures/activities of multiple people in the same room. Both types of experiments were performed under a train-and-test split strategy with 80% of the random data was considered as training data while the remaining 20% was taken as the testing data. Furthermore, each experiment was repeated 10 times to get the average accuracy rates for both sets of experiments. The proposed 1-D CNN architecture consists of 100 epochs and Adamax as the optimiser with 0.001 learning rate. A detailed discussion on the experimental results related to both experiments is given in the following subsections.

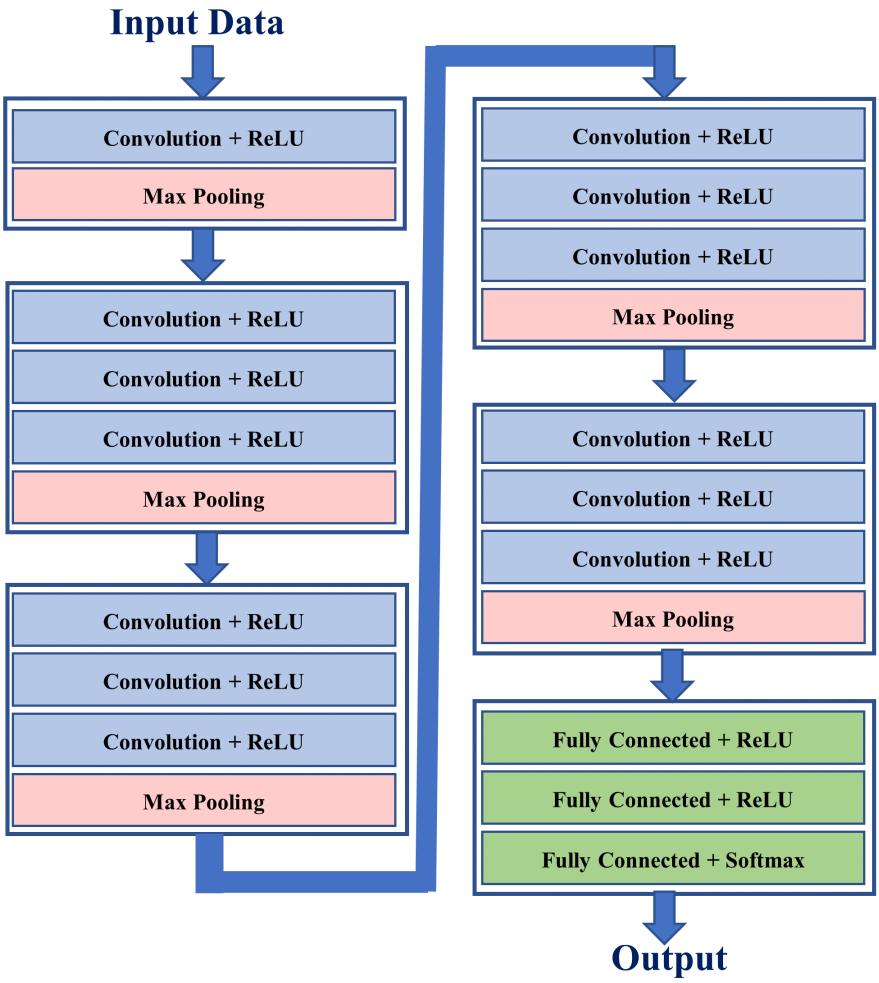

Figure 5.7: Architectural diagram of the proposed 1-D CNN.

5.3.1 Multi-User Presence

The purpose of this experiment is to determine the number of people in an indoor setting. The experiment is done in multiple phases to gradually incorporate different activities as shown in Table 5.4.

- In the first phase, the experiment involves only standing activity performed by a different number of subjects in parallel. The data is divided into 5 classes including the "Empty" class that represents "no-subject in the room" as shown in Table 5.4. For this phase of the experiment, the total number of data samples used is 557, out of which 80% (i.e. 445 samples) are randomly selected to train the model and the remaining 20% (i.e. 112 samples) are used to test the system.

- The second phase involves only the sitting activity data of all the subjects. Again, the total number of samples are 557 and the data is divided into 5 classes, 4 sitting activity classes

Table 5.3: Parameter values used in 1-D CNN.

Architecture	Parameter		Value
	Block-1	1D Conv layers	1
		Kernels for each layer	8
		Kernel size	5
	Block-2	1D Conv layers	3
		Kernels for each layer	16
		Kernel size	5
	Block-3	1D Conv layers	3
		Kernels for each layer	16
		Kernel size	5
	Block-4	1D Conv layers	3
		Kernels for each layer	32
		Kernel size	5
	Block-5	1D Conv layers	3
		Kernels for each layer	64
		Kernel size	5
	Block-6	1D Conv layers	3
		Kernels for each layer	64
		Kernel size	5
	Block-7	1D Conv layers	480
		Kernels for each layer	40
		Kernel size	16
Training	Learning Algorithm		Adamax
	Batch Size		32
	Epochs		100
	Learning Rate		0.001

and 1 “Empty” class.

- In the third phase, sitting and standing activity data for each number of subjects are merged to form the 4 activity classes and 1 “Empty” class. Therefore, the total number of data samples becomes 1417 out of which 80% (i.e. 1133 samples) are used to train the system while the remaining 20% (i.e. 284) samples are used for the test purpose. This data also includes the data for mixed activities like one subject sitting and one standing.

- Similarly, in the fourth phase sitting, standing, and walking data are used together to make 4 activity classes plus 1 “Empty” class. In this phase, the total number of data samples used are 1777 (1421 training samples and 356 testing samples). This data also includes mixed activity data as described previously.

The average classification percentage accuracies for all the phases across all the 10 repetitions of each experiment are shown in the bar graph given in Fig.5.8. It is observed that, in general, the proposed system works well for all the cases. However, it works better when the sitting and standing activities (Phase-1 and Phase-2) are used separately to form the activity

classes. Whereas due to an increase in intra-class variation and a decrease in inter-class variation, when the sitting and standing activities are merged in Phase-3 and a new activity "walking" is introduced along with the other mixed activities in Phase-4, the overall accuracy shows a decrease.

A further analysis of the confusion matrices, shown in Fig.5.9, reveals that maximum misclassifications are due to 3-subject class or 4-subject class. That can be due to more subjects in a relatively smaller space that causes more noise in the USRP data. The performance can be further improved by changing the experimental environment.

In this experiment, the aim is to classify human activity in one of the 16 classes given in Table 5.2. For this experiment, 80-20% hold-out validation is utilised and all 1777 data samples are split into training (80%) and test (20%) data and the experiment is repeated 10 times to get the average performance results. The average percentage accuracy across all 10 repetitions comes as 79.5% $(+/-2.6)$ which is very promising considering a large number of classes and lots of variation within the data. Figure 5.10 shows the normalised confusion matrix with the highest accuracy that is 83% for the activity recognition experiment. Here, the numbers $1, 2, \cdots, 16$ are representing the 16 classes given in Table 5.2, respectively.

Table 5.4: Number of classes for all 4 phases for the subject count experiment

Class Number	Class Labels	Phase-1	Phase-2	Phase-3	Phase-4
1	No-Subject	Empty	Empty	Empty	Empty
2	1-Subject	1-Standing	1-Sitting	1-Standing / Sitting	1-All Activities
3	2-Subject	2-Standing	2-Sitting	2-Standing / Sitting	2-All Activities
4	3-Subject	3-Standing	3-Sitting	3-Standing / Sitting	3-All Activities
5	4-Subject	4-Standing	4-Sitting	4-Standing / Sitting	4-All Activities

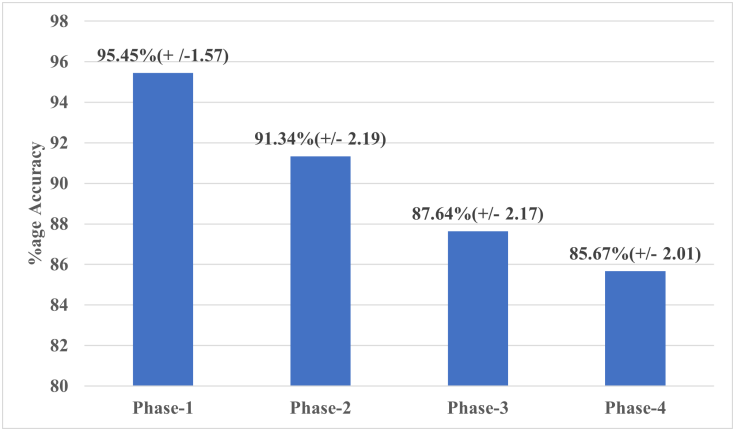

Figure 5.8: Percentage classification accuracy for all 4 phases of the subject counting experiment

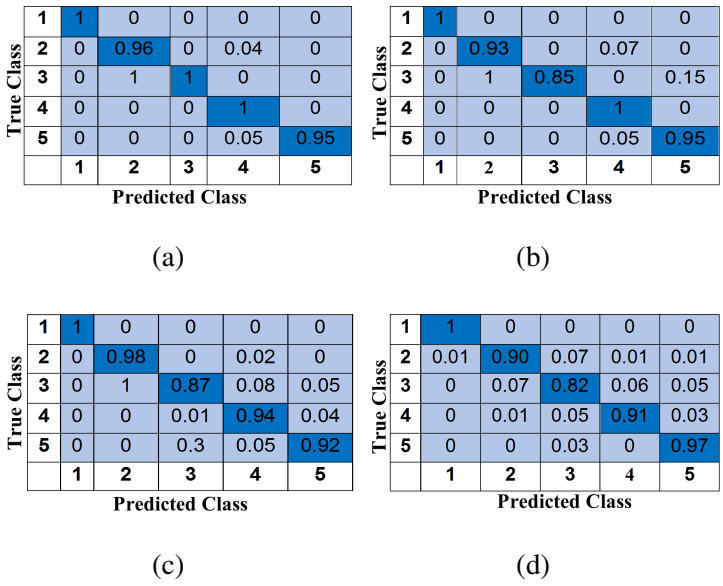

Figure 5.9: Normalised confusion matrices with maximum accuracy for all 4 phases of the experiment. The class labels for classes 1 to 5 are given in Table 5.4. In here a) is representing Phase-1 with an accuracy of 98.22%, b) is for Phase-2 with an accuracy of 94.64%, c) is the Phase-3 with an accuracy of 93.31% whereas d) is representing Phase-4 with an accuracy of 90.17%.

5.3.2 Activity Recognition

It can be seen in the given normalised confusion matrix that in general classification performance is good for most of the activities except a few classes. The normalised confusion matrix provides the highest accuracy for empty (class 1), 1 subject sitting (class 2) and 1 subject walking (class 4) of 100%, 90% and 93%, respectively. However, there is a resemblance in CSI variations in sitting and standing activities as they are similar movements. The 1 subject standing, however, has been misclassified as standing in 14% of the samples resulting in lower accuracy of 82%. Overall, as expected the 1 subject activities provide higher accuracies due to lesser variations in CSI data as compared to multi-subject activities.

In the multi-subject case, some activities have similar patterns and are difficult to differentiate such as “1 sit + 1 stand” (class 5), “2 sitting” (class 7) and “2 standing” (class 8). Since sitting and standing movements result in quite similar motions, whether moving up or down. Also “1 sit + 1 stand” has at least 1 subject performing similar motion with “2 sitting” and “2 standing”, resulting in 15% and 10% misclassification rate of “1 sit + 1 stand” activity as “2 sitting” and “2 standing”, respectively.

Moreover, “1 walking + 1 sitting” (class 6) and “1 walking + 2 sitting” (class 10) result in a higher misclassification rate between the two activities with accuracies of 80% and 75%, respectively. As illustrated in the confusion matrix 21% of “1 walking + 2 sitting” is misclassified as “1 walking + 1 sitting” and 15% of “1 walking + 1 sitting” activity is misclassified as “1 walk-

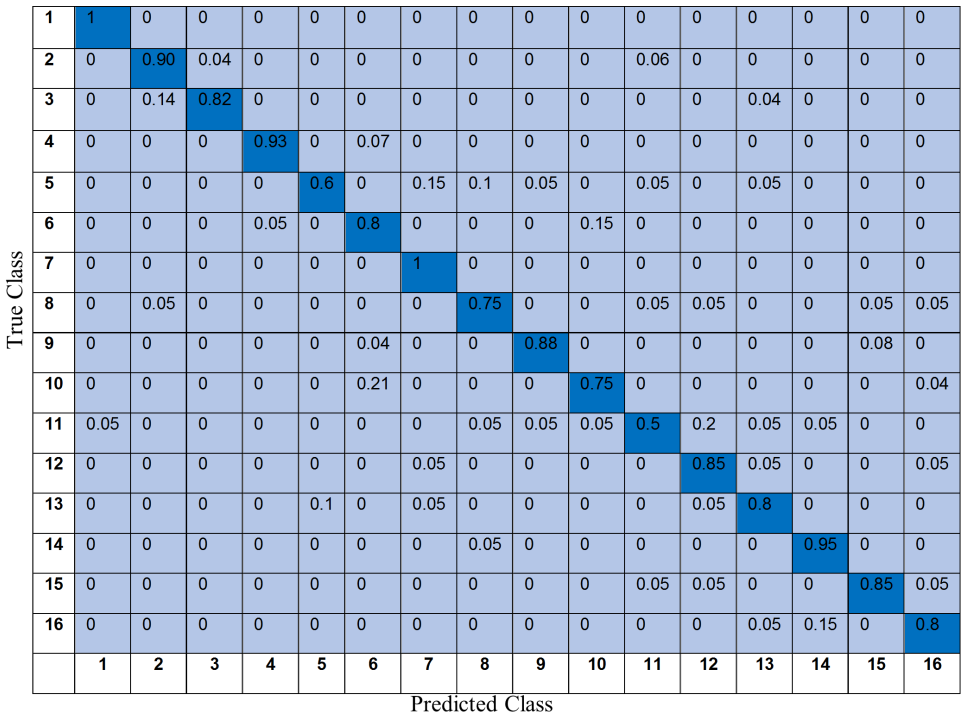

Figure 5.10: Activity monitoring: Normalised confusion matrix for the fold with accuracy of 83%.

ing + 2 sitting" activity resulting in the decrease of respective class accuracies. Similarly, "2 sit + 1 stand" (class 11) and "3 sitting" (class 12) resemble each other due to the same activities performed by at least two subjects. Furthermore, standing as mentioned before is quite similar to sitting in terms of similar motion resulting in 20% misclassification of class 11 samples as class 12. Also, similar CSI patterns exist between "4 sitting" and "2sit + 2 stand".

Due to the above-mentioned reasons and several classes performing sitting and standing activities with a different number of subjects, class 5 which represents two subjects (1 sitting and 1 standing) and class 11 that represents three subjects (1 sitting and 2 standing) provide the least accuracy rates of 60% and 50%, respectively in our deep learning classification model.

5.4 Summary

In this chapter, a novel 5G-enabled contactless RF sensing system has been presented to monitor the human presence and to detect multi-user parallel activity using CSI signals. The system's frequency of operation was $3.75GHz$, which falls within the 3.4 to $3.8GHz$ band of $5G$, and to the best of the author's knowledge, no other study has implemented $5G$-sensing before. The main idea of the work was to present a 5G-sensing based non-invasive system that is capable of detecting the presence and activities of multiple users in the same room. Furthermore, the results presented earlier in the work have shown that by combining RF-sensing technology with standard machine learning algorithms such as CNN, it is possible to detect different human ac-

tivities including counting the number of people in the room with a high accuracy. The system was tested to evaluate its capability of counting as well as detecting parallel activities amongst a variable number of subject, that is, between 0 and 4, as highlighted in sections 5.3.1 and 5.3.1, respectively. The subject counting experiment reported high accuracy results between approximately 86% and 95%, with the accuracy decreasing with the increase in inter-class variations. On the other hand, the activity recognition experiment has reported approximately 80% accuracy in recognising multiple activities performed amongst all test subjects. The reported accuracy in the activity recognition experiment was greatly impacted by the intra-class variation introduced in the data. however, the variation was introduced to train the system on the maximum possible combination of input activities, to mimic a real-life scenario. the results obtained in this experiment are promising and have a high potential to be improved through more data collection and the implementation of different learning algorithms.

Furthermore, as the major focus of this work is to show the significance and effectiveness of 5G-sensing in capturing variation in CSI data caused due to human activities, therefore the work currently focuses on a small setting, such as rooms in a care home, with four persons performing three major and common activities i.e Sitting, Standing and Walking. In future, the aim is to scale it up to cover most of the human activity spectrum performed by a larger group in multiple rooms. Moreover, current implementation of the proposed system is based on one transmitter/receiver antenna pair and is giving better performance in comparison with most of the existing work where more than one transmitter and receiver antenna have been used for the same purpose. Moreover, and given the current system is a proof of concept with focus on showing the significance and effectiveness of 5G frequency band in capturing variation in CSI data, in future the experiments will be performed to assess the impact of number of rooms vs the number of transmitter/receiver antennas on the performance of proposed system, as well different heights and positions for the transmitter and receiver devices. Furthermore, and as mentioned earlier, the data set used to achieve the previously reported results is made publicly available, at [209], to encourage other researchers and the wider communities to take this system a step further.

Chapter 6

Conclusion and Future work

6.1 Conclusion

Human activity detection using radio frequency (RF) technology can be used in a wide variety of human-centric applications and usher in a new era of contactless sensor technology. HAR system based on RF signals don't need any additional devices, Unlike wearable HAR systems that have a limited range and high installment cost, which limits their practical aspects, the user doesn't need to carry or wear a device. Furthermore, it does not impinge on privacy, and it has the capability of detect activities through walls.

In this thesis, we developed a stable portable and multi-band wireless communication platform for the creation of smart health care systems using SDR technology. The design is tested through simulations and real-time experimental results, then a comprehensive background overview of activity recognition with wire and wireless sensing systems have been reviewed . In addition, a contactless platform for monitoring human movement has been presented, we begin by explaining the basics of wireless signal propagation and extraction of channel state information CSI. Afterward, MATLAB Simulink modeled and demonstrated the working principle of generating the channel sensing model using Universal Software Radio Peripheral Platform USRP. Besides, data collection and machine learning process of our data has been presented in this chapter, then we show the experimental result and discussion of the results for recognizing the activity of single subject in indoor environment. The five human activities are classified by using four machine learning algorithms, the KNN classifier provide the best accuracy recognition among all four algorithms which was 89%. The experiment findings demonstrate that the built platform is dependable, portable, scalable, flexible, and capable of performing several functions.

Furthermore, Due to COVID-19, people have trouble breathing, which can lead to a variety of health complications, both physical and mental. It is essential to create novel approaches to provide non-contact and remote assistance, which might provide better care to patients. This work demonstrates that wireless communication technologies are not utilised for multimedia applications, but it also connects devices for connected health applications. a non contact sensing

platform is exploited to diagnose breathing abnormalities in a non-contact manner. It employs Orthogonal Frequency Division Multiplexing (OFDM) with 64 subcarriers to obtain the amplitude response of the Wireless Channel State Information (WCSI). We used wearable sensors (Ground truth) to ensure that the data collected was accurate, then four machine learning algorithms are used to classify the three different breathing patterns with a maximum classification accuracy of 99.3%, the KNN is the best of the four algorithms.
Building upon these successes, a non-invasive system based on 5 G-sensing that can detect the presence and activities of multiple users in the same room has been presented. We first discussed the methodology and framework adopted to conduct the experiments, followed by a thorough explanation of the experimental design stage, covering experimental variables, data collecting, data processing, system training, and testing procedures. The system was evaluated in order to determine its capacity for counting and detecting parallel actions among a varying number of subjects. The subject counting result confirms data with an accuracy of approximately 86% to 95%. On the other hand, the activity recognition experiment demonstrated an accuracy of around 80% in identifying numerous activities conducted by all test subjects.

6.2 Future work

For future work, our aim is to make this system more generalize, acquiring data in elderly care centre or hospitals in different geometrical settings. The CSI at heterogenous environment varies also, we will develop an algorithm for calibration in future work that in independent of geometrical structure.

We have made significant progress toward enabling accurate and adaptive human activity identification over SDR technology. There are still various avenues that can be studied in future work.

• Although the research undertaken classifies the breathing pattern and activity recognition accurately. However, the limitation of this research is that it cannot be applied to health problems that are not directly related to bodily, such as sleep disorders, temperature, diabetics, etc. This research can also be applied to the early detection and monitoring of breast cancer, sleep disorders, gait disorders, and a variety of other diseases that are affected by human body motion.

• Smart sensing based on SDR technology has the potential to cover a wider area in the future by improving system gain, sample rate, and Multiple Input Multiple Output (MIMO) antennas. The phase response is another technique for identifying concurrent human activities in the same environment based on the measurement of phase delays.The wireless channel is robust in nature, and it is difficult to predict responses in changing environmental conditions. By util-

ising state-of-the-art deep and machine learning methods, it is possible to improve recognition accuracy by exploiting time and frequency domain features from extraction WCSI data.

• The proposed system works when only one person performs a single activity at a time. However, the volunteers sometimes implement more than one activity at the same time. For example, peaking on the phone while walking or eating while watching television. Distinguishing signals caused by the activity of various body sections is another challenge and future direction that is worth exploring.

• Future research will examine a substantially more diverse collection of datasets to gain a better understanding of the intricate statistical linkages between classification rate, dataset complexity/size, and the type of feature extractor/learner employed to achieve the highest accuracy.

• Future wireless sensing systems will be based on ubiquitous advanced commercial SDR technology to deliver a variety of high-precision, high-reliability, high-security, and consumer application services, the basis of which is available to the public human activities recognition technology.

• Increasing the transmission power is essential for the detection range and precision of the wireless sensing system. As a future consumer electronics product, however, high-power wireless devices are prohibited. Therefore, identifying how to perceive efficient environmental states using low-power wireless signals becomes a difficulty that must be solved by the researchers.

• Heart rate and blood pressure monitors have become more and more popular. Many families' daily needs mean that people are slowly becoming more aware of their health. Monitoring devices may be replaced in the future by wireless monitoring devices. In the future, people will be able to use medical health monitoring systems that make it easier for them to keep track of their health. Families can use a wireless sensing system so that everyone in the family can keep an eye on things like breathing and heart rate.

• Falling is one of the biggest health risks and problems for older people who want to live on their own. It also adds to the pressure on health care and injury rescue services for older people around the world. the delay of medical treatment following a fall might raise the risk of death, particularly for elderly individuals who live alone. For instance, falls among older persons cost the U.S. health care system more than $19 billion in 2000, and the figure grew to $30 billion in 2010; falls among younger adults cost the system less than $1 billion in 2000. This suffices to illustrate the far-reaching consequences of extensively deployed wireless sensing systems for medical health monitoring.

• After a natural disaster such as a fire or earthquake, the disaster scene environment is so incredibly complicated that it impedes the progress of search and rescue efforts. Therefore, rapidly and properly identifying the location of the wounded and locating the signs of life can rescue more lives in the ruins. The wireless sensing system's accurate vital signs monitoring and localization capabilities can assist rescuers in locating survivors more quickly and efficiently.

Bibliography

[1] Przemyslaw Woznowski, Alison Burrows, Tom Diethe, Xenofon Fafoutis, Jake Hall, Sion Hannuna, Massimo Camplani, Niall Twomey, Michal Kozlowski, Bo Tan, et al. Sphere: A sensor platform for healthcare in a residential environment. In *Designing, developing, and facilitating smart cities*, pages 315–333. Springer, 2017.

[2] Rajib Rana, Brano Kusy, Josh Wall, and Wen Hu. Novel activity classification and occupancy estimation methods for intelligent hvac (heating, ventilation and air conditioning) systems. *Energy*, 93:245–255, 2015.

[3] Koji Yatani and Khai N Truong. Bodyscope: a wearable acoustic sensor for activity recognition. In *Proceedings of the 2012 ACM Conference on Ubiquitous Computing*, pages 341–350, 2012.

[4] Ling Bao and Stephen S Intille. Activity recognition from user-annotated acceleration data. In *International conference on pervasive computing*, pages 1–17. Springer, 2004.

[5] Tian Hao, Guoliang Xing, and Gang Zhou. isleep: Unobtrusive sleep quality monitoring using smartphones. In *Proceedings of the 11th ACM Conference on Embedded Networked Sensor Systems*, pages 1–14, 2013.

[6] Bo Wei, Wen Hu, Mingrui Yang, and Chun Tung Chou. Radio-based device-free activity recognition with radio frequency interference. In *Proceedings of the 14th International Conference on Information Processing in Sensor Networks*, pages 154–165, 2015.

[7] Jennifer R Kwapisz, Gary M Weiss, and Samuel A Moore. Activity recognition using cell phone accelerometers. *ACM SigKDD Explorations Newsletter*, 12(2):74–82, 2011.

[8] Nishkam Ravi, Nikhil Dandekar, Preetham Mysore, and Michael L Littman. Activity recognition from accelerometer data. In *Aaai*, volume 5, pages 1541–1546. Pittsburgh, PA, 2005.

[9] Isaac Cohen and Hongxia Li. Inference of human postures by classification of 3d human body shape. In *2003 IEEE international SOI conference. Proceedings (cat. No. 03CH37443)*, pages 74–81. IEEE, 2003.

[10] Michael Harville and Dalong Li. Fast, integrated person tracking and activity recognition with plan-view templates from a single stereo camera. In *Proceedings of the 2004 IEEE Computer Society Conference on Computer Vision and Pattern Recognition, 2004. CVPR 2004.*, volume 2, pages II–II. IEEE, 2004.

[11] SU Park, JH Park, MA Al-Masni, MA Al-Antari, Md Z Uddin, and T-S Kim. A depth camera-based human activity recognition via deep learning recurrent neural network for health and social care services. *Procedia Computer Science*, 100:78–84, 2016.

[12] Nuria Oliver, Eric Horvitz, and Ashutosh Garg. Layered representations for human activity recognition. In *Proceedings. Fourth IEEE International Conference on Multimodal Interfaces*, pages 3–8. IEEE, 2002.

[13] Tao Zhao, Manoj Aggarwal, Rakesh Kumar, and Harpreet Sawhney. Real-time wide area multi-camera stereo tracking. In *2005 IEEE Computer Society Conference on Computer Vision and Pattern Recognition (CVPR'05)*, volume 1, pages 976–983. IEEE, 2005.

[14] Wei Wang, Alex X Liu, Muhammad Shahzad, Kang Ling, and Sanglu Lu. Understanding and modeling of wifi signal based human activity recognition. In *Proceedings of the 21st annual international conference on mobile computing and networking*, pages 65–76, 2015.

[15] Yu Gu, Lianghu Quan, and Fuji Ren. Wifi-assisted human activity recognition. In *2014 IEEE Asia Pacific Conference on Wireless and Mobile*, pages 60–65. IEEE, 2014.

[16] Jing Chen, Xinyu Huang, Hao Jiang, and Xiren Miao. Low-cost and device-free human activity recognition based on hierarchical learning model. *Sensors*, 21(7):2359, 2021.

[17] Xue Ding, Ting Jiang, Yi Zhong, Yan Huang, and Zhiwei Li. Wi-fi-based location-independent human activity recognition via meta learning. *Sensors*, 21(8):2654, 2021.

[18] Shangyue Zhu, Junhong Xu, Hanqing Guo, Qiwei Liu, Shaoen Wu, and Honggang Wang. Indoor human activity recognition based on ambient radar with signal processing and machine learning. In *2018 IEEE international conference on communications (ICC)*, pages 1–6. IEEE, 2018.

[19] Baris Erol and Moeness G Amin. Radar data cube processing for human activity recognition using multisubspace learning. *IEEE Transactions on Aerospace and Electronic Systems*, 55(6):3617–3628, 2019.

[20] Akash Deep Singh, Sandeep Singh Sandha, Luis Garcia, and Mani Srivastava. Radhar: Human activity recognition from point clouds generated through a millimeter-wave radar. In *Proceedings of the 3rd ACM Workshop on Millimeter-wave Networks and Sensing Systems*, pages 51–56, 2019.

[21] Xinyu Li, Yuan He, Francesco Fioranelli, and Xiaojun Jing. Semisupervised human activity recognition with radar micro-doppler signatures. *IEEE Transactions on Geoscience and Remote Sensing*, 2021.

[22] Aboajeila Milad Ashleibta, Adnan Zahid, Syed Aziz Shah, Muhammad Ali Imran, and Qammer H Abbasi. Software defined radio based testbed for large scale body movements. In *2020 IEEE International Symposium on Antennas and Propagation and North American Radio Science Meeting*, pages 2079–2080. IEEE, 2020.

[23] William Taylor, Syed Aziz Shah, Kia Dashtipour, Adnan Zahid, Qammer H Abbasi, and Muhammad Ali Imran. An intelligent non-invasive real-time human activity recognition system for next-generation healthcare. *Sensors*, 20(9):2653, 2020.

[24] Muhammad Bilal Khan, Xiaodong Yang, Aifeng Ren, Mohammed Ali Mohammed Al-Hababi, Nan Zhao, Lei Guan, Dou Fan, and Syed Aziz Shah. Design of software defined radios based platform for activity recognition. *IEEE Access*, 7:31083–31088, 2019.

[25] Yi Zhong, Ju Wang, Siliang Wu, Ting Jiang, Yan Huang, and Qiang Wu. Multilocation human activity recognition via mimo-ofdm-based wireless networks: An iot-inspired device-free sensing approach. *IEEE Internet of Things Journal*, 8(20):15148–15159, 2020.

[26] Changzhi Li, Victor M Lubecke, Olga Boric-Lubecke, and Jenshan Lin. A review on recent advances in doppler radar sensors for noncontact healthcare monitoring. *IEEE Transactions on microwave theory and techniques*, 61(5):2046–2060, 2013.

[27] Juris Klonovs, Mohammad A Haque, Volker Krueger, Kamal Nasrollahi, Karen Andersen-Ranberg, Thomas B Moeslund, and Erika G Spaich. Monitoring technology. In *Distributed Computing and Monitoring Technologies for Older Patients*, pages 49–84. Springer, 2016.

[28] Xingfa Shen, Zhenxian Ni, Lili Liu, Jian Yang, and Kabir Ahmed. Wipass: 1d-cnn-based smartphone keystroke recognition using wifi signals. *Pervasive and Mobile Computing*, 73:101393, 2021.

[29] Guanhua Wang, Yongpan Zou, Zimu Zhou, Kaishun Wu, and Lionel M Ni. We can hear you with wi-fi! *IEEE Transactions on Mobile Computing*, 15(11):2907–2920, 2016.

[30] Ju Wang, Jie Xiong, Hongbo Jiang, Kyle Jamieson, Xiaojiang Chen, Dingyi Fang, and Chen Wang. Low human-effort, device-free localization with fine-grained subcarrier information. *IEEE Transactions on Mobile Computing*, 17(11):2550–2563, 2018.

[31] Jaime Lien, Nicholas Gillian, M Emre Karagozler, Patrick Amihood, Carsten Schwesig, Erik Olson, Hakim Raja, and Ivan Poupyrev. Soli: Ubiquitous gesture sensing with millimeter wave radar. *ACM Transactions on Graphics (TOG)*, 35(4):1–19, 2016.

[32] Yu Gu, Fuji Ren, and Jie Li. Paws: Passive human activity recognition based on wifi ambient signals. *IEEE Internet of Things Journal*, 3(5):796–805, 2015.

[33] Souvik Sen, Romit Roy Choudhury, Bozidar Radunovic, and Tom Minka. Precise indoor localization using phy layer information. In *Proceedings of the 10th ACM Workshop on hot topics in networks*, pages 1–6, 2011.

[34] Ennio Gambi, Giulia Temperini, Rossana Galassi, Linda Senigagliesi, and Adelmo De Santis. Adl recognition through machine learning algorithms on iot air quality sensor dataset. *IEEE Sensors Journal*, 20(22):13562–13570, 2020.

[35] Syed Aziz Shah and Francesco Fioranelli. Rf sensing technologies for assisted daily living in healthcare: A comprehensive review. *IEEE Aerospace and Electronic Systems Magazine*, 34(11):26–44, 2019.

[36] Jake K Aggarwal and Michael S Ryoo. Human activity analysis: A review. *Acm Computing Surveys (Csur)*, 43(3):1–43, 2011.

[37] Xiaodong Yang and YingLi Tian. Super normal vector for human activity recognition with depth cameras. *IEEE transactions on pattern analysis and machine intelligence*, 39(5):1028–1039, 2016.

[38] Cuong Tran and Mohan Manubhai Trivedi. 3-d posture and gesture recognition for interactivity in smart spaces. *IEEE Transactions on Industrial Informatics*, 8(1):178–187, 2011.

[39] Aaron F. Bobick and James W. Davis. The recognition of human movement using temporal templates. *IEEE Transactions on pattern analysis and machine intelligence*, 23(3):257–267, 2001.

[40] Ali Al-Raziqi and Joachim Denzler. Unsupervised group activity detection by hierarchical dirichlet processes. In *International Conference Image Analysis and Recognition*, pages 399–407. Springer, 2017.

[41] Zhiwei Deng, Arash Vahdat, Hexiang Hu, and Greg Mori. Structure inference machines: Recurrent neural networks for analyzing relations in group activity recognition. In *Proceedings of the IEEE conference on computer vision and pattern recognition*, pages 4772–4781, 2016.

[42] Andreas Bulling, Ulf Blanke, and Bernt Schiele. A tutorial on human activity recognition using body-worn inertial sensors. *ACM Computing Surveys (CSUR)*, 46(3):1–33, 2014.

[43] Oscar D Lara and Miguel A Labrador. A survey on human activity recognition using wearable sensors. *IEEE communications surveys & tutorials*, 15(3):1192–1209, 2012.

[44] Yin Zhang, Raffaele Gravina, Huimin Lu, Massimo Villari, and Giancarlo Fortino. Pea: Parallel electrocardiogram-based authentication for smart healthcare systems. *Journal of Network and Computer Applications*, 117:10–16, 2018.

[45] Zhenghua Chen, Qingchang Zhu, Yeng Chai Soh, and Le Zhang. Robust human activity recognition using smartphone sensors via ct-pca and online svm. *IEEE Transactions on Industrial Informatics*, 13(6):3070–3080, 2017.

[46] Yi-Ting Chiang, Kuo-Chung Hsu, Ching-Hu Lu, Li-Chen Fu, and Jane Yung-Jen Hsu. Interaction models for multiple-resident activity recognition in a smart home. In *2010 IEEE/RSJ International Conference on Intelligent Robots and Systems*, pages 3753–3758. IEEE, 2010.

[47] Masayuki Nakatsuka, H Iwatani, and Jiro Katto. A study on passive crowd density estimation using wireless sensors. In *The 4th Intl. Conf. on Mobile Computing and Ubiquitous Networking (ICMU 2008)*. Citeseer, 2008.

[48] Heba Abdelnasser, Moustafa Youssef, and Khaled A Harras. Wigest: A ubiquitous wifi-based gesture recognition system. In *2015 IEEE conference on computer communications (INFOCOM)*, pages 1472–1480. IEEE, 2015.

[49] Moustafa Youssef, Matthew Mah, and Ashok Agrawala. Challenges: device-free passive localization for wireless environments. In *Proceedings of the 13th annual ACM international conference on Mobile computing and networking*, pages 222–229, 2007.

[50] Neal Patwari and Joey Wilson. Spatial models for human motion-induced signal strength variance on static links. *IEEE Transactions on Information Forensics and Security*, 6(3):791–802, 2011.

[51] Robert Moore, Richard Howard, Pavel Kuksa, and Richard P Martin. A geometric approach to device-free motion localization using signal strength. 2010.

[52] Ahmed E Kosba, Ahmed Saeed, and Moustafa Youssef. Rasid: A robust wlan device-free passive motion detection system. In *2012 IEEE International Conference on Pervasive Computing and Communications*, pages 180–189. IEEE, 2012.

[53] Stephan Sigg, Shuyu Shi, Felix Buesching, Yusheng Ji, and Lars Wolf. Leveraging rf-channel fluctuation for activity recognition: Active and passive systems, continuous and

rssi-based signal features. In *Proceedings of International Conference on Advances in Mobile Computing & Multimedia*, pages 43–52, 2013.

[54] Stephan Sigg, Markus Scholz, Shuyu Shi, Yusheng Ji, and Michael Beigl. Rf-sensing of activities from non-cooperative subjects in device-free recognition systems using ambient and local signals. *IEEE Transactions on Mobile Computing*, 13(4):907–920, 2013.

[55] Apidet Booranawong, Nattha Jindapetch, and Hiroshi Saito. A system for detection and tracking of human movements using rssi signals. *IEEE sensors journal*, 18(6):2531–2544, 2018.

[56] Wenfeng He, Kaishun Wu, Yongpan Zou, and Zhong Ming. Wig: Wifi-based gesture recognition system. In *2015 24th International Conference on Computer Communication and Networks (ICCCN)*, pages 1–7. IEEE, 2015.

[57] Pedro Melgarejo, Xinyu Zhang, Parameswaran Ramanathan, and David Chu. Leveraging directional antenna capabilities for fine-grained gesture recognition. In *Proceedings of the 2014 ACM International Joint Conference on pervasive and ubiquitous computing*, pages 541–551, 2014.

[58] Xiang Li, Daqing Zhang, Jie Xiong, Yue Zhang, Shengjie Li, Yasha Wang, and Hong Mei. Training-free human vitality monitoring using commodity wi-fi devices. *Proceedings of the ACM on Interactive, Mobile, Wearable and Ubiquitous Technologies*, 2(3):1–25, 2018.

[59] Sang-Chul Kim, Tae Gi Kim, and Sung Hyun Kim. Human activity recognition and prediction based on wi-fi channel state information and machine learning. In *2019 International Conference on Artificial Intelligence in Information and Communication (ICAIIC)*, pages 418–422. IEEE, 2019.

[60] Hoonyong Lee, Changbum R Ahn, Nakjung Choi, Toseung Kim, and Hyunsoo Lee. The effects of housing environments on the performance of activity-recognition systems using wi-fi channel state information: An exploratory study. *Sensors*, 19(5):983, 2019.

[61] Fangxin Wang, Wei Gong, and Jiangchuan Liu. On spatial diversity in wifi-based human activity recognition: A deep learning-based approach. *IEEE Internet of Things Journal*, 6(2):2035–2047, 2018.

[62] Daqing Zhang, Hao Wang, and Dan Wu. Toward centimeter-scale human activity sensing with wi-fi signals. *Computer*, 50(1):48–57, 2017.

[63] Neena Damodaran, Elis Haruni, Muyassar Kokhkharova, and Jörg Schäfer. Device free human activity and fall recognition using wifi channel state information (csi). *CCF Transactions on Pervasive Computing and Interaction*, 2(1):1–17, 2020.

[64] Wei Wang, Alex X Liu, Muhammad Shahzad, Kang Ling, and Sanglu Lu. Device-free human activity recognition using commercial wifi devices. *IEEE Journal on Selected Areas in Communications*, 35(5):1118–1131, 2017.

[65] Jiguang Lv, Dapeng Man, Wu Yang, Xiaojiang Du, and Miao Yu. Robust wlan-based indoor intrusion detection using phy layer information. *IEEE Access*, 6:30117–30127, 2017.

[66] Mauro De Sanctis, Ernestina Cianca, Simone Di Domenico, Daniele Provenziani, Giuseppe Bianchi, and Marina Ruggieri. Wibecam: Device free human activity recognition through wifi beacon-enabled camera. In *Proceedings of the 2nd workshop on Workshop on Physical Analytics*, pages 7–12, 2015.

[67] Yan Wang, Jian Liu, Yingying Chen, Marco Gruteser, Jie Yang, and Hongbo Liu. E-eyes: device-free location-oriented activity identification using fine-grained wifi signatures. In *Proceedings of the 20th annual international conference on Mobile computing and networking*, pages 617–628, 2014.

[68] Kun Qian, Chenshu Wu, Zheng Yang, Yunhao Liu, Fugui He, and Tianzhang Xing. Enabling contactless detection of moving humans with dynamic speeds using csi. *ACM Transactions on Embedded Computing Systems (TECS)*, 17(2):1–18, 2018.

[69] Sameera Palipana, Piyush Agrawal, and Dirk Pesch. Channel state information based human presence detection using non-linear techniques. In *Proceedings of the 3rd ACM International Conference on Systems for Energy-Efficient Built Environments*, pages 177–186, 2016.

[70] Meiguang Liu, Lei Zhang, Panlong Yang, Liangfu Lu, and Liangyi Gong. Wi-run: Device-free step estimation system with commodity wi-fi. *Journal of Network and Computer Applications*, 143:77–88, 2019.

[71] Dan Wu, Daqing Zhang, Chenren Xu, Yasha Wang, and Hao Wang. Widir: walking direction estimation using wireless signals. In *Proceedings of the 2016 ACM international joint conference on pervasive and ubiquitous computing*, pages 351–362, 2016.

[72] Simone Di Domenico, Mauro De Sanctis, Ernestina Cianca, and Marina Ruggieri. Wifi-based through-the-wall presence detection of stationary and moving humans analyzing the doppler spectrum. *IEEE Aerospace and Electronic Systems Magazine*, 33(5-6):14–19, 2018.

[73] Qizhen Zhou, Jianchun Xing, and Qiliang Yang. Device-free occupant activity recognition in smart offices using intrinsic wi-fi components. *Building and Environment*, 172:106737, 2020.

[74] Sheheryar Arshad, Chunhai Feng, Yonghe Liu, Yupeng Hu, Ruiyun Yu, Siwang Zhou, and Heng Li. Wi-chase: A wifi based human activity recognition system for sensorless environments. In *2017 IEEE 18th International Symposium on A World of Wireless, Mobile and Multimedia Networks (WoWMoM)*, pages 1–6. IEEE, 2017.

[75] Linlin Guo, Lei Wang, Chuang Lin, Jialin Liu, Bingxian Lu, Jian Fang, Zhonghao Liu, Zeyang Shan, Jingwen Yang, and Silu Guo. Wiar: A public dataset for wifi-based activity recognition. *IEEE Access*, 7:154935–154945, 2019.

[76] Heju Li, Xin He, Xukai Chen, Yinyin Fang, and Qun Fang. Wi-motion: A robust human activity recognition using wifi signals. *IEEE Access*, 7:153287–153299, 2019.

[77] Syed Aziz Shah, Jawad Ahmad, Ahsen Tahir, Fawad Ahmed, Gordon Russell, Syed Yaseen Shah, William J Buchanan, and Qammer H Abbasi. Privacy-preserving non-wearable occupancy monitoring system exploiting wi-fi imaging for next-generation body centric communication. *Micromachines*, 11(4):379, 2020.

[78] Linsong Cheng and Jiliang Wang. Walls have no ears: A non-intrusive wifi-based user identification system for mobile devices. *IEEE/ACM Transactions on Networking*, 27(1):245–257, 2019.

[79] Muhammad Bilal Khan, Ali Mustafa, Mubashir Rehman, Najah Abed AbuAli, Chang Yuan, Xiaodong Yang, Fiaz Hussain Shah, and Qammer H Abbasi. Non-contact smart sensing of physical activities during quarantine period using sdr technology. *Sensors*, 22(4):1348, 2022.

[80] Tahmid Z Chowdhury. *Using Wi-Fi channel state information (CSI) for human activity recognition and fall detection*. PhD thesis, University of British Columbia, 2018.

[81] Xu Yang, Fangyuan Xiong, Yuan Shao, and Qiang Niu. Wmfall: Wifi-based multistage fall detection with channel state information. *International Journal of Distributed Sensor Networks*, 14(10):1550147718805718, 2018.

[82] Sankalp Dayal, Hirokazu Narui, and Paraskevas Deligiannis. Human fall detection in indoor environments using channel state information of wi-fi signals. *Stanford University, Published*, 2015.

[83] Hao Wang, Daqing Zhang, Yasha Wang, Junyi Ma, Yuxiang Wang, and Shengjie Li. Rt-fall: A real-time and contactless fall detection system with commodity wifi devices. *IEEE Transactions on Mobile Computing*, 16(2):511–526, 2016.

[84] Wenchang Cao, Xinhua Liu, and Fangmin Li. Robust device-free fall detection using fine-grained wi-fi signatures. In *2017 IEEE 2nd Advanced Information Technology, Electronic and Automation Control Conference (IAEAC)*, pages 1404–1408. IEEE, 2017.

[85] Yuxi Wang, Kaishun Wu, and Lionel M Ni. Wifall: Device-free fall detection by wireless networks. *IEEE Transactions on Mobile Computing*, 16(2):581–594, 2016.

[86] Alireza Borhani and Matthias Pätzold. A non-stationary channel model for the development of non-wearable radio fall detection systems. *IEEE Transactions on Wireless Communications*, 17(11):7718–7730, 2018.

[87] Daniyal Haider, Xiaodong Yang, and Qammer Hussain Abbasi. Post-surgical fall detection by exploiting the 5 g c-band technology for ehealth paradigm. *Applied Soft Computing*, 81:105537, 2019.

[88] Usman Mahmood Khan, Zain Kabir, and Syed Ali Hassan. Wireless health monitoring using passive wifi sensing. In *2017 13th International Wireless Communications and Mobile Computing Conference (IWCMC)*, pages 1771–1776. IEEE, 2017.

[89] Zizheng Zhang, Shigemi Ishida, Shigeaki Tagashira, and Akira Fukuda. Danger-pose detection system using commodity wi-fi for bathroom monitoring. *Sensors*, 19(4):884, 2019.

[90] Sangeeta Goyal, Shobha Sundar Ram, and Vivek Ashok Bohara. *USRP based through wall radar*. PhD thesis, 2016.

[91] Xiaolin Ma, Running Zhao, Xinhua Liu, Hailan Kuang, and Mohammed AA Al-Qaness. Classification of human motions using micro-doppler radar in the environments with micro-motion interference. *Sensors*, 19(11):2598, 2019.

[92] Sandra Costanzo, Francesco Spadafora, Giuseppe Di Massa, Antonio Borgia, Antonio Costanzo, Ginaluca Aloi, Pasquale Pace, Valeria Loscri, and Hugo Oswaldo Moreno. Potentialities of usrp-based software defined radar systems. *Progress In Electromagnetics Research B*, 53, 2013.

[93] Adel Alzogaiby. *Using micro-Doppler radar signals for human gait detection*. PhD thesis, Stellenbosch: Stellenbosch University, 2014.

[94] Youngwook Kim, Sungjae Ha, and Jihoon Kwon. Human detection using doppler radar based on physical characteristics of targets. *IEEE Geoscience and Remote Sensing Letters*, 12(2):289–293, 2014.

[95] Fadel Adib and Dina Katabi. See through walls with wifi! In *Proceedings of the ACM SIGCOMM 2013 conference on SIGCOMM*, pages 75–86, 2013.

[96] Jingmiao Wu, Jie Wang, Qinghua Gao, Miao Pan, and Haixia Zhang. Path-independent device-free gait recognition using mmwave signals. *IEEE Transactions on Vehicular Technology*, 70(11):11582–11592, 2021.

[97] Fadel Adib, Zach Kabelac, Dina Katabi, and Robert C Miller. 3d tracking via body radio reflections. In *11th USENIX Symposium on Networked Systems Design and Implementation (NSDI 14)*, pages 317–329, 2014.

[98] Xiaodong Yang, Syed Aziz Shah, Aifeng Ren, Nan Zhao, Dou Fan, Fangming Hu, Masood Ur Rehman, Karen M von Deneen, and Jie Tian. Wandering pattern sensing at s-band. *IEEE journal of biomedical and health informatics*, 22(6):1863–1870, 2017.

[99] Francesco Fioranelli, Julien Le Kernec, and Syed Aziz Shah. Radar for health care: Recognizing human activities and monitoring vital signs. *IEEE Potentials*, 38(4):16–23, 2019.

[100] Qian Wan, Yiran Li, Changzhi Li, and Ranadip Pal. Gesture recognition for smart home applications using portable radar sensors. In *2014 36th annual international conference of the IEEE engineering in medicine and biology society*, pages 6414–6417. IEEE, 2014.

[101] Zhenyuan Zhang, Zengshan Tian, and Mu Zhou. Latern: Dynamic continuous hand gesture recognition using fmcw radar sensor. *IEEE Sensors Journal*, 18(8):3278–3289, 2018.

[102] Qifan Pu, Sidhant Gupta, Shyamnath Gollakota, and Shwetak Patel. Whole-home gesture recognition using wireless signals. In *Proceedings of the 19th annual international conference on Mobile computing & networking*, pages 27–38, 2013.

[103] Chuanwei Ding, Yu Zou, Li Sun, Hong Hong, Xiaohua Zhu, and Changzhi Li. Fall detection with multi-domain features by a portable fmcw radar. In *2019 IEEE MTT-S International Wireless Symposium (IWS)*, pages 1–3. IEEE, 2019.

[104] Syed Aziz Shah and Francesco Fioranelli. Human activity recognition: Preliminary results for dataset portability using fmcw radar. In *2019 International Radar Conference (RADAR)*, pages 1–4. IEEE, 2019.

[105] Fei Luo, Stefan Poslad, and Eliane Bodanese. Human activity detection and coarse localization outdoors using micro-doppler signatures. *IEEE Sensors Journal*, 19(18):8079–8094, 2019.

[106] Ram M Narayanan, Mahesh C Shastry, Pin-Heng Chen, and Mark Levi. Through-the-wall detection of stationary human targets using doppler radar. *Progress In Electromagnetics Research B*, 20:147–166, 2010.

[107] Bahri Çağlıyan and Sevgi Zübeyde Gürbüz. Micro-doppler-based human activity classification using the mote-scale bumblebee radar. *IEEE Geoscience and Remote Sensing Letters*, 12(10):2135–2139, 2015.

[108] Wenda Li, Bo Tan, and Robert Piechocki. Passive radar for opportunistic monitoring in e-health applications. *IEEE journal of translational engineering in health and medicine*, 6:1–10, 2018.

[109] Håkan Jonsson and Pierre Nugues. Group affiliation detection in a challenging environment. *Procedia Computer Science*, 141:507–512, 2018.

[110] Claudio Guerra, Valentina Bianchi, Ilaria De Munari, and Paolo Ciampolini. Action tagging in a multi-user indoor environment for behavioural analysis purposes. In *2015 37th Annual International Conference of the IEEE Engineering in Medicine and Biology Society (EMBC)*, pages 5036–5039. IEEE, 2015.

[111] Alvarez Jose, Leppanen Teemu, Iwai Masayuki, Kobayashi Hiroki, and Sezaki Kaoru. A method for grouping smartphone users based on wi-fi signal strength. In *11th International Conference on Frontiers of Information Technology (FIT)*, pages 449–452, 2013.

[112] Sheng Tan, Linghan Zhang, Zi Wang, and Jie Yang. Multitrack: Multi-user tracking and activity recognition using commodity wifi. In *Proceedings of the 2019 CHI Conference on Human Factors in Computing Systems*, pages 1–12, 2019.

[113] Raghav H Venkatnarayan, Griffin Page, and Muhammad Shahzad. Multi-user gesture recognition using wifi. In *Proceedings of the 16th Annual International Conference on Mobile Systems, Applications, and Services*, pages 401–413, 2018.

[114] Zihao Zhao, Yue Li, Zhijun Yan, Yiyang Luo, Hushan Wang, Qizhen Sun, Deming Liu, and Lin Zhang. Highly polarized multiwavelength er-doped fibre laser using all fibre lyot filter. In *2017 16th International Conference on Optical Communications and Networks (ICOCN)*, pages 1–3. IEEE, 2017.

[115] Adrian Lin and Hao Ling. Doppler and direction-of-arrival (ddoa) radar for multiple-mover sensing. *IEEE transactions on aerospace and electronic systems*, 43(4):1496–1509, 2007.

[116] Saandeep Depatla, Arjun Muralidharan, and Yasamin Mostofi. Occupancy estimation using only wifi power measurements. *IEEE Journal on Selected Areas in Communications*, 33(7):1381–1393, 2015.

[117] Chenren Xu, Bernhard Firner, Robert S Moore, Yanyong Zhang, Wade Trappe, Richard Howard, Feixiong Zhang, and Ning An. Scpl: Indoor device-free multi-subject counting and localization using radio signal strength. In *Proceedings of the 12th international conference on Information Processing in Sensor Networks*, pages 79–90, 2013.

[118] Moustafa Seifeldin, Ahmed Saeed, Ahmed E Kosba, Amr El-Keyi, and Moustafa Youssef. Nuzzer: A large-scale device-free passive localization system for wireless environments. *IEEE Transactions on Mobile Computing*, 12(7):1321–1334, 2012.

[119] Wei Xi, Jizhong Zhao, Xiang-Yang Li, Kun Zhao, Shaojie Tang, Xue Liu, and Zhiping Jiang. Electronic frog eye: Counting crowd using wifi. In *IEEE INFOCOM 2014-IEEE Conference on Computer Communications*, pages 361–369. IEEE, 2014.

[120] Yaoxuan Yuan, Chen Qiu, Wei Xi, and Jizhong Zhao. Crowd density estimation using wireless sensor networks. In *2011 seventh international conference on mobile Ad-hoc and sensor networks*, pages 138–145. IEEE, 2011.

[121] He Li, Kaoru Ota, Mianxiong Dong, and Minyi Guo. Learning human activities through wi-fi channel state information with multiple access points. *IEEE Communications Magazine*, 56(5):124–129, 2018.

[122] Masaya Arai, Hidenori Kawamura, and Keiji Suzuki. Estimation of zigbee's rssi fluctuated by crowd behavior in indoor space. In *Proceedings of SICE Annual Conference 2010*, pages 696–701. IEEE, 2010.

[123] Fadel Adib, Zachary Kabelac, Hongzi Mao, Dina Katabi, and Robert C Miller. Real-time breath monitoring using wireless signals. In *Proceedings of the 20th annual international conference on Mobile computing and networking*, pages 261–262, 2014.

[124] Wenda Li, Bo Tan, and Robert J Piechocki. Non-contact breathing detection using passive radar. In *2016 IEEE International Conference on Communications (ICC)*, pages 1–6. IEEE, 2016.

[125] Muhammad Bilal Khan, Mubashir Rehman, Ali Mustafa, Raza Ali Shah, and Xiaodong Yang. Intelligent non-contact sensing for connected health using software defined radio technology. *Electronics*, 10(13):1558, 2021.

[126] Aboajeila Milad Ashleibta, Qammer H Abbasi, Syed Aziz Shah, Muhammad Arslan Khalid, Najah Abed AbuAli, and Muhammad Ali Imran. Non-invasive rf sensing for detecting breathing abnormalities using software defined radios. *IEEE Sensors Journal*, 21(4):5111–5118, 2020.

[127] Mubashir Rehman, Raza Ali Shah, Muhammad Bilal Khan, Najah Abed Abu Ali, Abdullah Alhumaidi Alotaibi, Turke Althobaiti, Naeem Ramzan, Syed Aziz Shah, Xiaodong Yang, Akram Alomainy, et al. Contactless small-scale movement monitoring system using software defined radio for early diagnosis of covid-19. *IEEE Sensors Journal*, 21(15):17180–17188, 2021.

[128] Sandra Costanzo. Software-defined doppler radar sensor for human breathing detection. *Sensors*, 19(14):3085, 2019.

[129] Fadel Adib, Hongzi Mao, Zachary Kabelac, Dina Katabi, and Robert C Miller. Smart homes that monitor breathing and heart rate. In *Proceedings of the 33rd annual ACM conference on human factors in computing systems*, pages 837–846, 2015.

[130] Sangyoun Lee, Young-Deok Park, Young-Joo Suh, and Seokseong Jeon. Design and implementation of monitoring system for breathing and heart rate pattern using wifi signals. In *2018 15th IEEE Annual Consumer Communications & Networking Conference (CCNC)*, pages 1–7. IEEE, 2018.

[131] Xuyu Wang, Chao Yang, and Shiwen Mao. Tensorbeat: Tensor decomposition for monitoring multiperson breathing beats with commodity wifi. *ACM Transactions on Intelligent Systems and Technology (TIST)*, 9(1):1–27, 2017.

[132] Jian Liu, Yan Wang, Yingying Chen, Jie Yang, Xu Chen, and Jerry Cheng. Tracking vital signs during sleep leveraging off-the-shelf wifi. In *Proceedings of the 16th ACM international symposium on mobile ad hoc networking and computing*, pages 267–276, 2015.

[133] Neal Patwari, Lara Brewer, Quinn Tate, Ossi Kaltiokallio, and Maurizio Bocca. Breathfinding: A wireless network that monitors and locates breathing in a home. *IEEE Journal of Selected Topics in Signal Processing*, 8(1):30–42, 2013.

[134] Ossi Kaltiokallio, Hüseyin Yiğitler, Riku Jäntti, and Neal Patwari. Non-invasive respiration rate monitoring using a single cots tx-rx pair. In *IPSN-14 Proceedings of the 13th International Symposium on Information Processing in Sensor Networks*, pages 59–69. IEEE, 2014.

[135] Heba Abdelnasser, Khaled A Harras, and Moustafa Youssef. Ubibreathe: A ubiquitous non-invasive wifi-based breathing estimator. In *Proceedings of the 16th ACM International Symposium on Mobile Ad Hoc Networking and Computing*, pages 277–286, 2015.

[136] Zhicheng Yang, Parth H Pathak, Yunze Zeng, Xixi Liran, and Prasant Mohapatra. Monitoring vital signs using millimeter wave. In *Proceedings of the 17th ACM international symposium on mobile ad hoc networking and computing*, pages 211–220, 2016.

[137] Neal Patwari, Joey Wilson, Sai Ananthanarayanan, Sneha K Kasera, and Dwayne R Westenskow. Monitoring breathing via signal strength in wireless networks. *IEEE Transactions on Mobile Computing*, 13(8):1774–1786, 2013.

[138] Youwei Zeng, Dan Wu, Ruiyang Gao, Tao Gu, and Daqing Zhang. Fullbreathe: Full human respiration detection exploiting complementarity of csi phase and amplitude of wifi signals. *Proceedings of the ACM on Interactive, Mobile, Wearable and Ubiquitous Technologies*, 2(3):1–19, 2018.

[139] Hao Wang, Daqing Zhang, Junyi Ma, Yasha Wang, Yuxiang Wang, Dan Wu, Tao Gu, and Bing Xie. Human respiration detection with commodity wifi devices: do user location and body orientation matter? In *Proceedings of the 2016 ACM International Joint Conference on Pervasive and Ubiquitous Computing*, pages 25–36, 2016.

[140] Xuefeng Liu, Jiannong Cao, Shaojie Tang, and Jiaqi Wen. Wi-sleep: Contactless sleep monitoring via wifi signals. In *2014 IEEE Real-Time Systems Symposium*, pages 346–355. IEEE, 2014.

[141] Fan Li, Cheng Xu, Yang Liu, Yun Zhang, Zhuo Li, Kashif Sharif, and Yu Wang. Mosleep: Unobtrusive sleep and movement monitoring via wi-fi signal. In *2016 IEEE 35th International Performance Computing and Communications Conference (IPCCC)*, pages 1–8. IEEE, 2016.

[142] Jiang Wang, Zicheng Liu, Ying Wu, and Junsong Yuan. Mining actionlet ensemble for action recognition with depth cameras. In *2012 IEEE Conference on Computer Vision and Pattern Recognition*, pages 1290–1297. IEEE, 2012.

[143] Isah A Lawal and Sophia Bano. Deep human activity recognition using wearable sensors. In *Proceedings of the 12th ACM International Conference on PErvasive Technologies Related to Assistive Environments*, pages 45–48, 2019.

[144] Markus Scholz, Till Riedel, Mario Hock, and Michael Beigl. Device-free and device-bound activity recognition using radio signal strength. In *Proceedings of the 4th augmented human international conference*, pages 100–107, 2013.

[145] Neena Damodaran and Jörg Schäfer. Device free human activity recognition using wifi channel state information. In *2019 IEEE SmartWorld, Ubiquitous Intelligence & Computing, Advanced & Trusted Computing, Scalable Computing & Communications, Cloud & Big Data Computing, Internet of People and Smart City Innovation (SmartWorld/SCALCOM/UIC/ATC/CBDCom/IOP/SCI)*, pages 1069–1074. IEEE, 2019.

[146] Syed Aziz Shah, Aifeng Ren, Dou Fan, Zhiya Zhang, Nan Zhao, Xiaodong Yang, Ming Luo, Weigang Wang, Fangming Hu, Masood Ur Rehman, et al. Internet of things for sensing: A case study in the healthcare system. *Applied sciences*, 8(4):508, 2018.

[147] Matt Ettus. Usrp users and developers guide. *www. olifantasia. com/gnuradio/usrp/files/usrp_guide. pdf*, 2005.

[148] Lei Zhang. *Implementation of wireless communication based on software defined radio*. PhD thesis, E_Telecomunicacion, 2013.

[149] Chao Wang, Siwen Chen, Yanwei Yang, Feng Hu, Fugang Liu, and Jie Wu. Literature review on wireless sensing-wi-fi signal-based recognition of human activities. *Tsinghua Science and Technology*, 23(2):203–222, 2018.

[150] Chenshu Wu, Zheng Yang, Zimu Zhou, Xuefeng Liu, Yunhao Liu, and Jiannong Cao. Non-invasive detection of moving and stationary human with wifi. *IEEE Journal on Selected Areas in Communications*, 33(11):2329–2342, 2015.

[151] Chih-Yu Wang and Hung-Yu Wei. Ieee 802.11 n mac enhancement and performance evaluation. *Mobile Networks and Applications*, 14(6):760–771, 2009.

[152] Daniel Halperin, Wenjun Hu, Anmol Sheth, and David Wetherall. Predictable 802.11 packet delivery from wireless channel measurements. *ACM SIGCOMM computer communication review*, 40(4):159–170, 2010.

[153] Xiaodong Yang, Syed Aziz Shah, Aifeng Ren, Nan Zhao, Zhiya Zhang, Dou Fan, Jianxun Zhao, Weigang Wang, and Masood Ur-Rehman. Freezing of gait detection considering leaky wave cable. *IEEE Transactions on Antennas and Propagation*, 67(1):554–561, 2018.

[154] Noushin Karimian. *Design and analysis of OFDM system for powerline based communication*. PhD thesis, University of Central Lancashire, 2012.

[155] Zhengjie Wang, Kangkang Jiang, Yushan Hou, Zehua Huang, Wenwen Dou, Chengming Zhang, and Yinjing Guo. A survey on csi-based human behavior recognition in through-the-wall scenario. *IEEE Access*, 7:78772–78793, 2019.

[156] Y Lu, SH Lv, XD Wang, XM Zhou, et al. A survey on wifi based human behavior analysis technology. *Chin. J. Comput*, 41(27):1–22, 2018.

[157] Jiangang Hao and Tin Kam Ho. Machine learning made easy: a review of scikit-learn package in python programming language. *Journal of Educational and Behavioral Statistics*, 44(3):348–361, 2019.

[158] Luca Pappalardo, Filippo Simini, Gianni Barlacchi, and Roberto Pellungrini. scikit-mobility: A python library for the analysis, generation and risk assessment of mobility data. *arXiv preprint arXiv:1907.07062*, 2019.

[159] Banu Saçlı, Cemanur Aydınalp, Gökhan Cansız, Sulayman Joof, Tuba Yilmaz, Mehmet Çayören, Bülent Önal, and Ibrahim Akduman. Microwave dielectric property based clas-

sification of renal calculi: Application of a knn algorithm. *Computers in biology and medicine*, 112:103366, 2019.

[160] Kunming Li, Yijun Gu, Peijing Zhang, Wang An, and Wenzheng Li. Research on knn algorithm in malicious pdf files classification under adversarial environment. In *Proceedings of the 2019 4th International Conference on Big Data and Computing*, pages 156–159, 2019.

[161] Torgyn Shaikhina, Dave Lowe, Sunil Daga, David Briggs, Robert Higgins, and Natasha Khovanova. Decision tree and random forest models for outcome prediction in antibody incompatible kidney transplantation. *Biomedical Signal Processing and Control*, 52:456–462, 2019.

[162] Zhefu Wu, Qiang Xu, Jianan Li, Chenbo Fu, Qi Xuan, and Yun Xiang. Passive indoor localization based on csi and naive bayes classification. *IEEE Transactions on Systems, Man, and Cybernetics: Systems*, 48(9):1566–1577, 2017.

[163] Daniel De Backer, Fabio Silvio Taccone, Roland Holsten, Fayssal Ibrahimi, and Jean-Louis Vincent. Influence of respiratory rate on stroke volume variation in mechanically ventilated patients. *The Journal of the American Society of Anesthesiologists*, 110(5):1092–1097, 2009.

[164] Racheal Parkes. Rate of respiration: the forgotten vital sign. *Emergency Nurse*, 19(2), 2011.

[165] Nastaran Hesam Shariati and Edmond Zahedi. Comparison of selected parametric models for analysis of the photoplethysmographic signal. In *2005 1st International Conference on Computers, Communications, & Signal Processing with Special Track on Biomedical Engineering*, pages 169–172. IEEE, 2005.

[166] L Robert Mogue and Boerje Rantala. Capnometers. *Journal of clinical monitoring*, 4(2):115–121, 1988.

[167] Marek Bartula, Timo Tigges, and Jens Muehlsteff. Camera-based system for contactless monitoring of respiration. In *2013 35th Annual International Conference of the IEEE Engineering in Medicine and Biology Society (EMBC)*, pages 2672–2675. IEEE, 2013.

[168] Ming-Zher Poh, Daniel J McDuff, and Rosalind W Picard. Non-contact, automated cardiac pulse measurements using video imaging and blind source separation. *Optics express*, 18(10):10762–10774, 2010.

[169] Amy D Droitcour, Olga Boric-Lubecke, and Gregory TA Kovacs. Signal-to-noise ratio in doppler radar system for heart and respiratory rate measurements. *IEEE transactions on microwave theory and techniques*, 57(10):2498–2507, 2009.

[170] Amy D Droitcour, Olga Boric-Lubecke, Victor M Lubecke, Jenshan Lin, and Gregory TA Kovacs. Range correlation and i/q performance benefits in single-chip silicon doppler radars for noncontact cardiopulmonary monitoring. *IEEE Transactions on Microwave Theory and Techniques*, 52(3):838–848, 2004.

[171] Yifan Chen and Predrag Rapajic. Human respiration rate estimation using ultra-wideband distributed cognitive radar system. *International Journal of Automation and Computing*, 5(4):325–333, 2008.

[172] Antonio Lazaro, David Girbau, and Ramon Villarino. Analysis of vital signs monitoring using an ir-uwb radar. *Progress In Electromagnetics Research*, 100:265–284, 2010.

[173] Youwei Zeng, Dan Wu, Jie Xiong, Enze Yi, Ruiyang Gao, and Daqing Zhang. Farsense: Pushing the range limit of wifi-based respiration sensing with csi ratio of two antennas. *Proceedings of the ACM on Interactive, Mobile, Wearable and Ubiquitous Technologies*, 3(3):1–26, 2019.

[174] Syed Aziz Shah, Ahsen Tahir, Jawad Ahmad, Adnan Zahid, Haris Pervaiz, Syed Yaseen Shah, Aboajeila Milad Abdulhadi Ashleibta, Aamir Hasanali, Shadan Khattak, and Qammer H Abbasi. Sensor fusion for identification of freezing of gait episodes using wi-fi and radar imaging. *IEEE Sensors Journal*, 20(23):14410–14422, 2020.

[175] Darrell M West. How 5g technology enables the health internet of things. *Brookings Center for Technology Innovation*, 3:1–20, 2016.

[176] Diane J Cook, Maureen Schmitter-Edgecombe, and Prafulla Dawadi. Analyzing activity behavior and movement in a naturalistic environment using smart home techniques. *IEEE journal of biomedical and health informatics*, 19(6):1882–1892, 2015.

[177] Behdad Dehbandi, Alexandre Barachant, Anna H Smeragliuolo, John Davis Long, Silverio Joseph Bumanlag, Victor He, Anna Lampe, and David Putrino. Using data from the microsoft kinect 2 to determine postural stability in healthy subjects: A feasibility trial. *PloS one*, 12(2):e0170890, 2017.

[178] Ahmad Taha, Ruiheng Wu, Anthony Emeakaroha, and Jan Krabicka. Reduction of electricity costs in medway nhs by inducing pro-environmental behaviour using persuasive technology. *Future Cities and Environment*, 4(1), 2018.

[179] Basel Barakat, Ahmad Taha, Ryan Samson, Aiste Steponenaite, Shuja Ansari, Patrick M Langdon, Ian J Wassell, Qammer H Abbasi, Muhammad Ali Imran, and Simeon Keates. 6g opportunities arising from internet of things use cases: a review paper. *Future Internet*, 13(6):159, 2021.

[180] Ahmad Taha, Jan Krabicka, Ruiheng Wu, Peter Kyberd, and Neil Adams. Design of an occupancy monitoring unit: a thermal imaging based people counting solution for socio-technical energy saving systems in hospitals. In *2019 11th Computer Science and Electronic Engineering (CEEC)*, pages 1–6. IEEE, 2019.

[181] F Valentina, A Rune, and P Stefano. A methodology for modelling energy-related human behavior: Application to window opening behavior in residential buildings [j]. In *Building Simulation*, volume 6, pages 415–427, 2013.

[182] Davide Calì, Tanja Osterhage, Rita Streblow, and Dirk Müller. Energy performance gap in refurbished german dwellings: Lesson learned from a field test. *Energy and buildings*, 127:1146–1158, 2016.

[183] Rune Vinther Andersen. Occupant behaviour with regard to control of the indoor environment. *Technical University of Denmark*, 776:777, 2009.

[184] Vytautas Martinaitis, Edmundas Kazimieras Zavadskas, Violeta Motuzienė, and Tatjana Vilutienė. Importance of occupancy information when simulating energy demand of energy efficient house: A case study. *Energy and Buildings*, 101:64–75, 2015.

[185] David Caicedo, Ashish Pandharipande, and Frans MJ Willems. Detection performance analysis of an ultrasonic presence sensor. In *2013 IEEE International Conference on Acoustics, Speech and Signal Processing*, pages 2780–2784. IEEE, 2013.

[186] Shijia Pan, Tong Yu, Mostafa Mirshekari, Jonathon Fagert, Amelie Bonde, Ole J Mengshoel, Hae Young Noh, and Pei Zhang. Footprintid: Indoor pedestrian identification through ambient structural vibration sensing. *Proceedings of the ACM on Interactive, Mobile, Wearable and Ubiquitous Technologies*, 1(3):1–31, 2017.

[187] Jeffrey D Poston, Javier Schloemann, R Michael Buehrer, VVN Sriram Malladi, Americo G Woolard, and Pablo A Tarazaga. Towards indoor localization of pedestrians via smart building vibration sensing. In *2015 international conference on localization and GNSS (ICL-GNSS)*, pages 1–6. IEEE, 2015.

[188] Shijia Pan, Mario Berges, Juleen Rodakowski, Pei Zhang, and Hae Young Noh. Fine-grained recognition of activities of daily living through structural vibration and electrical sensing. In *Proceedings of the 6th ACM International Conference on Systems for Energy-Efficient Buildings, Cities, and Transportation*, pages 149–158, 2019.

[189] Md Osman Gani, Taskina Fayezeen, Richard J Povinelli, Roger O Smith, Muhammad Arif, Ahmed J Kattan, and Sheikh Iqbal Ahamed. A light weight smartphone based human activity recognition system with high accuracy. *Journal of Network and Computer Applications*, 141:59–72, 2019.

[190] William Taylor, Kia Dashtipour, Syed Aziz Shah, Amir Hussain, Qammer H Abbasi, and Muhammad A Imran. Radar sensing for activity classification in elderly people exploiting micro-doppler signatures using machine learning. *Sensors*, 21(11):3881, 2021.

[191] Markus Scholz, Stephan Sigg, Hedda R Schmidtke, and Michael Beigl. Challenges for device-free radio-based activity recognition. In *Workshop on Context Systems, Design, Evaluation and Optimisation*, 2011.

[192] Kristen Woyach, Daniele Puccinelli, and Martin Haenggi. Sensorless sensing in wireless networks: Implementation and measurements. In *2006 4th International Symposium on Modeling and Optimization in Mobile, Ad Hoc and Wireless Networks*, pages 1–8. IEEE, 2006.

[193] SangUk Han and SangHyun Lee. A vision-based motion capture and recognition framework for behavior-based safety management. *Automation in Construction*, 35:131–141, 2013.

[194] Emre Ertin, Nathan Stohs, Santosh Kumar, Andrew Raij, Mustafa Al'Absi, and Siddharth Shah. Autosense: unobtrusively wearable sensor suite for inferring the onset, causality, and consequences of stress in the field. In *Proceedings of the 9th ACM conference on embedded networked sensor systems*, pages 274–287, 2011.

[195] Fang-Jing Wu and Gurkan Solmaz. We hear your activities through wi-fi signals. In *2016 IEEE 3rd World Forum on Internet of Things (WF-IoT)*, pages 251–256. IEEE, 2016.

[196] Qimeng Li, Raffaele Gravina, Ye Li, Saeed H Alsamhi, Fangmin Sun, and Giancarlo Fortino. Multi-user activity recognition: Challenges and opportunities. *Information Fusion*, 63:121–135, 2020.

[197] Zheng Yang, Zimu Zhou, and Yunhao Liu. From rssi to csi: Indoor localization via channel response. *ACM Computing Surveys (CSUR)*, 46(2):1–32, 2013.

[198] Chunhai Feng, Sheheryar Arshad, Siwang Zhou, Dun Cao, and Yonghe Liu. Wi-multi: A three-phase system for multiple human activity recognition with commercial wifi devices. *IEEE Internet of Things Journal*, 6(4):7293–7304, 2019.

[199] Junhuai Li, Pengjia Tu, Huaijun Wang, Kan Wang, and Lei Yu. A novel device-free counting method based on channel status information. *Sensors*, 18(11):3981, 2018.

[200] Xiaodong Yang, Dou Fan, Aifeng Ren, Nan Zhao, and Muhammad Alam. 5g-based user-centric sensing at c-band. *IEEE Transactions on Industrial Informatics*, 15(5):3040–3047, 2019.

[201] Daniyal Haider, Aifeng Ren, Dou Fan, Nan Zhao, Xiaodong Yang, Shujaat Ali Khan Tanoli, Zhiya Zhang, Fangming Hu, Syed Aziz Shah, and Qammer H Abbasi. Utilizing a 5g spectrum for health care to detect the tremors and breathing activity for multiple sclerosis. *Transactions on Emerging Telecommunications Technologies*, 29(10):e3454, 2018.

[202] Ahsen Tahir, Jawad Ahmad, Syed Aziz Shah, Gordon Morison, Dawn A Skelton, Hadi Larijani, Qammer H Abbasi, Muhammad Ali Imran, and Ryan M Gibson. Wifreeze: Multiresolution scalograms for freezing of gait detection in parkinson's leveraging 5g spectrum with deep learning. *Electronics*, 8(12):1433, 2019.

[203] Bahareh Gholampooryazdi et al. Walking speed detection from 5g prototype system. 2017.

[204] Tan Zhang, Ning Leng, and Suman Banerjee. A vehicle-based measurement framework for enhancing whitespace spectrum databases. In *Proceedings of the 20th annual international conference on Mobile computing and networking*, pages 17–28, 2014.

[205] Shuangquan Wang and Gang Zhou. A review on radio based activity recognition. *Digital Communications and Networks*, 1(1):20–29, 2015.

[206] Zafar Ayyub Qazi, Cheng-Chun Tu, Luis Chiang, Rui Miao, Vyas Sekar, and Minlan Yu. Simple-fying middlebox policy enforcement using sdn. In *Proceedings of the ACM SIGCOMM 2013 conference on SIGCOMM*, pages 27–38, 2013.

[207] Aboajeila Milad Ashleibta, Adnan Zahid, Syed Aziz Shah, Qammer H Abbasi, and Muhammad Ali Imran. Flexible and scalable software defined radio based testbed for large scale body movement. *Electronics*, 9(9):1354, 2020.

[208] Qammer H Abbasi, Hasan Tahir Abbas, Akram Alomainy, and Muhammad Ali Imran. *Backscattering and RF Sensing for Future Wireless Communication*. John Wiley & Sons, 2021.

[209] Aboajeila Milad Ashleibta, Ahmad Taha, Muhammad Aurangzeb Khan, William Taylor, Ahsen Tahir, Ahmed Zoha, Qammer H Abbasi, and Muhammad Ali Imran. 5g-enabled contactless multi-user presence and activity detection for independent assisted living. *Scientific Reports*, 11(1):1–15, 2021.

[210] Alex Krizhevsky, Ilya Sutskever, and Geoffrey E Hinton. Imagenet classification with deep convolutional neural networks. *Advances in neural information processing systems*, 25, 2012.

[211] Siamak Azodolmolky, Jordi Perelló, Marianna Angelou, Fernando Agraz, Luis Velasco, Salvatore Spadaro, Yvan Pointurier, Antonio Francescon, Chava Vijaya Saradhi, Panagiotis Kokkinos, et al. Experimental demonstration of an impairment aware network planning and operation tool for transparent/translucent optical networks. *Journal of Lightwave Technology*, 29(4):439–448, 2011.

[212] Serkan Kiranyaz, Onur Avci, Osama Abdeljaber, Turker Ince, Moncef Gabbouj, and Daniel J Inman. 1d convolutional neural networks and applications: A survey. *Mechanical systems and signal processing*, 151:107398, 2021.